CONTROL OF ATMOSPHERIC FINE PRIMARY CARBON PARTICLE CONCENTRATIONS

by

Harry Andrew Gray

Project Principal Investigator:
Glen R. Cass

EQL Report 23

Environmental Quality Laboratory
California Institute of Technology
Pasadena, California 91125

7 February 1986

Final report prepared for
California Air Resources Board

in

completion of research under
ARB contract no. A1-071-32

"Characterization and Control of Primary
Carbon Particle Air Quality in the
South Coast Air Basin"

by

Environmental Quality Laboratory
California Institute of Technology
Pasadena, California 91125

7 February 1986

Disclaimer

The statements and conclusions in this report are those of the authors and not necessarily those of the California Air Resources Board. The mention of commercial products, their source or their use in connection with material reported herein is not to be construed as either an actual or an implied endorsement of such products.

to my family

and Melissa

ACKNOWLEDGEMENTS

The author would like to gratefully acknowledge the contributions of many individuals and organizations toward the completion of this thesis. My principal advisor, Dr. Glen Cass, has been instrumental in providing guidance during this project. His insights into the problems and importance of air pollution control led me to undertake this work. This study would have been impossible if it were not for previous investigations into air pollution control conducted by Dr. Cass, especially his Ph.D. thesis work. I am especially thankful to Dr. Cass for the genuine interest he has shown toward me, and the many long hours he has spent discussing this work and providing a comfortable environment for executing it.

The air quality monitoring program conducted during 1982 was greatly facilitated by the South Coast Air Quality Management District (SCAQMD). They allowed me to use a number of their monitoring locations. Many SCAQMD staff members were extremely helpful, not only during the monitoring program, but also in providing meteorological and emissions data used during the air quality model application. In particular, I would like to thank the following SCAQMD staff members for their assistance: Tony Hernandez, William Holland, William Bope, Margaret Brunelle, Eric Lemke, Margil Wadley, Sam Witz, Dominick Mercadante, Wiliam Baylor, Mike Nazemi, Chung Liu, Joe Cassmassi, and especially, Arthur Davidson and John Grisinger.

Duane Lea of the U.S. Navy (Pt. Mugu) was extremely cooperative in arranging for access to the San Nicolas Island weather station for

use as a remote off-shore monitoring location. Darwin Tolzin and Carl Otten went out of their way to assist in the operation of that monitoring site.

Design and construction of the fine aerosol samplers was performed with the generous assistance of Caltech's Environmental Engineering shop staff members Joe Fontana, Rich Eastvedt, Leonard Montenegro, and especially, Elton Daly. Jim Huntzicker, Emily Heyerdahl, and John Rau, at the Oregon Graduate Center, performed the aerosol carbon analyses on the filter samples. John Cooper and Cliff Frazier, at NEA Labs, were responsible for the X-ray fluorescence analysis which provided trace metal data. Daniel Jacob performed the ion chromatography analyses at Caltech.

Many staff members at Caltech's Environmental Quality Laboratory (EQL) assisted with portions of this work. Especially noteworthy was the contribution made by Shohreh Gharib, whose unselfish dedication was instrumental to the success of this thesis. She prepared almost all of the filters for the air quality monitoring program, spent many hours entering data onto a computer keyboard, and also gathered much of the fuel use data of Appendix B. Ted Russell Lynn Hildemann, Richard Honrath, and Barbara Turpin also helped in the collection of emissions inventory information. Andrew Ranzieri, of the California Air Resources Board, provided a large portion of the emissions inventory data. Jim Houseworth and Jim Tilden assisted in the deployment and retrieval of the fine particle samplers. Discussion of air quality modeling procedures with William Goodin was

very instructive. Robert Koh was helpful in answering questions on computing and his universal data handling system called MAGIC was used throughout to expedite computations and to prepare computer-generated graphics. Previous work by Susan Hunts and Ken McCue proved to be very useful during the control strategy analysis. I would like also to thank Dr. Norman Brooks, the director of EQL, for his generous support.

A great deal was learned about the nature of air pollution from Drs. John Seinfeld and Richard Flagan. Dr. Joel Franklin's instruction in applied mathematics was useful in devising the control strategy optimization technique and in formulation of the air quality model. Librarians Rayma Harrison and Gunilla Hastrup were very helpful in locating hard to find literature. I would also like to thank Kiku Matsumoto of Caltech's Computing Support Services department for her assistance in removing many obstacles, and hence allowing me to successfully run the air quality model programs.

Finally, I would like to especially thank Pat Houseworth and Christina Conti for the typing and preparation of this manuscript. Their assistance and friendship in the office has been greatly appreciated. Theresa Fall and Nancy Tomer prepared many of the graphics contained in this thesis.

The California Air Resources Board provided most of the monetary support needed to conduct this research project under Agreement A1-071-32. I am grateful that they have had the foresight to realize that it is necessary to conduct long-term research into the

problems of air pollution if progress is to be made. Doug Lawson, Jack Suder, Eric Fujita, and Chuck Unger were the contract monitors.

This report was submitted in fulfillment of ARB contract no. A1-071-32 "Characterization and Control of Primary Carbon Particle Air Quality in the South Coast Air Basin" by the Environmental Quality Laboratory, California Institute of Technology, Pasadena, California 91125, under the sponsorship of the California Air Resources Board. Work was completed as of 7 February 1986.

ABSTRACT

The adverse health effects and urban visibility degradation associated with atmospheric carbon particle concentrations suggest that control of this class of air pollutants is desirable, especially in the event of an increase in the usage of diesel vehicles. In this study, procedures for the engineering design of fine carbonaceous particulate matter abatement strategies have been developed and tested in the Los Angeles area. Carbon particle abatement strategies are evaluated based on the results of an emissions to air quality model, the performance of which is verified by comparison to measurements of ambient aerosol concentrations taken in the South Coast Air Basin during 1982.

As a result of this research, the long-term average behavior of fine aerosol carbon concentrations has been characterized in the Los Angeles area for the first time. The highest concentrations of fine particulate total carbon were observed in areas of heavy traffic density. The annual average fine total carbon concentration at downtown Los Angeles was 12.2 $\mu g\ m^{-3}$ during 1982, which constituted 37% of the fine aerosol (particle diameter $< 2.1\ \mu m$) mass collected at that location. Aerosol carbon concentrations were observed to decrease with distance inland from downtown Los Angeles. The 1982 annual average fine total carbon concentration at Rubidoux, which is about 80 km east of Los Angeles, was only 8.2 $\mu g\ m^{-3}$. There is a pronounced winter peak and summer minimum in carbonaceous aerosol concentrations in the western portion of the air basin. The monthly

average fine total carbon concentration at downtown Los Angeles reached a high of 22.3 $\mu g\ m^{-3}$ during December 1982, and dropped to 7.4 $\mu g\ m^{-3}$ during June 1982. At eastern locations in the air basin, the seasonal trend becomes less significant, with monthly average fine total carbon concentrations at Rubidoux observed to be between 6.4 and 10.8 $\mu g\ m^{-3}$ during all months of 1982.

Elemental carbon in the atmosphere is inert and is due solely to direct (primary) aerosol emissions from sources, while organic carbon could be directly emitted as primary aerosol or could be formed in part from condensation of the low vapor pressure products of atmospheric chemical reactions (secondary formation). Examination of the spatial and temporal trends of the ratio of fine total carbon to fine elemental carbon concentration leads to the conclusion that secondary organic carbon aerosol formed in the atmosphere from hydrocarbon precursors was not the overwhelming contributor to overall long-term average total carbon levels in the Los Angeles area during the year 1982. At downwind locations, such as Azusa or Rubidoux, it was found that, at most, between 16% and 22% of the annual average total carbon concentration (or 27% to 38% of the organic carbon) may be due to secondary aerosol formation in excess of that found at Lennox (a near-coastal site next to a heavily travelled freeway source of primary aerosol). Comparison of fine elemental and organic carbon particle concentrations against the ratio of those two aerosol species found in basin-wide source emissions further indicates that, over long averaging times during 1982, primary aerosol carbon particle emissions

are responsible for the majority of atmospheric carbon particle concentrations.

The particulate air quality data collected during 1982 were used to verify the performance of a mathematical model for long-term average air quality. The Lagrangian particle-in-cell air quality model previously developed by Cass (1977, 1981) was improved to handle near-source dispersion from ground level sources. The model was tested against emissions, elemental carbon air quality, and meteorological data for 1982 in the Los Angeles area. It was found that the model adequately predicts the long-term average concentration of this primary pollutant. The predictions and observations of monthly average elemental carbon particle concentrations have a positive correlation coefficient of 0.78. The model also determines the source classes responsible for fine carbon particle air quality. Many source types, including highway vehicles, charcoal broilers, and fireplaces contribute to primary total carbon particle concentrations, while elemental carbon concentrations are due mostly to emissions from diesel engines.

The source class contributions computed by the air quality model were used to determine the optimal emission control strategy for attaining any desired level of improved carbon particle air quality. Linear programming techniques were employed to solve for the least costly set of emission control measures which would enable an air quality goal to be met. Solutions indicate that application of a few control measures, aimed almost entirely at diesel engines, will reduce

the basin-wide maximum annual average fine elemental carbon concentration approximately by half at an annual cost of about $69 million. The maximum annual average fine primary particulate total carbon concentration may be reduced by about 35% at a cost of $102 million per year. A control program for visibility improvement would preferentially require the reduction of atmospheric fine elemental carbon particle concentrations, whereas a program designed to control fine aerosol mass would benefit from total carbon particle concentration reductions. It was determined that a control strategy that is optimal for total carbon control may be near-optimal for elemental carbon control. However, an emissions control strategy designed to optimize for elemental carbon control may produce peak total carbon concentrations that exceed those which would result from a control strategy optimized for total carbon by as much as 8%.

In summary, it has been demonstrated that the air quality model is useful both in predicting long-term average carbon particle air quality and in determining the sources responsible for that air quality outcome. It was found that emissions from diesel engines were responsible for a large portion of the atmospheric fine carbon particle concentrations in the Los Angeles area during 1982. Control of emissions from diesel engines is therefore important, and it was determined that the least costly set of emission control measures for reducing carbon particle concentrations includes diesel engine emission controls.

TABLE OF CONTENTS

	Page
ACKNOWLEDGEMENTS	iv
ABSTRACT	viii
LIST OF FIGURES	xvi
LIST OF TABLES	xxii
GLOSSARY	xxv
CHAPTER 1 INTRODUCTION	1
1.1 Problem Definition	1
1.2 Approach of the Present Study	3
1.3 References for Chapter 1	8
CHAPTER 2 CHARACTERISTICS OF ATMOSPHERIC ORGANIC AND ELEMENTAL CARBON PARTICLE CONCENTRATIONS IN LOS ANGELES	11
2.1 Introduction	11
2.2 Experimental Design	13
2.3 Fine Particle Concentration and Composition	20
2.4 Characteristics of Elemental and Organic Carbon Concentrations	23
2.5 Comparison to Emission Data	40
2.6 Summary and Discussion	56
2.7 References for Chapter 2	60

TABLE OF CONTENTS (Continued)

	Page
CHAPTER 3 DEVELOPMENT OF A SIMULATION MODELING TECHNIQUE FOR LONG-TERM AVERAGE PRIMARY CARBON PARTICLE AIR QUALITY	64
3.1 Introduction	64
3.2 An Overview of Long-term Average Air Quality Models	65
3.3 A Simulation Model for Long-term Average Primary Carbon Particle Air Quality under Unsteady Meteorological Conditions	69
3.3.1 Single Particle Transport in the Horizontal Plane	73
3.3.2 Exchange in the Vertical Direction	78
3.3.3 Vertical Profile below Inversion Base	88
3.3.4 Computational Procedure for Air Quality Model Simulation	93
3.4 Summary	97
3.5 References for Chapter 3	99
CHAPTER 4 APPLICATION OF THE SIMULATION MODEL TO LOS ANGELES FINE PRIMARY CARBON PARTICULATE AIR QUALITY	100
4.1 Introduction	100
4.2 Data Requirements for Model Application	100
4.2.1 Emission Source Related Data	101
4.2.2 Meteorological Data	114
4.2.3 Estimation of Atmospheric Diffusive Dispersion Parameters	116
4.2.3.1 Horizontal Dispersion Parameter	116
4.2.3.2 Vertical Dispersion Parameter	117
4.2.4 Estimation of Particulate Dry Deposition Velocity	121

TABLE OF CONTENTS (Continued)

		Page
4.2.5	Background Concentrations of Fine Atmospheric Carbonaceous Particulate Matter	122
4.2.6	Selection of Time Step and Receptor Grid Cell Size	122
4.2.7	Model Validation Data	124
4.3	Air Quality Model Results	125
4.3.1	Predicted versus Observed Fine Elemental Carbon Particle Concentrations	125
4.3.2	Spatial-Temporal Correlation between Predicted and Observed Fine Elemental Carbon Particle Concentrations	133
4.3.3	Comparison of Primary Fine Total Carbon Concentration Predictions and Fine Total Carbon Air Quality Observations	137
4.3.4	Spatial Variations in Fine Carbon Particle Air Quality	147
4.3.5	Source Class Contributions to Atmospheric Fine Carbon Particle Concentrations	163
4.4	Summary	172
4.5	References for Chapter 4	174
CHAPTER 5	OPTIMAL STRATEGIES FOR THE CONTROL OF FINE PRIMARY PARTICULATE CARBON AIR QUALITY	176
5.1	Introduction	176
5.2	Formulation of the Linear Programming Technique	179
5.3	Application of the Linear Programming Technique for Control of Fine Primary Carbonaceous Particulate Matter in the Los Angeles Area	186
5.3.1	Introduction	186
5.3.2	Data Requirements	188
5.3.3	Results	198

TABLE OF CONTENTS (Continued)

	Page
5.4 Summary and Conclusions	207
5.5 References for Chapter 5	211
CHAPTER 6 FUTURE RESEARCH	213
6.1 Introduction	213
6.2 Air Quality Observations	213
6.3 Air Quality Model Application	215
6.4 Emission Control Strategies	216
6.5 Conclusions	217
6.6 References for Chapter 6	219
APPENDIX A 1982 EMISSIONS ESTIMATES IN THE 50X50-MILE MODELING GRID	220
APPENDIX B 1982 FUEL USE DATA	258
APPENDIX C 1982 EMISSIONS ESTIMATES IN THE 4 COUNTY SOUTH COAST AIR BASIN	273
APPENDIX D ESTIMATES OF THE COSTS AND EMISSION REDUCTIONS OF FINE PARTICLE CONTROL MEASURES	278
APPENDIX E FINE PARTICLE CONCENTRATIONS AT ELEVEN LOCATIONS IN THE SOUTH COAST AIR BASIN DURING 1982	327
APPENDIX F SOURCE CLASS CONTRIBUTIONS TO 1982 ANNUAL AVERAGE CARBON PARTICLE AIR QUALITY	328

LIST OF FIGURES

Figure		Page
2.1	Fine particle air monitoring network.	14
2.2	Ambient sampling protocol.	16
2.3	Comparison of fine particulate matter concentration to total suspended particulate matter concentration.	21
2.4	Material balance on the chemical composition of annual mean fine particle concentrations in the Los Angeles area--1982.	24
2.5	Fine carbonaceous particulate matter in the Los Angeles area.	25
2.6	Daily and monthly average carbonaceous aerosol concentrations at Lennox, CA. (a) daily OC, (b) monthly average OC, (c) daily EC, and (d) monthly average EC	28
2.7	Fine total carbon concentration. (a) daily TC and (b) monthly average TC at Los Angeles,	29
	(c) daily TC and (d) monthly average TC at Pasadena,	30
	(e) daily TC and (f) monthly average TC at Upland,	31
	(g) daily TC and (h) monthly average TC at Rubidoux,	32
	(i) daily TC and (j) monthly average TC at Lennox,	33
	(k) daily TC and (l) monthly average TC at Long Beach,	34
	(m) daily TC and (n) monthly average TC at West Los Angeles,	35
	(o) daily TC and (p) monthly average TC at Anaheim,	36
	(q) daily TC and (r) monthly average TC at Azusa,	37
	(s) daily TC and (t) monthly average TC at Burbank,	38
	(u) daily TC and (v) monthly average TC at San Nicolas Island	39
2.8	Aerosol carbon emissions in the greater Los Angeles area in particle sizes $\leq$ 10 μm diameter, winter 1980 (from Cass, Boone, and Macias 1982).	41
2.9	Ratio of total carbon to elemental carbon. (a) daily ratio and (b) monthly average ratio at Lennox,	44
	(c) daily ratio and (d) monthly average ratio at Los Angeles,	45
	(e) daily ratio and (f) monthly average ratio at Pasadena,	46
	(g) daily ratio and (h) monthly average ratio at Upland,	47

LIST OF FIGURES (Continued)

Figure		Page
2.9	(i) daily ratio and (j) monthly average ratio at Rubidoux,	48
	(k) daily ratio and (l) monthly average ratio at Long Beach,	49
	(m) daily ratio and (n) monthly average ratio at West Los Angeles,	50
	(o) daily ratio and (p) monthly average ratio at Anaheim,	51
	(q) daily ratio and (r) monthly average ratio at Azusa,	52
	(s) daily ratio and (t) monthly average ratio at Burbank	53
2.10	Annual average of the daily ratio of total carbon to elemental carbon in fine particles in the Los Angeles area--1982.	55
3.1	Air parcel insertion into the atmosphere (from Cass 1977).	82
3.2	Hypothetical time history of interaction between the inversion base and a fluid particle released at time t_o (from Cass 1977).	85
3.3	Air quality model calculation: mapping of emissions from a unit source into average pollutant concentration.	96
4.1	The central portion of the South Coast Air Basin showing the grid system used.	102
4.2	Fine aerosol carbon emissions in the 50X50-mile modeling grid.	107
4.3	Fine total carbon emissions within the 50X50-mile grid during December 1982.	109
4.4	Fine elemental carbon emissions within the 50X50-mile grid during December 1982.	110
4.5	Cross-wind standard deviation of plume spread as a function of travel time. St. Louis data from McElroy and Pooler (1968). Los Angeles data from Drivas and Shair (1975) and Shair (1977). Heavy solid line represents function for $\sigma_y(t)$ fit to the Los Angeles data, from Cass (1977).	118

LIST OF FIGURES (Continued)

Figure		Page
4.6	Effective vertical standard deviation of plume spread as a function of downwind distance in terms of Pasquill-Turner stability classes (from McElroy and Pooler, 1968).	119
4.7a	Monthly mean elemental carbon concentration at Lennox —Air quality model results vs. observed values.	126
4.7b	Source class contributions to elemental carbon concentrations at Lennox.	126
4.8a	Monthly mean elemental carbon concentration at Long Beach --Air quality model results vs. observed values.	127
4.8b	Source class contributions to elemental carbon concentrations at Long Beach.	127
4.9a	Monthly mean elemental carbon concentration at West Los Angeles--Air quality model results vs. observed values.	128
4.9a	Source class contributions to elemental carbon concentrations at West Los Angeles.	128
4.10a	Monthly mean elemental carbon concentration at Los Angeles--Air quality model results vs. observed values.	129
4.10b	Source class contributions to elemental carbon concentrations at Los Angeles.	129
4.11a	Monthly mean elemental carbon concentration at Anaheim --Air quality model results vs. observed values.	130
4.11b	Source class contributions to elemental carbon concentrations at Anaheim.	130
4.12a	Monthly mean elemental carbon concentration at Pasadena --Air quality model results vs. observed values.	131
4.12b	Source class contributions to elemental carbon concentrations at Pasadena.	131
4.13a	Monthly mean elemental carbon concentration at Azusa --Air quality model results vs. observed values.	132
4.13b	Source class contributions to elemental carbon concentrations at Azusa.	132

LIST OF FIGURES (Continued)

Figure		Page
4.14	Monthly average fine elemental carbon particle concentration at seven monitoring sites--observations vs. predictions.	135
4.15a	Monthly mean total carbon concentration at Lennox --Air quality model results vs. observed values.	138
4.15b	Source class contributions to total carbon concentrations at Lennox.	138
4.16a	Monthly mean total carbon concentration at Long Beach --Air quality model results vs. observed values.	139
4.16b	Source class contributions to total carbon concentrations at Long Beach.	139
4.17a	Monthly mean total carbon concentration at West Los Angeles--Air quality model results vs. observed values.	140
4.17b	Source class contributions to total carbon concentrations at West Los Angeles.	140
4.18a	Monthly mean total carbon concentration at Los Angeles --Air quality model results vs. observed values.	141
4.18b	Source class contributions to total carbon concentrations at Los Angeles.	141
4.19a	Monthly mean total carbon concentration at Anaheim --Air quality model results vs. observed values.	142
4.19b	Source class contributions to total carbon concentrations at Anaheim.	142
4.20a	Monthly mean total carbon concentration at Pasadena --Air quality model results vs. observed values.	143
4.20b	Source class contributions to total carbon concentrations at Pasadena.	143
4.21a	Monthly mean total carbon concentration at Azusa --Air quality model results vs. observed values.	144
4.21b	Source class contributions to total carbon concentrations at Azusa.	144

LIST OF FIGURES (Continued)

Figure		Page
4.22	Observations of monthly average fine total carbon particle concentrations vs. predictions of fine primary total carbon particle concentrations at seven monitoring sites.	145
4.23	Annual mean fine primary total carbon concentration isopleths computed by the air quality model simulation.	148
4.24	Annual mean fine elemental carbon concentration isopleths computed by the air quality model simulation.	149
4.25	Monthly average fine elemental carbon concentration isopleths computed by the air quality model simulation --January 1982.	150
4.26	Monthly average fine elemental carbon concentration isopleths computed by the air quality model simulation --February 1982.	151
4.27	Monthly average fine elemental carbon concentration isopleths computed by the air quality model simulation --March 1982.	152
4.28	Monthly average fine elemental carbon concentration isopleths computed by the air quality model simulation --April 1982.	153
4.29	Monthly average fine elemental carbon concentration isopleths computed by the air quality model simulation --May 1982.	154
4.30	Monthly average fine elemental carbon concentration isopleths computed by the air quality model simulation --June 1982.	155
4.31	Monthly average fine elemental carbon concentration isopleths computed by the air quality model simulation --July 1982.	156
4.32	Monthly average fine elemental carbon concentration isopleths computed by the air quality model simulation --August 1982.	157
4.33	Monthly average fine elemental carbon concentration isopleths computed by the air quality model simulation --September 1982.	158

LIST OF FIGURES (Continued)

Figure		Page
4.34	Monthly average fine elemental carbon concentration isopleths computed by the air quality model simulation --October 1982.	159
4.35	Monthly average fine elemental carbon concentration isopleths computed by the air quality model simulation --November 1982.	160
4.36	Monthly average fine elemental carbon concentration isopleths computed by the air quality model simulation --December 1982.	161
4.37	Fine primary total carbon air quality increment due to heavy diesel trucks--June 1982.	164
4.38	Fine primary total carbon air quality increment due to petroleum refinery fuel combustion--June 1982.	165
4.39	Fine primary total carbon air quality increment due to heavy diesel trucks--December 1982.	166
4.40	Fine primary total carbon air quality increment due to petroleum refinery fuel combustion--December 1982.	167
4.41	Monthly average fine primary total carbon concentration isopleths computed by the air quality model simulation --June 1982.	169
4.42	Monthly average fine primary total carbon concentration isopleths computed by the air quality model simulation --December 1982.	170
5.1	Optimal strategy for control of fine total carbon concentrations.	199
5.2	Optimal strategy for control of fine elemental carbon concentrations.	200
5.3	Control of elemental carbon concentrations: comparison of optimal strategy for EC reduction to EC concentrations that result from optimal strategy for TC reduction.	205
5.4	Control of total carbon concentrations: comparison of optimal strategy for TC reduction to TC concentrations that result from optimal strategy for EC reduction.	206

LIST OF TABLES

Table		Page
2.1	Material Balance on the Chemical Composition of Fine Particulate Matter Concentrations--Los Angeles Area (1982 Annual Mean)	22
2.2	Statistical Description of Aerosol Carbon Data Los Angeles Area--1982	26
4.1	Emissions Estimates for Mobile Sources Within the 50X50-mile Grid 1982	103
4.2	Emissions Estimates for Stationary Combustion Sources Within the 50X50-mile Grid 1982	104
4.3	Emissions Estimates for Industrial Processes Within the 50X50-mile Grid 1982	105
4.4	Emissions Estimates for Fugitive Sources Within the 50X50-mile Grid 1982	106
4.5	1982 Annual Average Fine Particulate Carbon Emissions Summary within the 50X50-mile Grid	108
4.6	Key to Stability Classes (from Turner 1969)	120
4.7	Coefficients of $\sigma_z = ax^b$ by Stability Class, Fit to the Data of McElroy and Pooler (1968)	121
4.8	Fine Particulate Carbon Background Concentrations	123
4.9	Observed versus Predicted 1982 Annual Average Fine Elemental Carbon Concentrations	134
5.1	Costs and Emissions Reductions of Control Measures Used in this Study	190
5.2	Groupings of Incompatible Control Measures	194

LIST OF TABLES (Continued)

Table		Page
A.1	Emissions Estimates for Mobile Sources Within the 50X50-mile Grid 1982	221
A.2	Emissions Estimates for Stationary Combustion Sources Within the 50X50-mile Grid 1982	227
A.3	Emissions Estimates for Industrial Processes Within the 50X50-mile Grid 1982	232
A.4	Emissions Estimates for Fugitive Sources Within the 50X50-mile Grid 1982	235
A.5	Fuel Economy Calculation for 1982 Automobile Fleet	239
A.6	Vehicle Miles Travelled and Fuel Usage for Each Vehicle Type in 1982	241
A.7	Tire Attrition 1982	243
A.8	Brake Lining Attrition 1982	245
A.9	Fireplace Emissions 1982	247
A.10	Correspondence Between Source Types Used in this Study and California Air Resources Board Category of Emission Source (CES, SCC) Numbers	250
B.1	1980 Population by Region	259
B.2	Electric Generating Stations 1982 Fuel Use	260
B.3	Refineries Fuel Use 1982	262
B.4	Residential and High Priority Commercial Natural Gas Sales, 1982	264
B.5	Industrial and Low Priority Commercial Natural Gas Sales, 1982	266
B.6	Deliveries of Fuels in 1982	268
C.1	Emissions Estimates for Mobile Sources in 4 County South Coast Air Basin	274
C.2	Emissions Estimates for Stationary Combustion Sources in 4 County South Coast Air Basin	275

LIST OF TABLES (Continued)

Table		Page
C.3	Emissions Estimates for Industrial Processes in 4 County South Coast Air Basin	276
C.4	Emissions Estimates for Fugitive Sources in 4 County South Coast Air Basin	277
D.38	Source Class List Correspondence	319

GLOSSARY

Coarse particles – airborne particulate matter with particle sizes greater than 2.1 μm in diameter.

Elemental carbon – black carbonaceous particulate matter with a chemical structure similar to impure graphite and that is non-volatile below 600°C in an inert atmosphere (helium).

Fine particles – airborne particulate matter with particle sizes smaller than 2.1 μm in diameter.

Particulate organic carbon – the carbon content of airborne organic compounds present as particulate matter in the atmosphere.

Particulate total carbon – The summation of the airborne particulate carbon content due to all particle types present, including organic carbon, carbonate carbon and elemental carbon.

Primary aerosol carbon – that fraction of the airborne carbonaceous particulate matter that was emitted to the atmosphere from its source as particulate matter (eg. as a solid or liquid) rather than as a hydrocarbon gas.

Secondary aerosol carbon – carbonaceous particulate matter formed in the atmosphere from the low vapor pressure products of reactions involving gaseous hydrocarbon precursors.

CHAPTER 1

INTRODUCTION

1.1 Problem Definition

Particulate air pollutants residing in particle sizes below about 2 μm aerodynamic diameter are largely responsible for the severe visibility deterioration observed in the South Coast Air Basin that surrounds the Los Angeles area (Hidy et al. 1974, White and Roberts 1977, Cass 1976, Conklin et al. 1981). Particles in that size range are easily respirable (Task Group 1966) and thus contribute to many of the adverse health effects attributed to high levels of total suspended particulate matter in the atmosphere (Middleton et al. 1969). Control of the fine particle fraction of the ambient aerosol is, therefore, a particularly important problem facing state and local air pollution control agencies.

Studies show that most of the fine particulate matter in the atmosphere of the South Coast Air Basin consists of sulfates, nitrates, and carbonaceous particles (Hidy et. al 1974). As will be seen in Chapter 2 of this study, aerosol carbon alone accounts for about 40% of the total fine particle mass in that air basin. Hence, its control is critical to any attempt to meet present total suspended particulate matter and future fine particle air quality standards. Black graphitic (elemental) carbon particles have been found to be the predominant light-absorbing aerosol species in the atmosphere (Rosen

et al. 1977) and are responsible for a major portion of the Los Angeles visibility problem (Conklin et al. 1981). Polynuclear aromatic hydrocarbons that are adsorbed onto soot particles have been shown to be carcinogenic in experimental animal studies (IARC Working Group 1980). Thus an assessment of approaches to reducing atmospheric soot concentrations may provide valuable insights concerning the control of toxic substances in the atmosphere.

Despite the importance of aerosol carbon particles as contributors to particulate air quality and visibility standard violations, relatively little is known about how to control such pollutants effectively. Routine air monitoring data bases sufficient to support aerosol carbon control strategy studies do not presently exist for the Los Angeles area (Wadley and Witz 1981, Tsou 1981). Inventory procedures for defining organic and elemental carbon emissions are in their earliest stages of development at present (Cass et al. 1982). Air quality modeling approaches designed to assess the sources responsible for atmospheric carbon particle concentrations previously have been limited to rollback and receptor model calculations that cannot be verified easily because the elemental composition of emissions from many different carbonaceous particulate source types is virtually identical. The problem is compounded due to the presence of secondary organic aerosol that is formed in the atmosphere from the low vapor pressure products of reactions involving gaseous hydrocarbon precursors (Grosjean and Friedlander 1975, Schuetzle 1975, Cronn et al. 1977, Grosjean 1977, Appel et al. 1979).

Better air quality modeling approaches are needed. Methods for identifying the least costly combination of control technologies required to attain any desired level of aerosol carbon air quality should be developed. Control strategies aimed at abating fine total carbon particle mass might look quite different than strategies directed at abating the visibility-reducing potential of elemental carbon particles alone.

The pursuit of methods for controlling atmospheric carbon particle air quality is particularly important in Los Angeles at this time. As noted by Pierson (1978), Los Angeles air quality is likely to be heavily affected by increased soot emissions if large numbers of diesel passenger cars are introduced into the vehicle fleet. Engineering research into control of aerosol carbon concentrations is needed before conversion of more of the vehicle fleet to diesel engines occurs.

1.2 Approach of the Present Study

The objective of the present study is to develop methods for the design of emission control strategies that can be employed to reduce atmospheric primary carbonaceous aerosol loadings, thereby improving visibility and reducing exposure to respirable fine particles. Methods developed will be tested during a case study of aerosol carbon abatement alternatives in the South Coast Air Basin.

At the start of this research effort, an air quality data base suitable to support control strategy development in the Los Angeles

area did not exist. As part of this study, a routine sampling program is conducted during the calendar year of 1982. Twenty-four hour average ambient fine particulate matter samples are collected at six-day intervals at ten monitoring locations in the South Coast Air Basin. The samples are analyzed for total carbon and elemental carbon (total carbon = elemental carbon + organic carbon) by the method of Johnson et al. (1981). Measurement of the trace metal content of samples provides the ability to use receptor modeling techniques (Cooper and Watson 1980, Gordon 1980) to confirm source class contributors to observed air quality. Measurement of $SO_4^=$, NO_3^-, and NH_4^+ ion concentrations completes a mass balance on the major aerosol components of the samples. The sampling program described in Chapter 2 results in a representative set of air quality data that is used to characterize an annual cycle of fine carbon particle air quality in the Los Angeles area. The air quality data set also can be used to verify the predictions of an air quality model describing the transport of primary pollutants in an urban airshed.

The relative importance of secondary organics formation is assessed in Chapter 2 by comparing measured ambient (primary plus secondary) total carbon to elemental carbon concentration ratios with the same ratios observed at emission sources (which yield primary aerosol only). Development of new methods for evaluating the magnitude of secondary aerosol formation is extremely important. The extent to which primary particulate sources versus gas phase hydrocarbon sources should be controlled depends on the outcome of

such an inquiry, and present methods for making such determinations have led to longstanding scientific disputes (Gundel 1978).

A mathematical description of the atmospheric transport of fresh emissions of a non-reactive pollutant over an air basin is developed in Chapter 3. The model employs a Lagrangian particle-in-cell technique to predict long-term average concentrations of an inert pollutant, such as elemental carbon. The calculation procedure is formulated to simulate atmospheric transport processes including ground-level dry deposition and vertical diffusion. Particular attention is given to the mixing of pollutants in the vertical direction at locations close to sources.

In Chapter 4 the model is used to predict 1982 monthly averaged fine carbonaceous particle concentrations in the Los Angeles atmosphere. Data requirements for the model application are outlined and satisfied. An inventory of fine carbonaceous particulate emissions is compiled for an 80X80-km (50X50-mile) grid centered over the western portion of the South Coast Air Basin. Over 70 source types are identified, and carbonaceous aerosol emissions are matched to the model in such a way as to represent spatial and temporal emissions trends. Source samples are collected and analyzed for a few source types to further improve inventory accuracy. Meteorological data are collected, and the characteristics of ventilation in the air basin are summarized. Other data requirements and approximations necessary for execution of the air quality model are discussed.

Results of the modeling exercise are examined in the latter

part of Chapter 4. Since elemental carbon particles are chemically very stable and are due solely to primary emissions, the non-reactive air quality model is verified by focusing on the comparison between predicted and observed fine elemental carbon particle air quality. The comparison of fine primary total carbon concentration predictions to fine total carbon concentration observations provides a new method for estimating the amount of secondary organics present in the atmosphere (i.e., organic particles formed from the condensation products of atmospheric hydrocarbon gas phase reactions). By subtracting calculated primary organic aerosol concentrations from the measured total organic aerosol present, an estimate of the magnitude of the secondary organics present can be obtained.

From the air quality modeling exercise, the contribution from each of many source types to primary aerosol carbon air quality is determined at a number of receptor sites. This source-to-receptor information is combined with data on emission control opportunities to evaluate alternative strategies for aerosol carbon air quality improvement. In Chapter 5, a linear programming algorithm is developed to identify optimal control strategies that provide the least costly combination of aerosol carbon emission control measures needed to attain any desired level of primary aerosol carbon air quality.

The trade-off implied by choice of a strategy optimized for control of total carbon particle concentrations versus an optimal strategy for elemental carbon particle concentrations is examined in

Chapter 5. The effects on visibility (and the likely effects on health) of organic and elemental carbon particles are quite different. Elemental carbon particles are very efficient light absorbers and, therefore, contribute disproportionately to visibility degradation. Hence, the preferential abatement of elemental carbon or organic carbon particles might be selected as an objective of future fine particle control efforts. Chapter 5 shows how preferential control of elemental carbon levels can be achieved.

It is concluded that the air quality model developed during this study is useful for identifying the major sources responsible for high air pollutant concentrations in an urban air basin. This modeling approach could be applied to the problem of designing control strategies for other pollutants and could be applied in other geographic areas. Opportunities for future research and model application are given in Chapter 6.

1.3 References for Chapter 1

Appel, B. R., E. M. Hoffner, E. L. Kothny, S. M. Wall, M. Haik, and R. L. Knights. 1979. Analysis of carbonaceous material in southern California atmospheric aerosols 2. Environmental Science and Technology 13:98-104.

Cass, G. R. 1976. The relationship between sulfate air quality and visibility at Los Angeles. California Institute of Technology. Environmental Quality Laboratory Memorandum no. 18. Pasadena.

Cass, G. R., P. M. Boone, and E. S. Macias. 1982. Emissions and air quality relationships for atmospheric carbon particles in Los Angeles. In Particulate carbon: Atmospheric life cycle, ed. G. T. Wolff and R. L. Klimisch. New York: Plenum Press.

Conklin, M. H., G. R. Cass, L-C. Chu, and E. S. Macias. 1981. Wintertime carbonaceous aerosols in Los Angeles: An exploration of the role of elemental carbon. In Atmospheric aerosols: Source/air quality relationships, ed. E. S. Macias and P. K. Hopke. Washington, D.C.: American Chemical Society.

Cooper, J. A., and J. G. Watson. 1980. Receptor oriented methods of air particulate source apportionment. J. Air Pollution Control Assoc. 30:1116-25.

Cronn, D. R., R.J. Charlson, R. L. Knights, A. L. Crittenden, and B. R. Appel. 1977. A survey of the molecular nature of primary and secondary components of particles in urban air by high-resolution mass spectrometry. Atmospheric Environment 11:929-37.

Gordon, G. E. 1980. Receptor models. Environmental Science and Technology 7:792-800.

Grosjean, D. 1977. Aerosols. In Ozone and other photochemical oxidants. Washington, D.C.: National Academy of Sciences.

Grosjean, D., and S. K. Friedlander. 1975. Gas-particle distribution factors for organic and other pollutants in the Los Angeles atmosphere. J. Air Pollut. Control Assoc. 25:1038-44.

Gundel, L. 1978. In Proceedings, carbonaceous particles in the atmosphere, ed. T. Novakov, p. 91. Lawrence Berkeley Laboratory. Berkeley, California.

Hidy, G. M., et al. 1974. Characterization of aerosols in California (ACHEX). Rockwell International. Science Center. Prepared under California Air Resources Board contract no. 358 (issued September 1974, revised April 1975).

IARC Working Group. 1980. An evaluation of chemicals and industrial processes associated with cancer in humans based on human and animal data. Cancer Research 40:1-12.

Johnson, R. L., J. J. Shah, R. A. Cary, and J. J. Huntzicker. 1981. An automated thermal-optical method for the analysis of carbonaceous aerosol. In Atmospheric aerosols: Source/air quality relationships, ed. E. S. Macias and P. K. Hopke. Washington, D.C.: American Chemical Society.

Middleton, J. T., et al. 1969. Air quality criteria for particulate matter. U.S. Department of Health, Education, and Welfare. National Air Pollution Control Administration Publication no. AP-49.

Pierson, W. R. 1978. Particulate organic matter and total carbon from vehicles on the road. In Proceedings, carbonaceous particles in the atmosphere, ed. T. Novakov, 221-228. Lawrence Berkeley Laboratory. Berkeley, California.

Rosen, H., A. D. A. Hansen, R. L. Dod, and T. Novakov. 1977. Application of the optical absorption technique to the characterization of the carbonaceous component of ambient and source particulate samples. In Proceedings, fourth joint conference on sensing of environmental pollutants. New Orleans. Paper 171.

Schuetzle, F., D. Cronn, A. L. Crittenden, and R. J. Charlson. 1975. Molecular composition of secondary aerosol and its possible origin. Environmental Science and Technology 9:838-45.

Task Group on Lung Dynamics. 1966. Deposition and retention models for internal dosimetry of the human respiratory tract. Health Physics 12:173-207.

Tsou, G., California Air Resources Board, El Monte. 1981. Personal communication confirms that data from ARB aerosol carbon studies in early 1970s are incomplete and are not suitable to the needs of this research project.

Wadley, M., and S. Witz, South Coast Air Quality Management District, El Monte, California. 1981. Personal communication confirms that the AQMD has no historical aerosol carbon data base.

White, W. H., and P. T. Roberts. 1977. On the nature and origins of visibility-reducing aerosols in the Los Angeles air basin. Atmospheric Environment 11:803-12.

CHAPTER 2

CHARACTERISTICS OF ATMOSPHERIC ORGANIC AND ELEMENTAL CARBON PARTICLE CONCENTRATIONS IN LOS ANGELES

2.1 Introduction

Fine carbonaceous particulate matter is emitted from most combustion processes (Siegla and Smith 1981, Wagner 1978, Muhlbaier and Williams 1982, Cass et al. 1982). These primary carbon particles consist of organic compounds accompanied by black non-volatile soot components that have a chemical structure similar to impure graphite (Rosen et al. 1978). The black portion of these particulate emissions, commonly referred to as elemental carbon, is a major contributor to visibility reduction in urban areas (Rosen et al. 1982, Waggoner and Charlson 1977, Pierson and Russell 1979, Conklin et al. 1981, Groblicki et al. 1981, Wolff et al. 1982), and some investigators recently have suggested that light absorption by elemental carbon plays an important role in the earth's radiation budget (Shaw and Stamnes 1980, Rosen et al. 1981, Patterson et al. 1982, Porch and MacCracken 1982, Cess 1983). Organic aerosol components present in vehicular emissions (Pierson et al. 1983) and in ambient samples (Pitts 1983) have been found to be mutagenic in the Ames test, and soots have been shown to be carcinogenic in animal studies (IARC Working Group 1980). As a result, there is considerable interest in the behavior of primary carbon particle concentrations in

the atmosphere, and in how those concentrations might be controlled.

Primary emissions of carbonaceous aerosols are not regulated separately from the remainder of the urban aerosol complex. Routine monitoring programs in the United States do not provide data on aerosol carbon concentrations in the atmosphere, and data on the emissions of carbonaceous aerosols are sparse. As a result, information sufficient to support engineering studies of methods for controlling fine carbon particle concentrations is lacking. This control strategy development problem is further complicated by the fact that several studies suggest that a large fraction of the organic aerosol is secondary in origin (i.e., formed in the atmosphere from the low vapor pressure products of reactions involving gaseous hydrocarbon precursors) (Grosjean and Friedlander 1975, Schuetzle et al. 1975, Cronn et al. 1977, Grosjean 1977, Appel et al. 1979). If the overwhelming majority of aerosol carbon was formed in the atmosphere as a secondary product of photochemical reactions, then controls on direct emissions of carbon particles from sources might have little effect on urban air quality.

The present chapter is the first of a series designed to describe methods for achieving deliberate control of urban fine carbon particle concentrations. In this work, the approach used to acquire an air quality model verification data set for organic and elemental carbon concentrations will be described. This method will be demonstrated in Los Angeles, and key characteristics of Los Angeles carbonaceous aerosol air quality will be defined. The spatial and

temporal distribution of aerosol carbon concentrations over an entire annual cycle will be described. The geographic areas that experience the highest aerosol carbon concentrations will be identified and related to source density and pollutant transport patterns. The ratio of total carbon to elemental carbon in the atmosphere will be examined as an indicator of the extent of secondary organic carbon aerosol formation. In subsequent chapters, air quality models will be tested against this data set. The importance of major source types to observed aerosol carbon air quality will be quantified through that modeling effort. Mathematical programming methods for defining the most attractive approaches to aerosol carbon control then will be illustrated, using the results of the air quality modeling study.

2.2 Experimental Design

Throughout the year 1982, a fine particle air monitoring network was operated in the Los Angeles area at the locations shown in Figure 2.1. The ten stations marked with solid circles in Figure 2.1 are located in the South Coast Air Basin within the ring of mountains that surrounds Los Angeles. Samples also were collected from March through December at a remote off-shore site, San Nicolas Island, in order to define pollutant concentrations in the marine environment upwind of Los Angeles. Twenty-four hour average fine particle filter

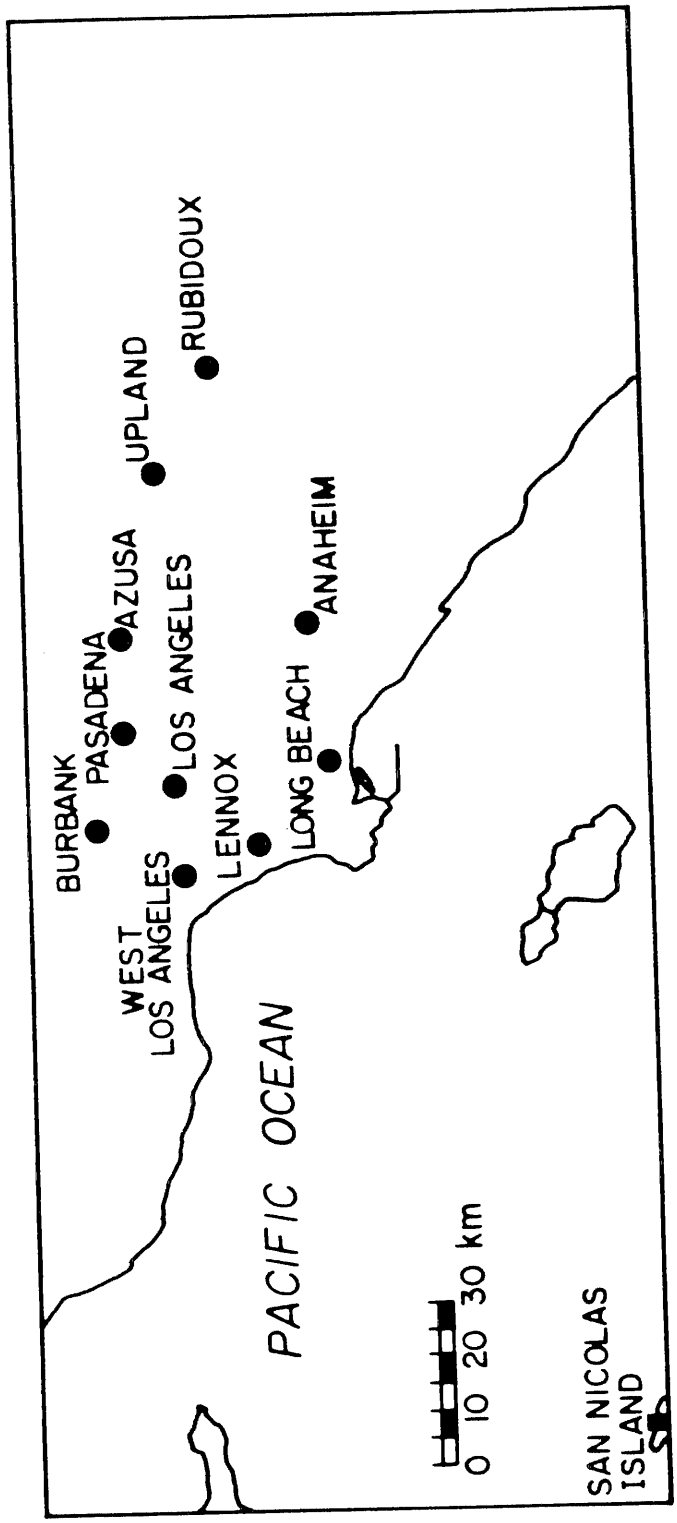

Figure 2.1 Fine particle air monitoring network.

samples were taken simultaneously throughout the network every sixth day during 1982 on a schedule coordinated with the National Air Surveillance Network (NASN) high volume sampling schedule.

The ambient sampling equipment constructed for use in this study is illustrated in Figure 2.2, and was designed to obtain a near mass balance on the chemically identifiable portion of the atmospheric fine particle loading. Ambient air at a flow rate of 25.9 lpm was drawn through an AIHL cyclone designed to remove particles with aerodynamic diameter larger than 2.1 μm (John and Reischl 1980). The air flow containing the fine particle fraction then was divided between four parallel filter assemblies. Each filter substrate was chosen for compatibility with a particular chemical or physical analysis procedure.

Samples taken for organic and elemental carbon determination were collected on 47 mm diameter quartz fiber filters (Pallflex Tissuquartz 2500 QAO) that had been heat treated to 600°C in air for more than 2 hours to lower their carbon blank. Filter samples were collected at a flow rate of 10 lpm, and all filters were refrigerated between collection and analysis to minimize losses due to volatilization and evaporation.

Organic and elemental carbon concentrations on these filters were measured by the method of Huntzicker et al. (1982) and Johnson et al. (1981). Four quartz fiber filter disks (0.25 cm^2 each) cut from a 47 mm filter are inserted into the combustion zone of a temperature programmed oven. Volatilization of organic carbon occurs

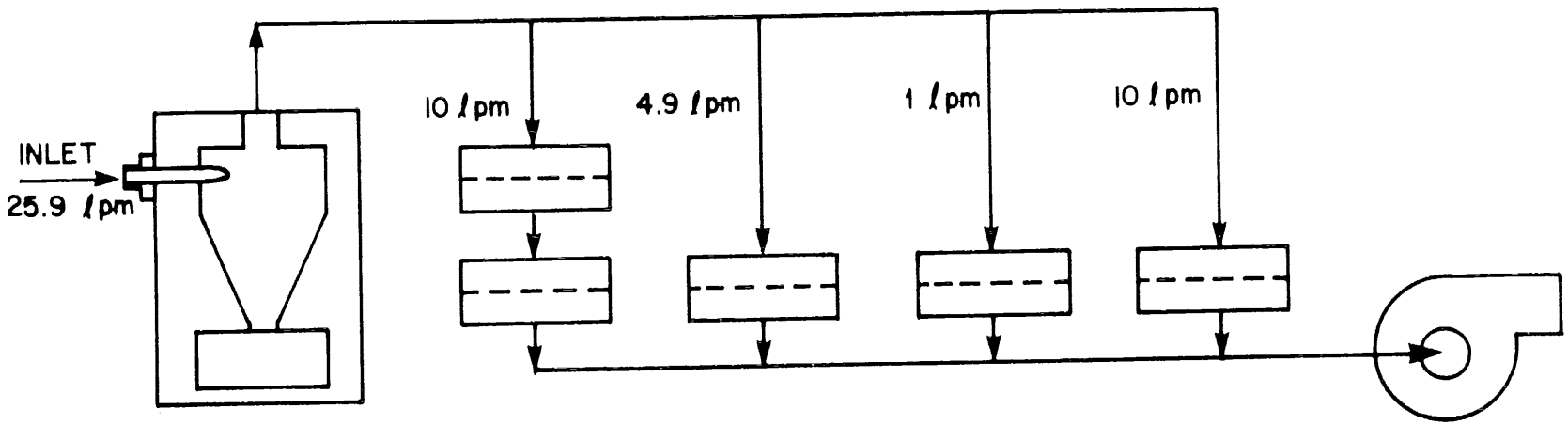

CYCLONE SEPARATOR

- REMOVE PARTICLES WITH $d_p > 2.1\ \mu m$

QUARTZ FIBER FILTERS

- ORGANIC CARBON
- ELEMENTAL CARBON

TEFLON FILTER

- MASS
- 34 TRACE METALS

NUCLEPORE FILTER

- $SO_4^{=}$
- NO_3^{-}
- NH_4^{+}
- b_{abs}

QUARTZ FIBER FILTER

- RESERVE FOR ORGANIC COMPOUND IDENTIFICATION

VACUUM PUMP

Figure 2.2 Ambient sampling protocol.

in two steps: at 400°C in flowing helium and at 600°C in flowing He. The volatilized carbon is oxidized to CO_2 over an MnO_2 catalyst at 1000°C, reduced to CH_4, and measured by a flame ionization detector. Elemental carbon is measured by combusting the residual carbon on the filter disks to CO_2 in an O_2(2%)-He(98%) mixture at 400°C, 500°C and at 750°C, followed by methanation and detection as described above. A calibration is performed at the end of each analysis by injecting a known amount of CH_4 into the oven and measuring the response. The reflectance of the filter sample is monitored continuously by a He-Ne laser during the volatilization and combustion process to detect any pyrolytic conversion of organic carbon to elemental carbon. Correction for pyrolytic conversion of organic carbon to elemental carbon is accomplished by measuring the amount of elemental carbon combustion required to return the filter reflectance to the value that it had prior to pyrolysis.

Replicate analysis of 53 filters taken from the present field experiment was used to determine the precision of the carbon analysis procedure. Analysis of variance showed the following analytical precisions (± 1 standard deviation): organic carbon (OC), ± 0.54 $\mu g\ m^{-3}$; elemental carbon (EC), ± 0.31 $\mu g\ m^{-3}$; total carbon (TC), ± 0.64 $\mu g\ m^{-3}$. The analytical precision of a single determination of the ratio of various carbon species concentrations was found to be (± 1 standard deviation): OC/TC, ± 0.025; OC/EC, ± 0.20; TC/EC, ± 0.20. The analytical accuracy of each single total carbon determination during this experimental program is estimated to

be ± 9.8% and includes the effects of uncertainties in carbon analyzer sample loop volume, calibration gas, area of the punches cut from each filter, temperature and pressure variations during analysis, filter surface area, and air volume sampled. The accuracy of total carbon measurements made by depositing known amounts of sucrose on filter disks and then analyzing the disks also was assessed. The average ratio of measured carbon to expected carbon was 1.01 ± 0.04 (95% confidence interval).

The filter intended for elemental and organic carbon aerosol collection was followed by a quartz fiber backup filter. This backup filter was included to permit assessment of the amount of organic carbon that can become attached to a clean filter due to adsorption of gas phase hydrocarbons or due to revaporization of organic material originally collected by the upstream aerosol filter. The extent of collection of aerosol and gas phase organics by aerosol sampling systems is dependent on the sample flow rate, temperature, and collection media used (Van Vaeck et al. 1979, Cadle et al. 1983, Appel et al. 1983, Grosjean 1983). Recent atmospheric sampling experiments conducted in Warren, Michigan, using dual filter units with quartz fiber filters showed that adsorption of organic compounds on backup filters as a result of sampling artifacts plus any contamination during handling accounted for at least 15% of the organic carbon collected on the upstream aerosol filter (Cadle et al. 1983). Analysis of three months of backup filters from the present set of Los Angeles area experiments showed that the backup filters adsorbed

organic carbon during sampling and handling equal to 17 ± 11% of the organic carbon found on the preceding aerosol filters, a value similar to results obtained during the Warren, Michigan, experiments (Cadle et al. 1983).

The second filter holder line shown in Figure 2.2 contained a 47 mm Teflon membrane filter (Membrana 0.5 μm pore size) operated at a flow rate of 4.9 lpm. Fine particulate matter collected on this filter was analyzed for the concentration of 34 trace elements by X-ray fluorescence. The Teflon filters were equilibrated at low relative humidity before and after sampling, then weighed repeatedly to obtain fine particle mass concentrations.

Samples collected on Nuclepore filters (47 mm diameter, 0.4 μm pore size) were intended for aerosol light absorption coefficient determination by the integrating plate technique (Lin et al. 1973). As a result, those filters must be lightly loaded, and a 1 lpm flow rate was chosen. A portion of each of these filters was analyzed for sulfates and nitrates by ion chromatography (Mueller et al. 1978), and for ammonium ion content by the phenolhypochlorite method (Solorzano 1967).

The remaining quartz fiber filter shown in Figure 2.2 was intended for determination of the detailed organic species present by gas chromatography/mass spectrometry. These filters were heat treated prior to use in the same manner as the other quartz fiber filters previously described in order to reduce their carbon blank. Results of the analysis of these filters will be reported elsewhere.

2.3 Fine Particle Concentration and Composition

Fine particle mass concentration during the year 1982 averaged between 23 $\mu g\ m^{-3}$ and 42 $\mu g\ m^{-3}$ within the metropolitan Los Angeles area, falling to 7 $\mu g\ m^{-3}$ at San Nicolas Island (SNI; see Figure 2.3a). Most of the fine particle air monitoring sites were co-located with a National Air Surveillance Network (NASN) or South Coast Air Quality Management District high volume sampler that operated on the same six-day schedule, and thus the average total suspended particulate matter concentration at these sites is known and is shown in Figure 2.3b. As a consistency check on the fine particle monitoring data, the fraction of the total aerosol mass found in particle sizes below 2.1 μm diameter was computed and found to constitute between 31% and 39% of the total particulate mass, as shown in Figure 2.3c. This result is in good agreement with South Coast Air Quality Management District special studies that show that 31% of TSP mass at El Monte in the Los Angeles area is present in particle sizes below 2.5 μm diameter (Witz 1982).

A mass balance was constructed at each air monitoring site by summing the chemically identified portions of the fine particulate matter samples. Trace metals were converted to their oxides, and organic carbon concentrations were multiplied by a factor of 1.2 (Countess et al. 1980) to convert them to an estimate of organic species concentration. Table 2.1 summarizes these results and shows that the material balance closed to within ± 10% of gravimetrically determined fine particle mass at all but one of the on-land monitoring

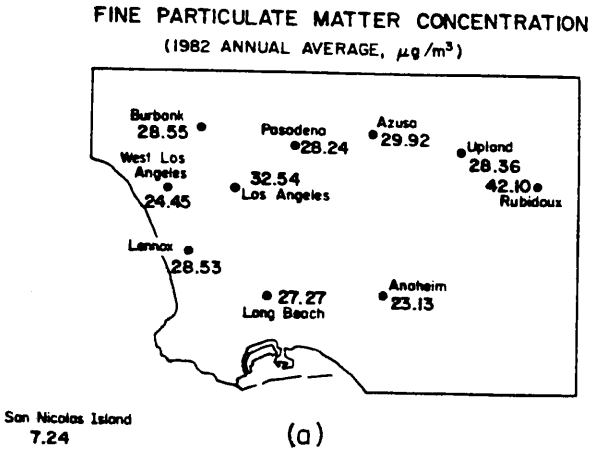

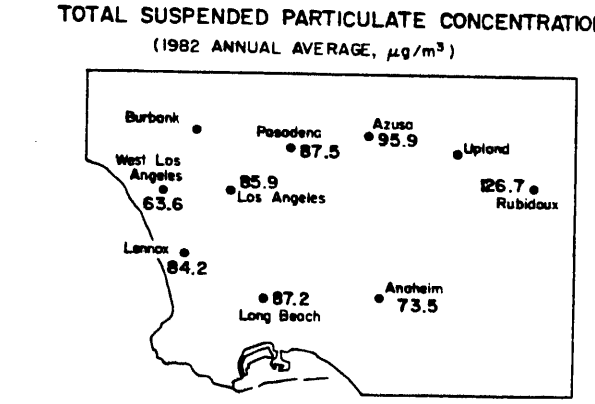

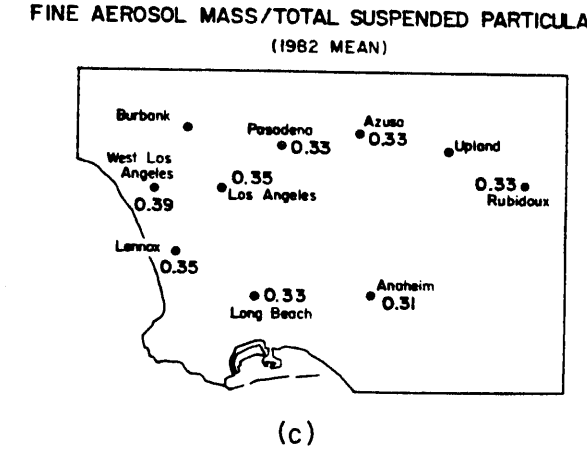

Figure 2.3 Comparison of fine particulate matter concentration to total suspended particulate matter concentration.

Table 2.1

Material Balance on the Chemical Composition of
Fine Particulate Matter Concentrations--Los Angeles Area
(1982 Annual Mean)

STATION	NUMBER OF SAMPLES (a)	FINE PARTICULATE MASS CONCENTRATION ($\mu g/m^3$) (b)	SUM OF IDENTIFIED CHEMICAL COMPONENTS ($\mu g/m^3$)	FRACTION IDENTIFIED (%)
Azusa	58	29.6	27.1	91.6
Burbank	58	28.6	30.0	105.6
Long Beach	58	27.5	25.9	94.2
Lennox	60	28.5	25.8	90.6
Pasadena	59	28.5	27.6	96.9
West Los Angeles	57	24.8	24.0	96.7
Los Angeles	60	32.7	30.4	92.8
Upland	55	27.7	25.4	91.5
Rubidoux	55	42.1	34.6	82.3
Anaheim	57	23.1	23.8	102.8
San Nicolas Island	43(c)	6.8	8.3	121.7

(a) Only those samples for which all scheduled chemical analyses are available. Averages thus differ slightly from those shown in Figure 2.3

(b) Determined gravimetrically.

(c) March-December 1982.

stations. Individual chemical species concentrations thus are consistent with a mass balance on the fine aerosol, and the major contributors to the fine aerosol loading have been identified.

Aerosol carbon species account for approximately 40% of the fine mass loading at most monitoring sites, as shown in Figure 2.4. At downtown Los Angeles, for example, the aerosol consists of 26.7% organics, 14.9% elemental carbon, 9.4% nitrate ion, 22.2% sulfate ion, 9.4% ammonium ion, 10.3% trace metal compounds, and 7.2% unidentified material (probably sea salt plus water retained on the filter despite desiccation). Results at the remaining stations are very similar except for Rubidoux and San Nicolas Island. The Rubidoux samples appear much lower in relative carbon content only because total fine particle mass concentration is higher there. This is due to addition of much more aerosol nitrate at Rubidoux than is found elsewhere, plus an added contribution from soil-like minerals when compared with other sites. The aerosol at San Nicolas Island is quite different from that found over the on-land portion of the air basin, being very low in elemental carbon content.

2.4 Characteristics of Elemental and Organic Carbon Concentrations

Fine total carbon concentrations are highest in heavily trafficked areas of the basin such as downtown Los Angeles and Burbank (see Figure 2.5a). Fine total carbon concentrations at those two sites averaged 12.2 and 13.7 $\mu g\ m^{-3}$, respectively, during 1982. Aerosol carbon concentrations decline with distance inland (the prevailing downwind direction), falling to 8.2 $\mu g\ m^{-3}$ for air masses

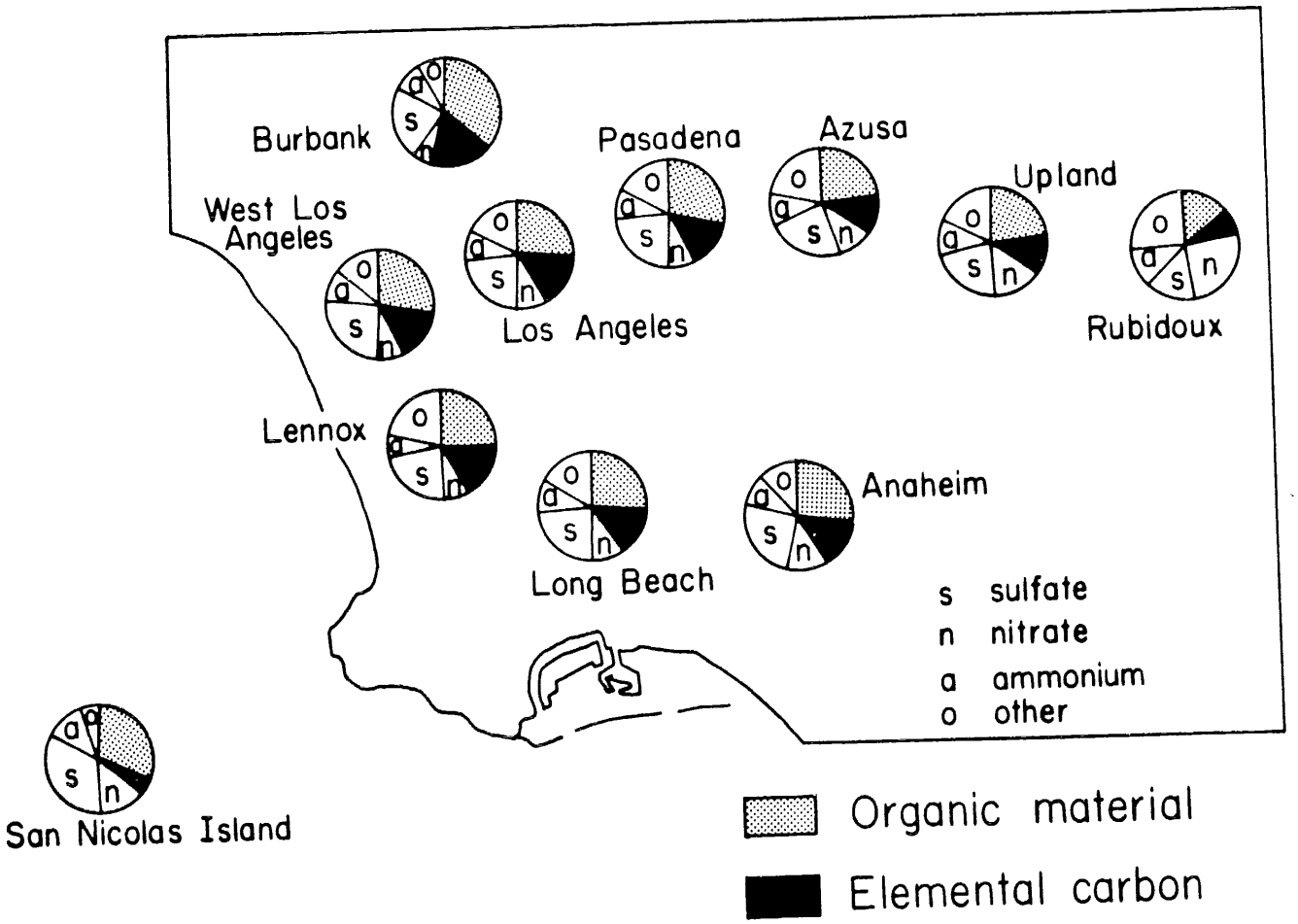

Figure 2.4 Material balance on the chemical composition of annual mean fine particle concentrations in the Los Angeles area--1982. Chart segments indicate the percentage contribution of each chemical species to the fine aerosol at each monitoring site.

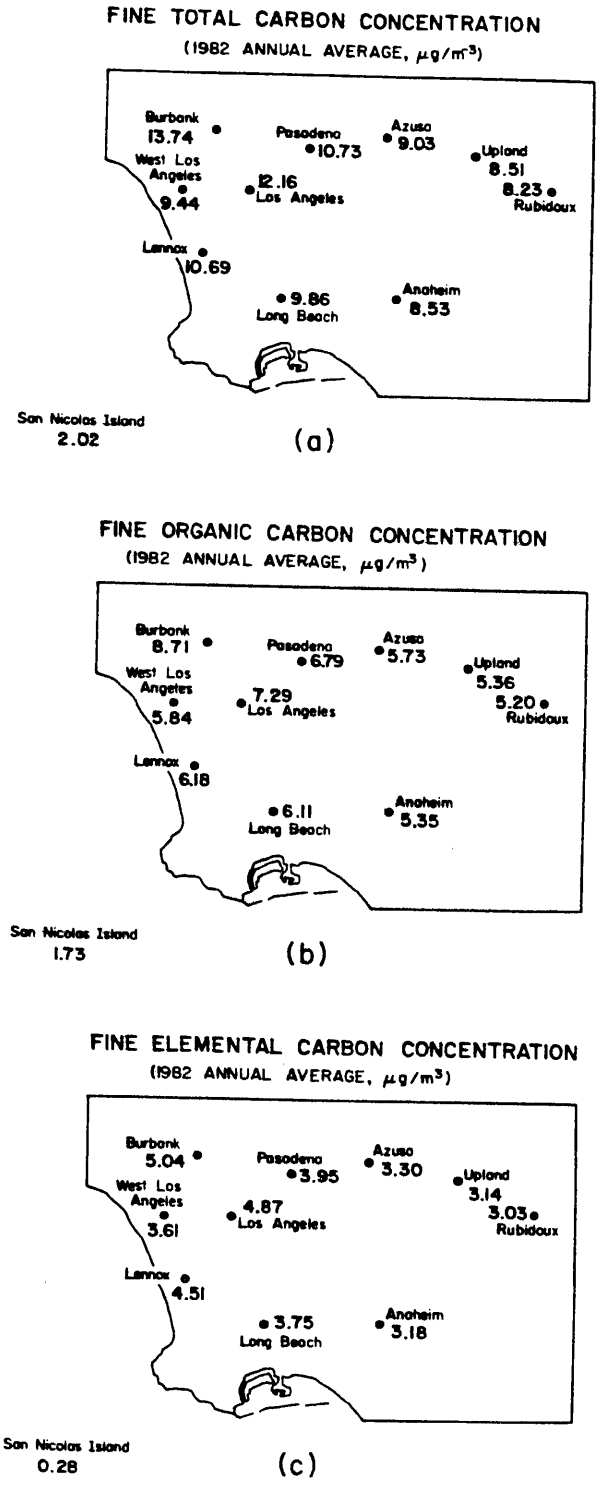

Figure 2.5 Fine carbonaceous particulate matter concentrations in the Los Angeles area.

TABLE 2.2

Statistical Description of Aerosol Carbon Data
Los Angeles Area - 1982

STATION	NUMBER OF CARBON SAMPLES	OC SAMPLE POPULATION		EC SAMPLE POPULATION		TC SAMPLE POPULATION		TC/EC POPULATION	
		Mean ($\mu g\ m^{-3}$)	Standard Deviation ($\mu g\ m^{-3}$)	Mean ($\mu g\ m^{-3}$)	Standard Deviation ($\mu g\ m^{-3}$)	Mean ($\mu g\ m^{-3}$)	Standard Deviation ($\mu g\ m^{-3}$)	Mean	Standard Deviation
Azusa	60	5.73	2.45	3.30	1.87	9.03	4.16	2.97	0.65
Burbank	58	8.71	4.50	5.04	3.20	13.74	7.56	2.89	0.46
Long Beach	59	6.11	4.65	3.75	3.00	9.86	7.57	2.77	0.46
Lennox	61	6.18	4.39	4.51	3.16	10.69	7.48	2.43	0.37
Pasadena	60	6.79	3.38	3.95	2.07	10.73	5.35	2.79	0.36
West Los Angeles	58	5.84	3.84	3.61	2.78	9.44	6.55	2.86	0.56
Los Angeles	61	7.29	4.30	4.87	3.24	12.16	7.44	2.59	0.35
Upland	56	5.36	1.99	3.14	1.34	8.51	3.07	2.83	0.63
Rubidoux	55	5.20	2.15	3.03	1.64	8.23	3.65	2.92	0.69
Anaheim	57	5.35	2.73	3.18	2.31	8.53	4.91	2.88	0.53
San Nicolas Is.	46	1.73	0.93	0.28	0.22	2.02	1.12	*	*

* Not computed because EC concentration approaches zero on a number of occasions.

passing Rubidoux in the Riverside area. A similar pattern is observed for both organic carbon (Figure 2.5b) and elemental carbon concentrations (Figure 2.5c). Note in Figure 2.5c that the elemental carbon concentration in marine air at San Nicolas Island is very low, about 0.3 $\mu g\ m^{-3}$ on the average. A statistical description of the aerosol carbon data set is provided in Table 2.2.

Aerosol carbon data at individual monitoring sites can be viewed on a seasonal basis. Figure 2.6a shows the time series of individual 24-hour average organic carbon samples at Lennox, a near-coastal site adjacent to a busy freeway. In Figure 2.6b, the time series of organic carbon concentrations has been smoothed by computing monthly average values. It is seen that the highest organic carbon values are observed in winter months, falling to a minimum in the summer. The same behavior is observed for elemental carbon at that site, as seen in Figures 2.6c and 2.6d. This pattern with high winter values and low summer concentrations is typical of primary automotive pollutants like CO and lead at that location (Hoggan et al. 1980).

Moving in the prevailing downwind direction from Lennox to downtown Los Angeles, a similar pattern of high winter values and a summer minimum in aerosol carbon levels is observed in 1982 (Figure 2.7ab). At Pasadena, a June minimum in fine carbon concentrations still is observed on average, but individual days during the late summer show total fine carbon concentrations that are as high as the winter values (Figure 2.7cd). Proceeding further downwind to Upland (Figure 2.7ef) and Rubidoux (Figure 2.7gh), the

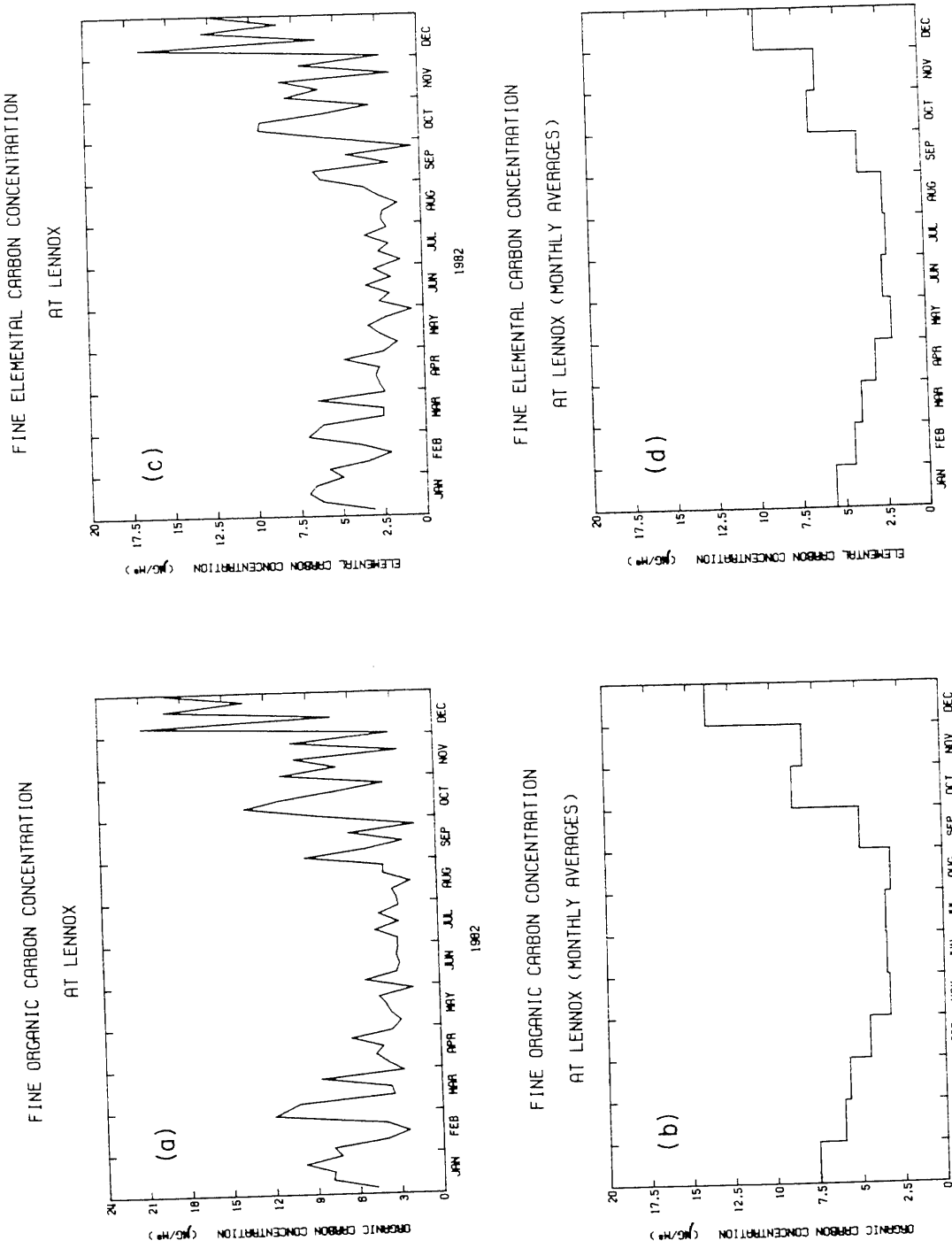

Figure 2.6 Daily and monthly average carbonaceous aerosol concentrations at Lennox, CA.

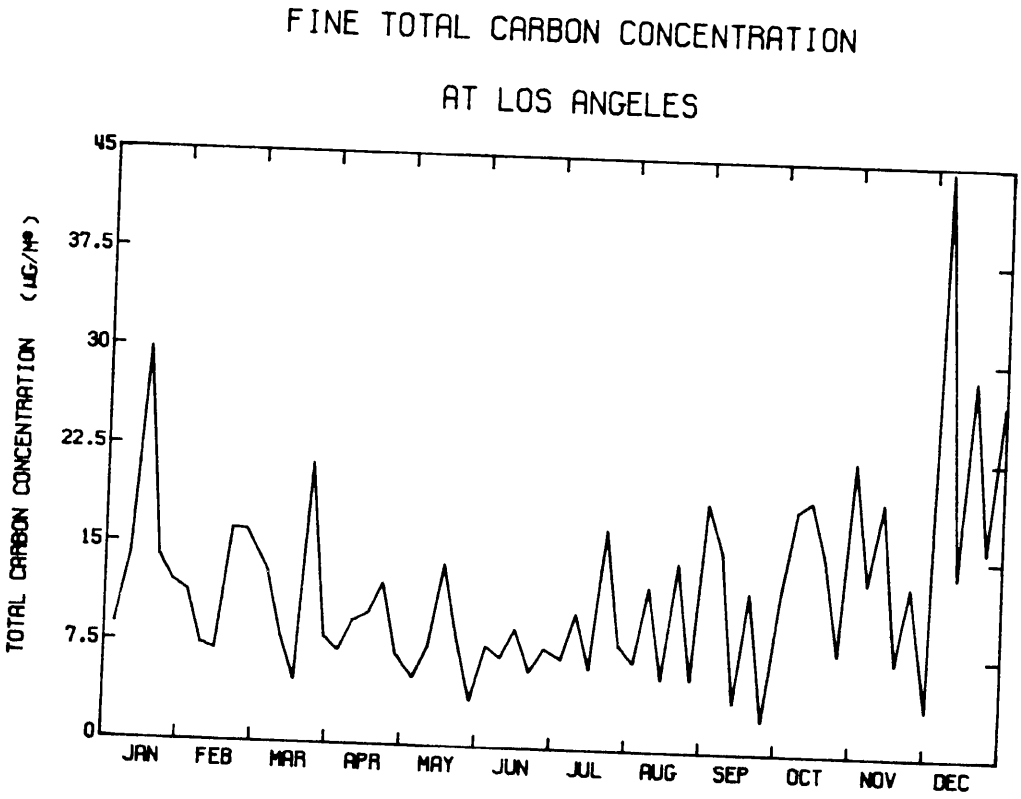

Figure 2.7a

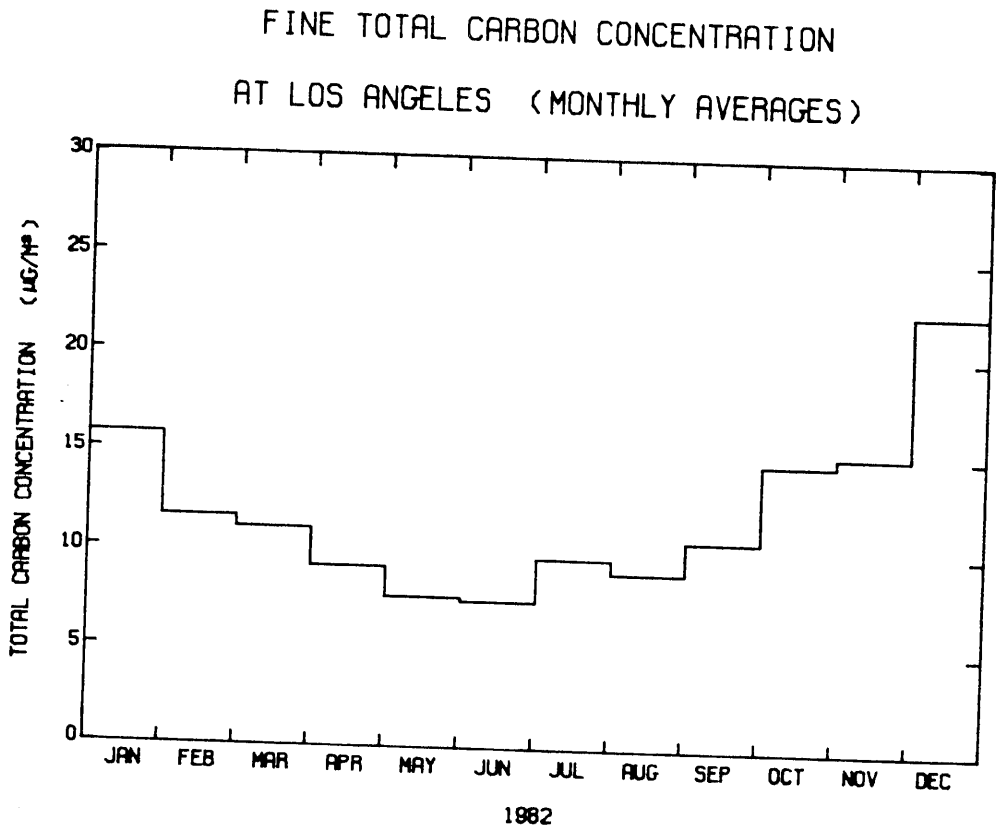

Figure 2.7b

FINE TOTAL CARBON CONCENTRATION

AT PASADENA

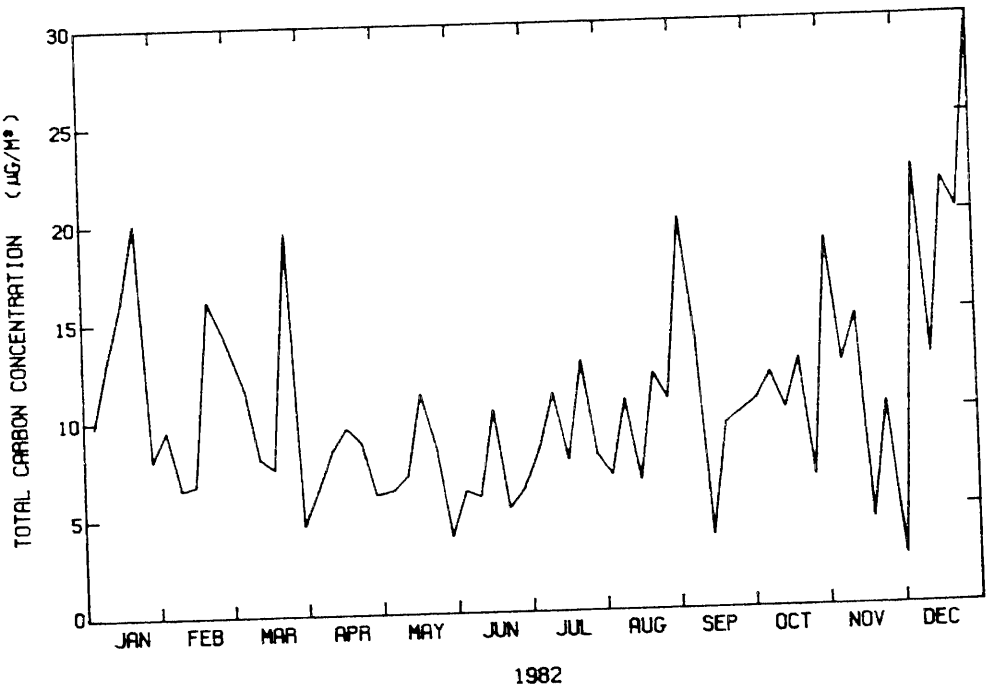

Figure 2.7c

FINE TOTAL CARBON CONCENTRATION

AT PASADENA (MONTHLY AVERAGES)

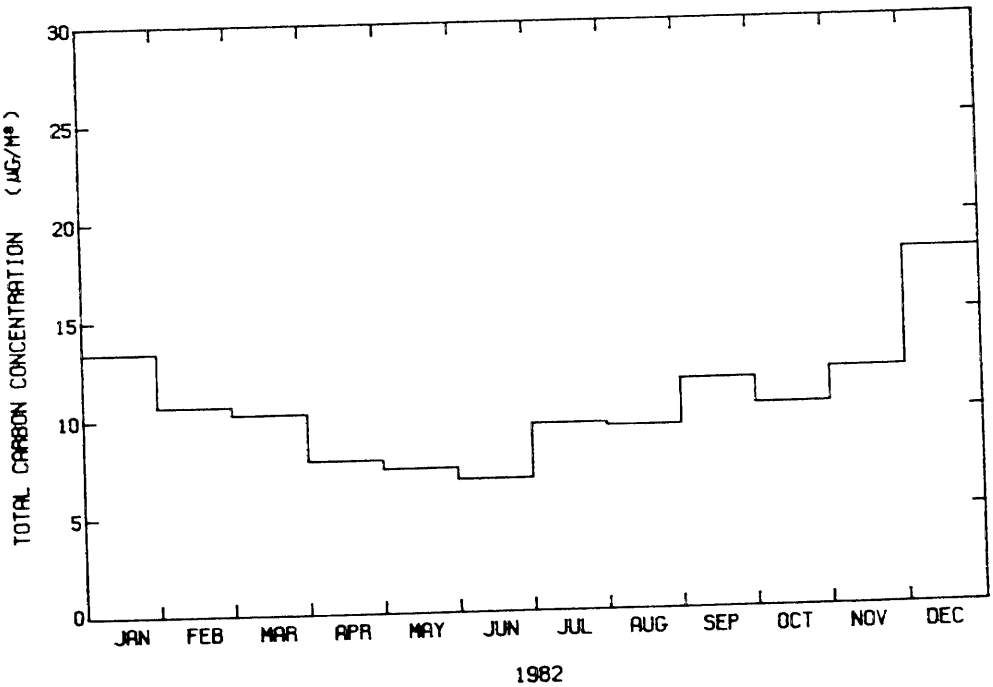

Figure 2.7d

FINE TOTAL CARBON CONCENTRATION

AT UPLAND

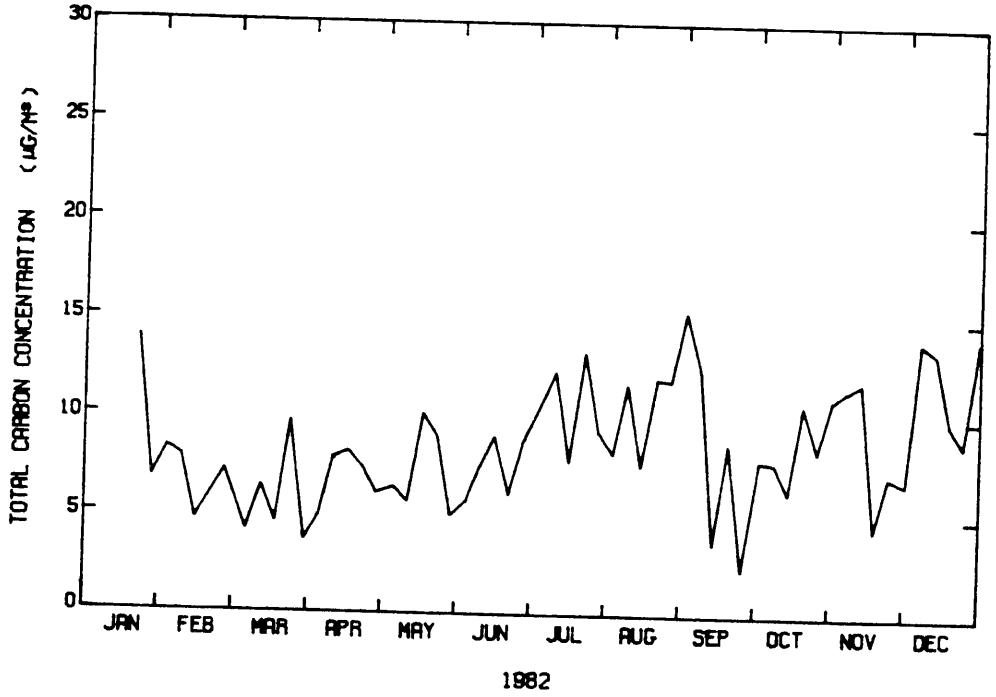

Figure 2.7e

FINE TOTAL CARBON CONCENTRATION

AT UPLAND (MONTHLY AVERAGES)

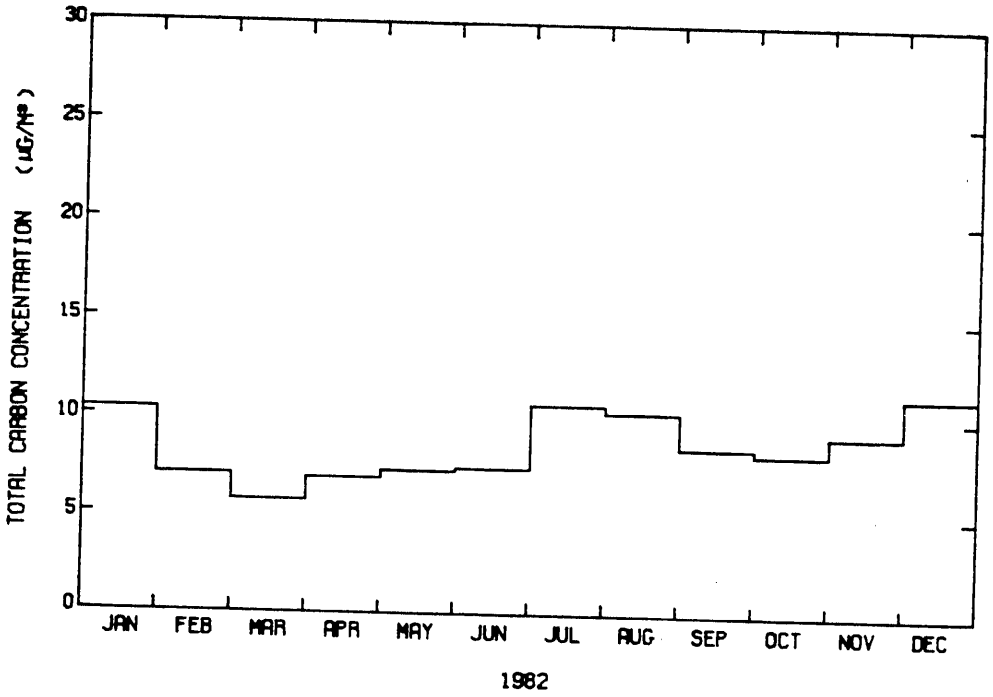

Figure 2.7f

FINE TOTAL CARBON CONCENTRATION

AT RUBIDOUX

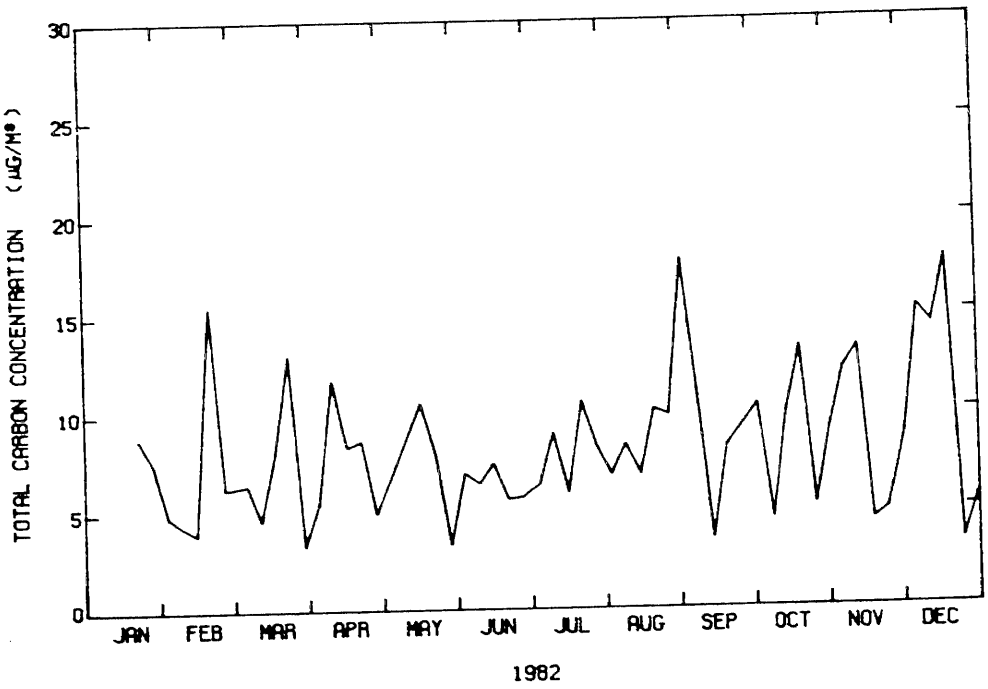

Figure 2.7g

FINE TOTAL CARBON CONCENTRATION

AT RUBIDOUX (MONTHLY AVERAGES)

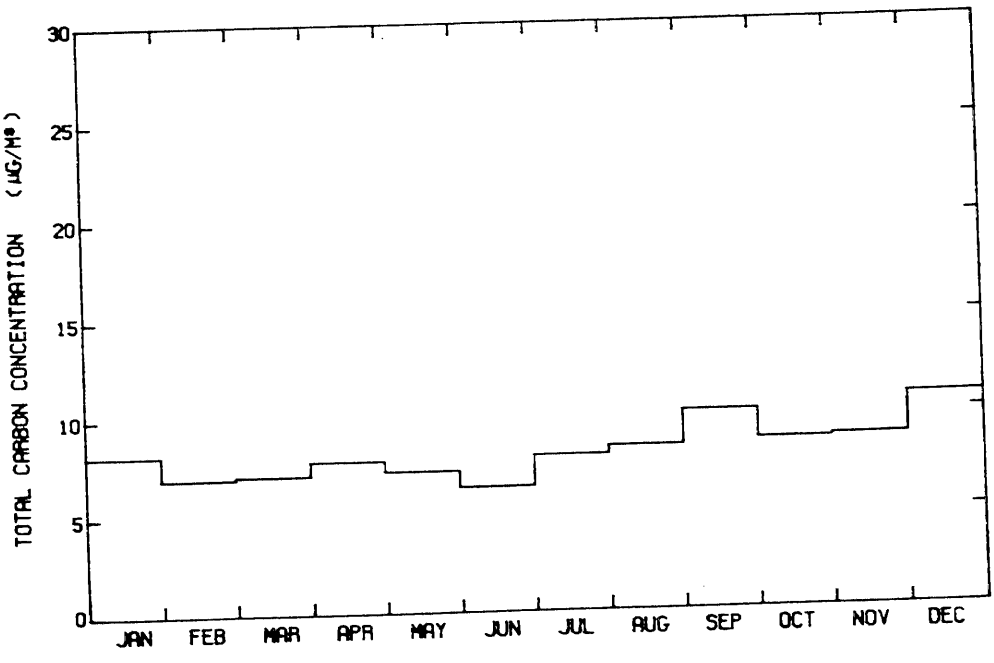

Figure 2.7h

FINE TOTAL CARBON CONCENTRATION

AT LENNOX

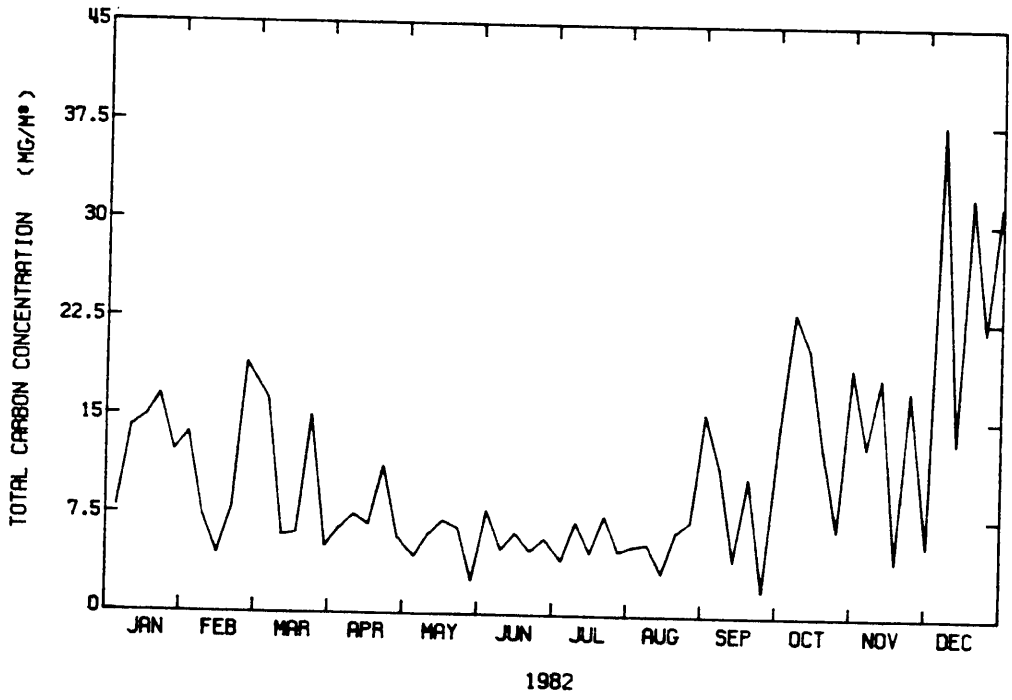

Figure 2.7i

FINE TOTAL CARBON CONCENTRATION

AT LENNOX (MONTHLY AVERAGES)

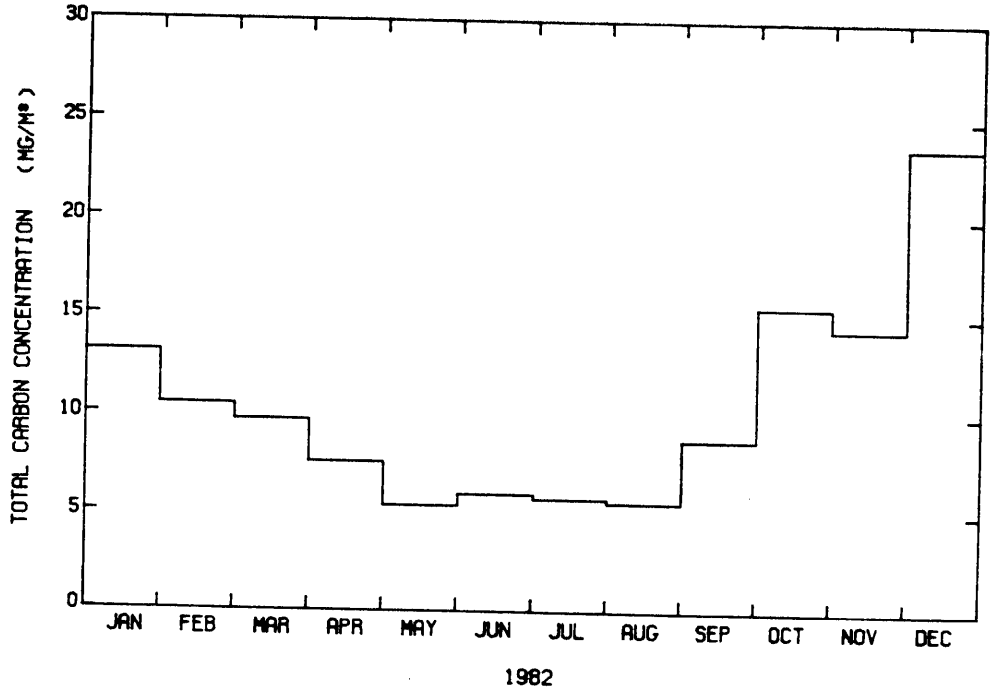

Figure 2.7j

FINE TOTAL CARBON CONCENTRATION

AT LONG BEACH

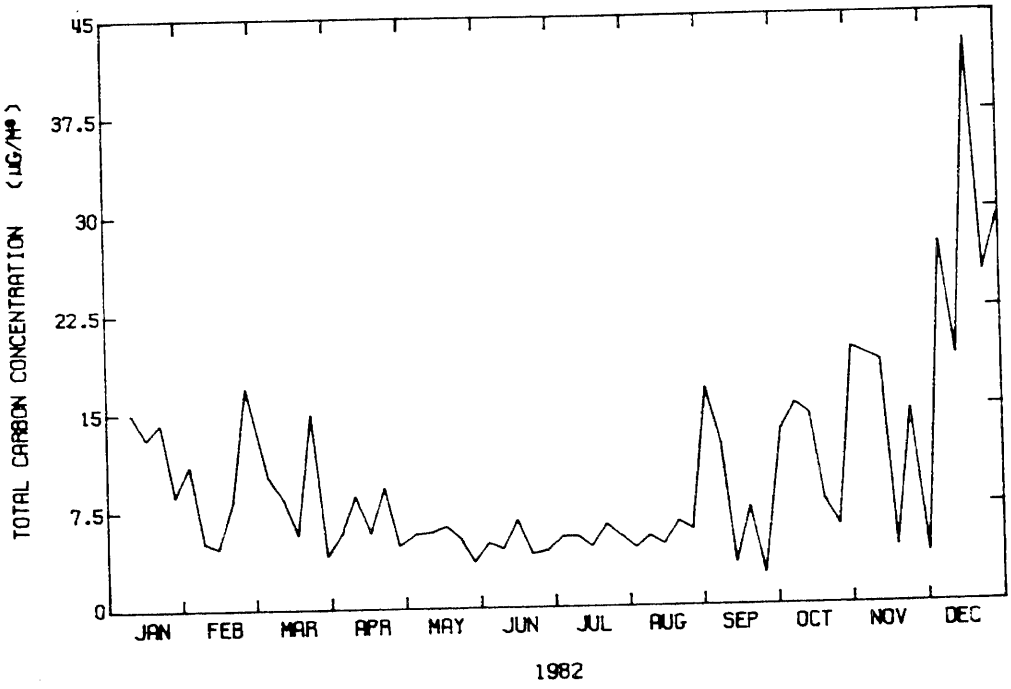

Figure 2.7k

FINE TOTAL CARBON CONCENTRATION

AT LONG BEACH (MONTHLY AVERAGES)

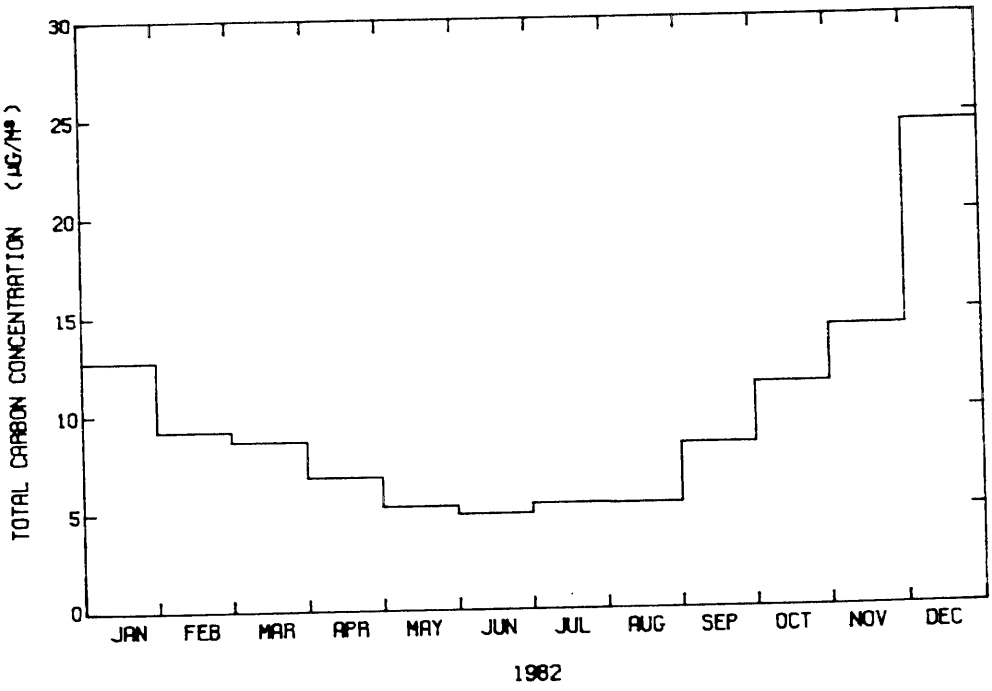

Figure 2.71

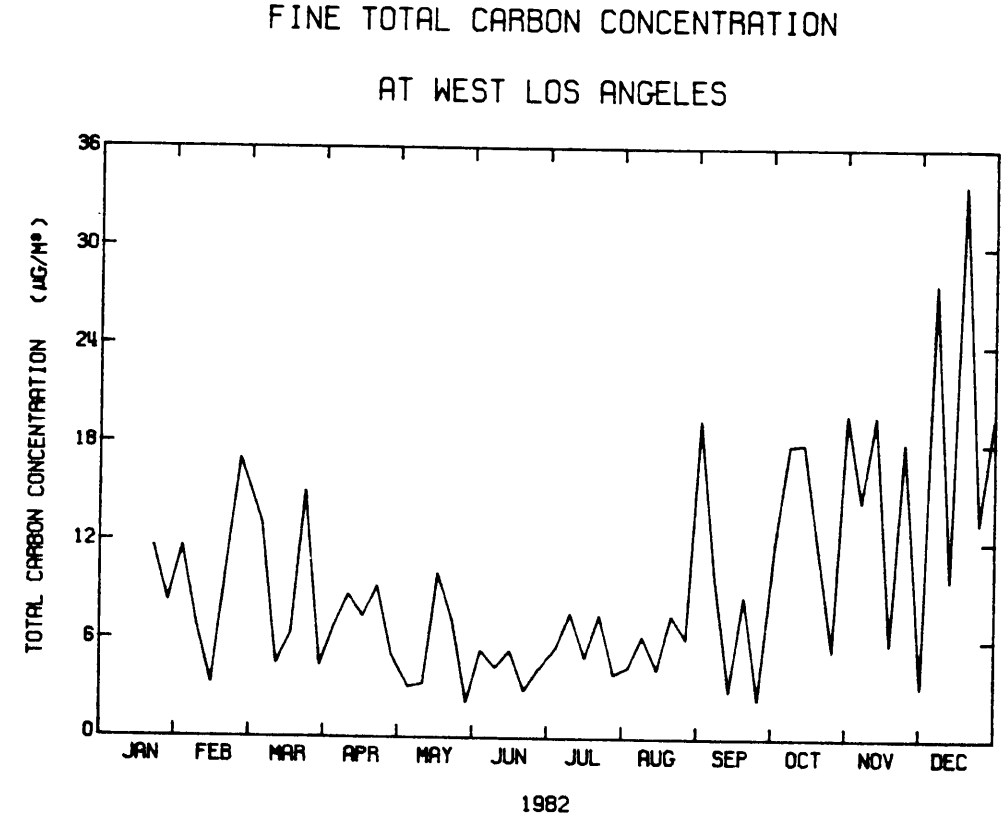

Figure 2.7m

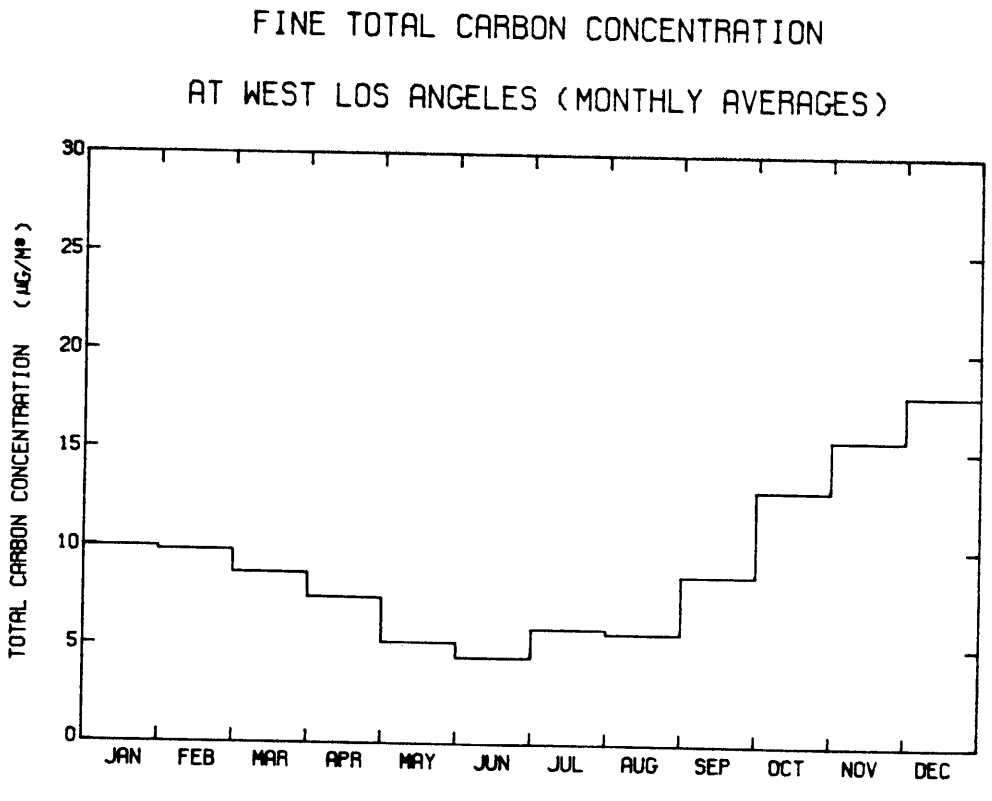

Figure 2.7n

FINE TOTAL CARBON CONCENTRATION

AT ANAHEIM

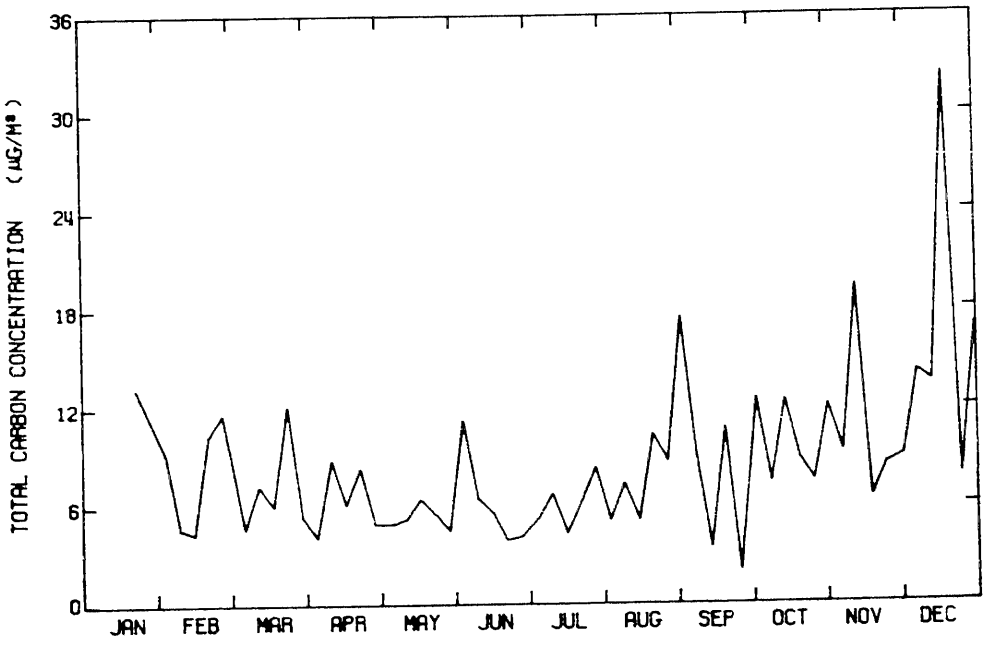

Figure 2.7o

FINE TOTAL CARBON CONCENTRATION

AT ANAHEIM (MONTHLY AVERAGES)

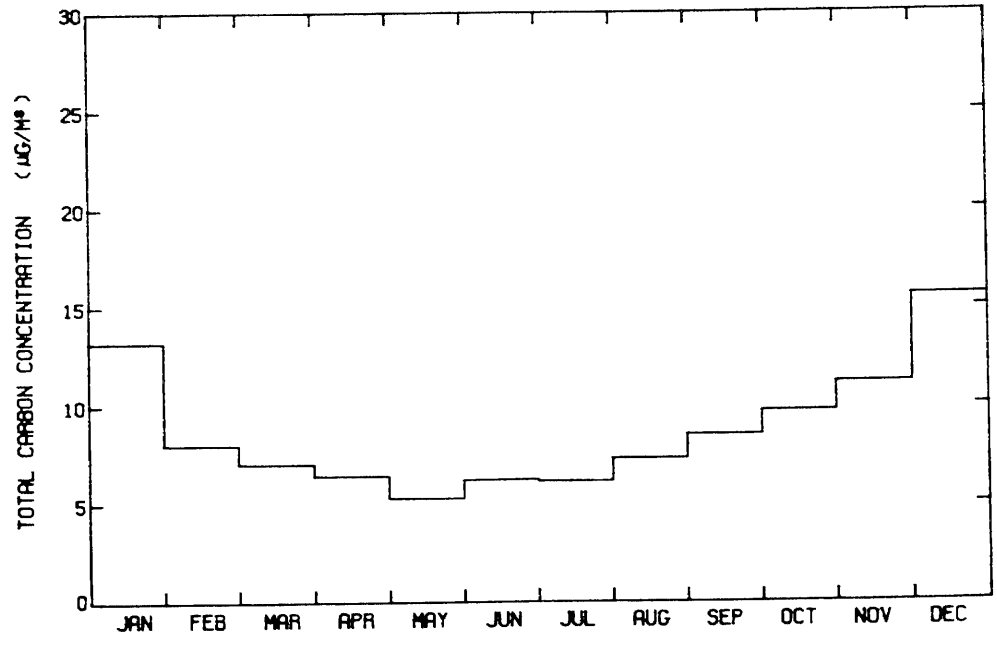

Figure 2.7p

FINE TOTAL CARBON CONCENTRATION

AT AZUSA

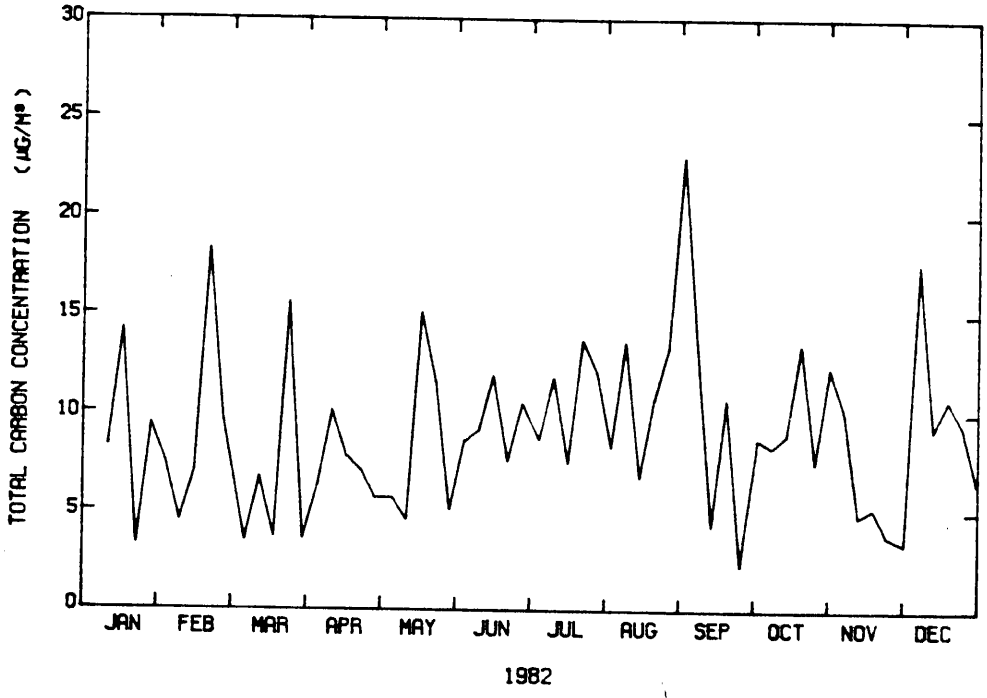

Figure 2.7q

FINE TOTAL CARBON CONCENTRATION

AT AZUSA (MONTHLY AVERAGES)

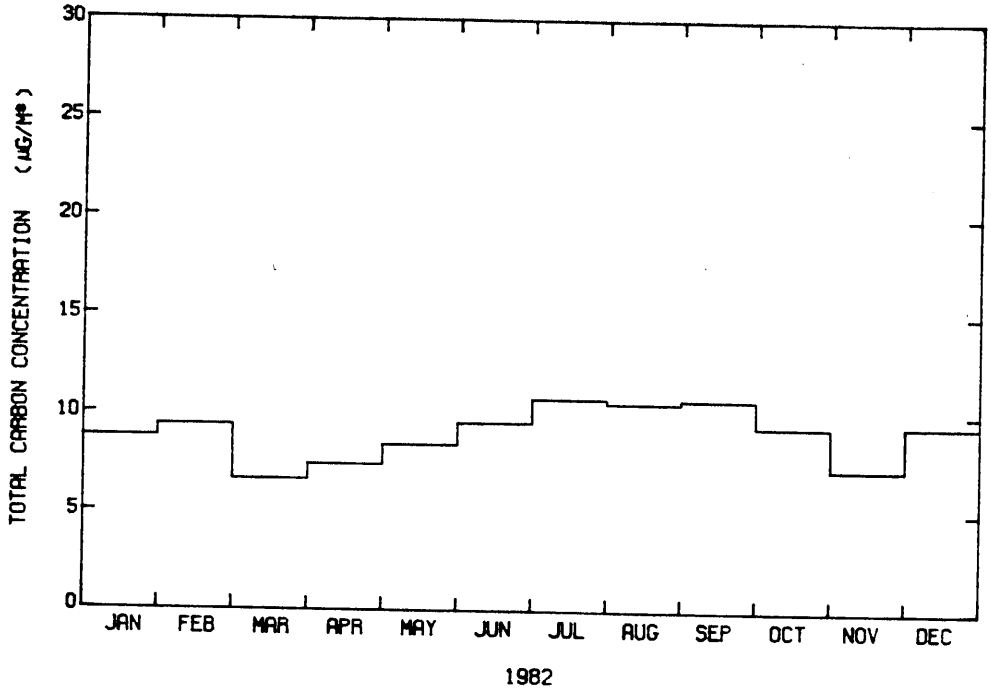

Figure 2.7r

FINE TOTAL CARBON CONCENTRATION

AT BURBANK

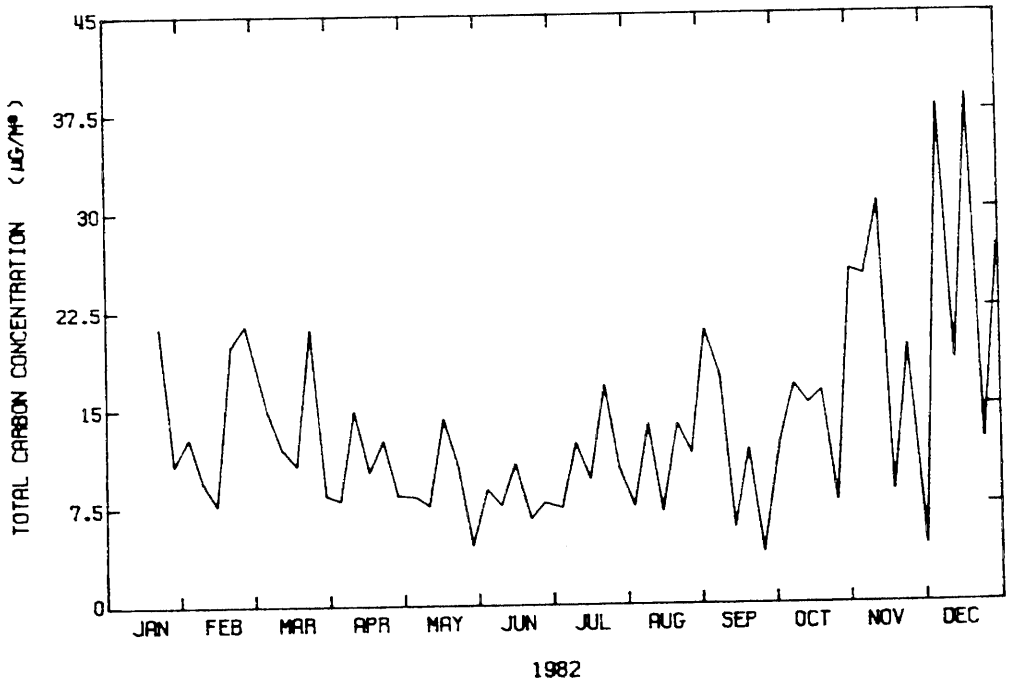

Figure 2.7s

FINE TOTAL CARBON CONCENTRATION

AT BURBANK (MONTHLY AVERAGES)

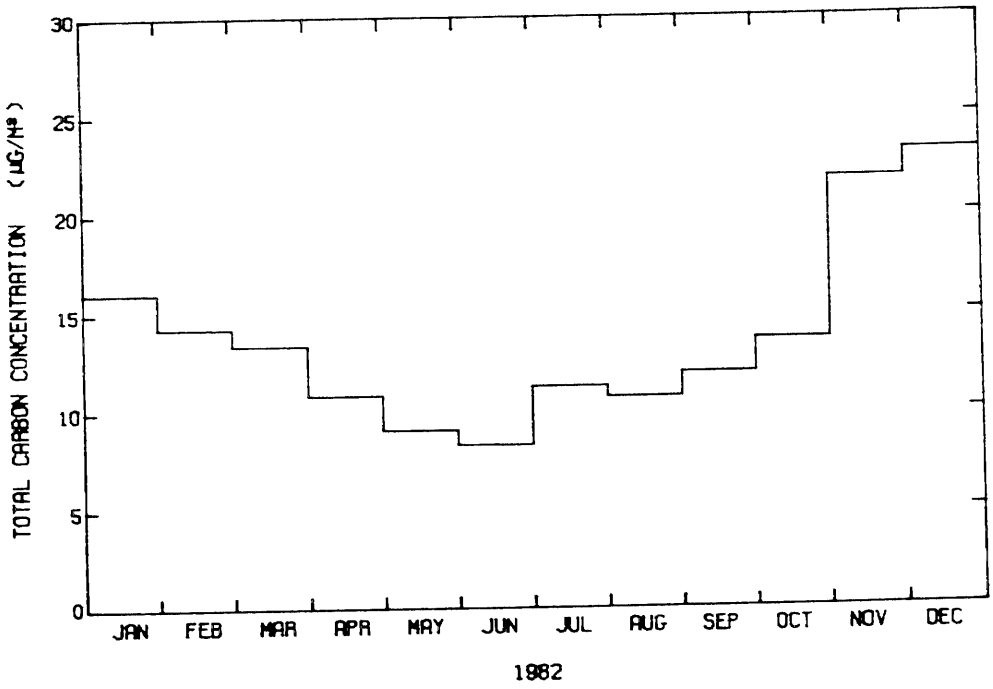

Figure 2.7t

FINE TOTAL CARBON CONCENTRATION

AT SAN NICOLAS ISLAND

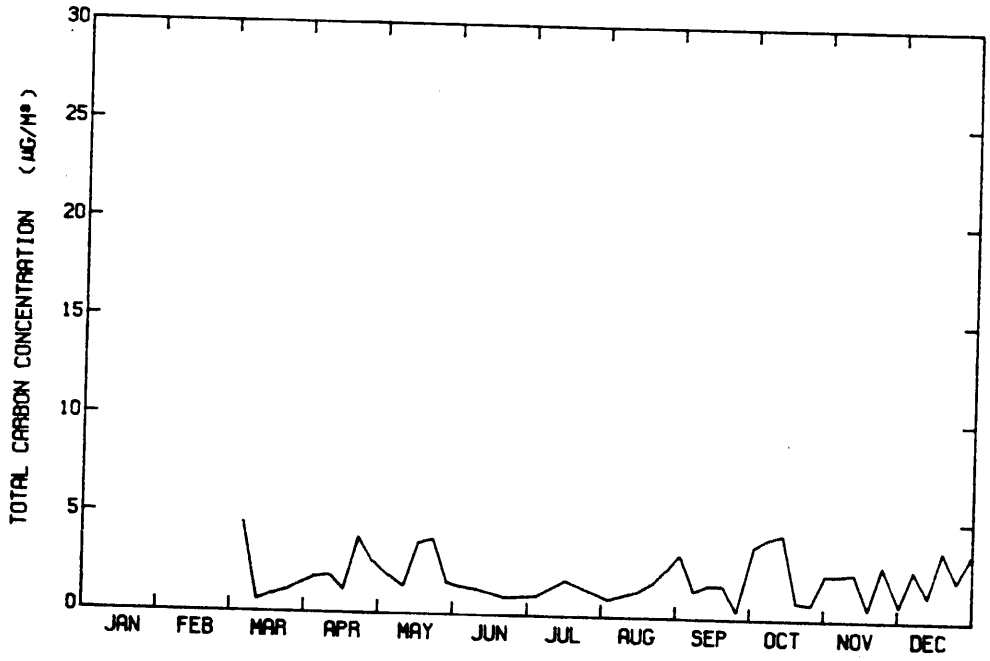

1982

Figure 2.7u

FINE TOTAL CARBON CONCENTRATION

AT SAN NICOLAS ISLAND (MONTHLY AVERAGES)

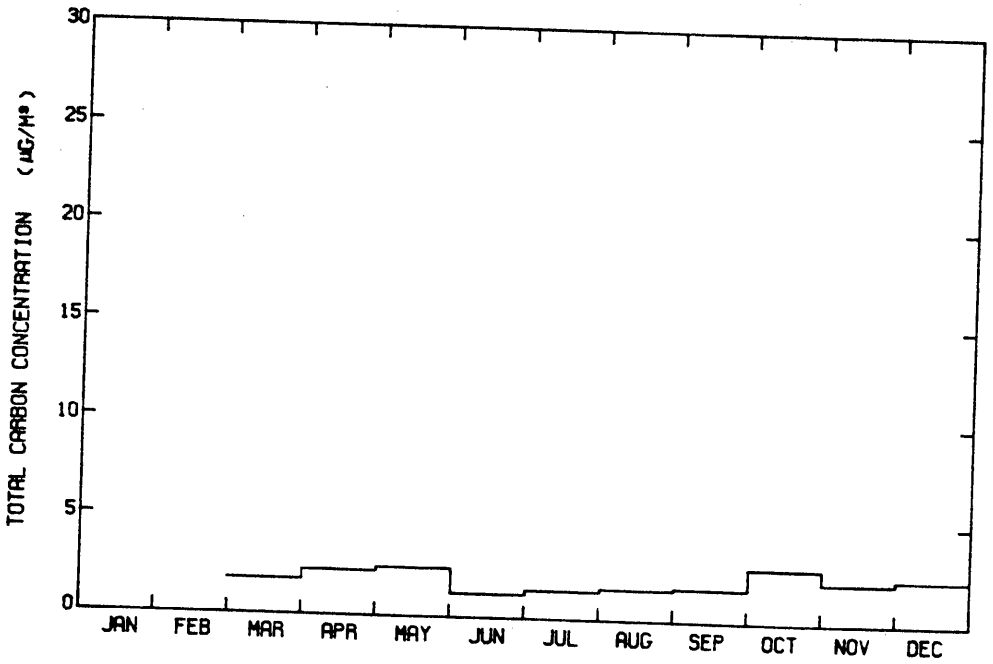

1982

Figure 2.7v

pronounced summer minimum in fine aerosol carbon levels is absent; there even may be a relative peak in aerosol carbon concentrations in the summer at Upland. Total carbon concentration data at the remaining monitoring sites are given in Figures 2.7i through 2.7v.

2.5 Comparison to Emission Data

An inventory of organic and elemental carbon particle emissions to the Los Angeles area atmosphere was developed for the year 1980 by Cass et al. (1982) and is summarized in Figure 2.8. Aerosol carbon emissions in particle sizes less than 10 μm were estimated to total about 46 tons per day. One quarter of that total came from gasoline powered vehicle exhaust, one fourth from diesel engine exhaust, and the remainder from a large variety of stationary fuel burning, industrial and fugitive sources. In contrast, the black elemental carbon particle emissions were dominated by diesel exhaust aerosol. The ratio of total carbon to elemental carbon in primary aerosol emissions was estimated to be about 3.2:1 averaged over all sources in the area in 1980. A weighted average highway traffic emission profile of gasoline fueled vehicle exhaust, diesel exhaust, tire dust and brake dust likewise indicated a total carbon to elemental carbon ratio of about 3.2:1. These total carbon to elemental carbon ratios obtained from the 1980 emissions survey may be slightly higher than would be obtained from a 1982 emission inventory for Los Angeles. One reason for this is that the relatively high organic carbon emissions from old non-catalyst automobiles are declining over time as catalyst-

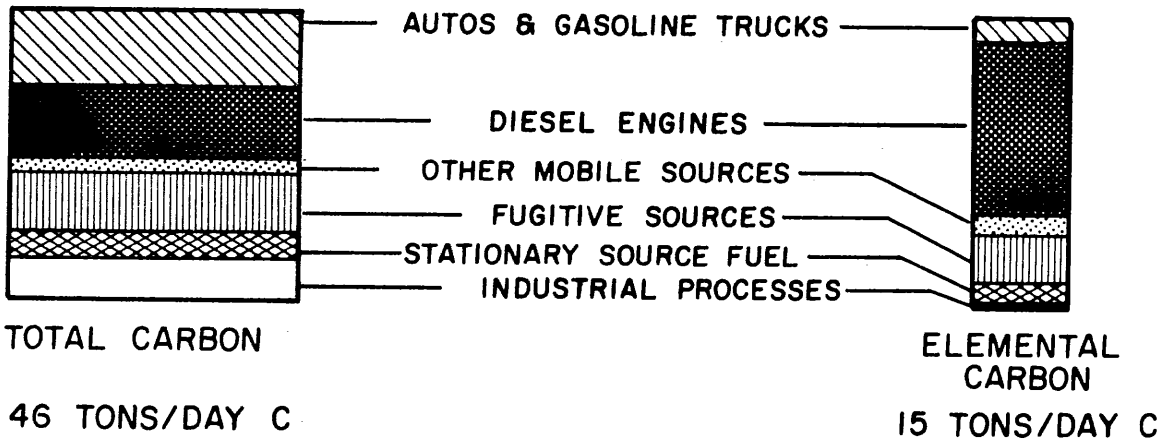

Figure 2.8 Aerosol carbon emissions in the greater Los Angeles area in particle sizes $\leq$ 10 μm diameter, winter 1980 (from Cass, Boone, and Macias 1982).

equipped new cars take their place in the vehicle fleet.

The ratio of total carbon to elemental carbon in source emissions when compared to the same ratio in atmospheric samples should be useful in detecting the presence of any large enrichment in organic aerosol in the atmosphere due to secondary aerosol formation. Fine elemental carbon aerosol is formed during combustion processes. This atmospheric elemental carbon is non-volatile, inert and is not formed in the atmosphere by reactions involving gaseous hydrocarbon precursors. Therefore, the entire concentration of elemental carbon observed in the atmosphere is from primary emission sources. Organic carbon may be emitted as primary aerosol directly from sources, but secondary organics also can be formed in the atmosphere from the low vapor pressure products of atmospheric chemical reactions (Grosjean 1977). If a large fraction of the atmospheric fine carbon particle burden in the Los Angeles area is contributed by secondary organics, three features might be expected. First, the ratio of total carbon to elemental carbon in atmospheric aerosol samples should exceed that found in primary source emissions. Second, a higher ratio of total carbon to elemental carbon might be expected during the summer peak photochemical smog season. Third, the ratio of total carbon to elemental carbon might be expected to increase as one moves inland from the coast to the San Fernando, San Gabriel and San Bernardino Valleys along the prevailing downwind transport direction, in a manner similar to other secondary photochemical pollutants, like ozone.

The atmospheric fine carbon particle data were examined to note

whether or not these likely indicators of high secondary aerosol levels were present during the year 1982. The discussion will begin at the upwind edge of the air basin near Lennox. Fine elemental and organic carbon concentrations at Lennox are shown in Figure 2.6ac. Elemental and organic aerosol concentrations are highly correlated. The daily ratio of total carbon (TC) to elemental carbon (EC) at Lennox is shown in Figure 2.9a. These values are contained entirely within the range 4.0:1 to 1.8:1. In Figure 2.9b, the daily values of the TC to EC ratio are averaged over each month of the year 1982. It is seen that there is very little seasonal variation, with an annual average value of the daily TC to EC ratio of 2.4:1. An alternative statistic, the ratio of annual average TC to annual average EC, can be computed from Figures 2.5ac, with similar results. When compared to 1980 estimates of the TC to EC ratio in primary source emissions (see Figure 2.8), the Lennox aerosol is not highly enriched in organic carbon relative to elemental carbon. This suggests that the carbonaceous aerosol at Lennox is dominated by primary source emissions on the average over long periods of time. This is not surprising since the Lennox site is located only about 100 m from a very large freeway, and shows the highest annual mean lead levels in the Los Angeles area (Davidson et al. 1979) (again an indicator of direct vehicle exhaust influence).

The situation at downtown Los Angeles is quite similar to that at Lennox (Figure 2.9cd). Peak TC to EC ratios of 4:1, little seasonal dependence, and an annual average value of the daily TC to EC

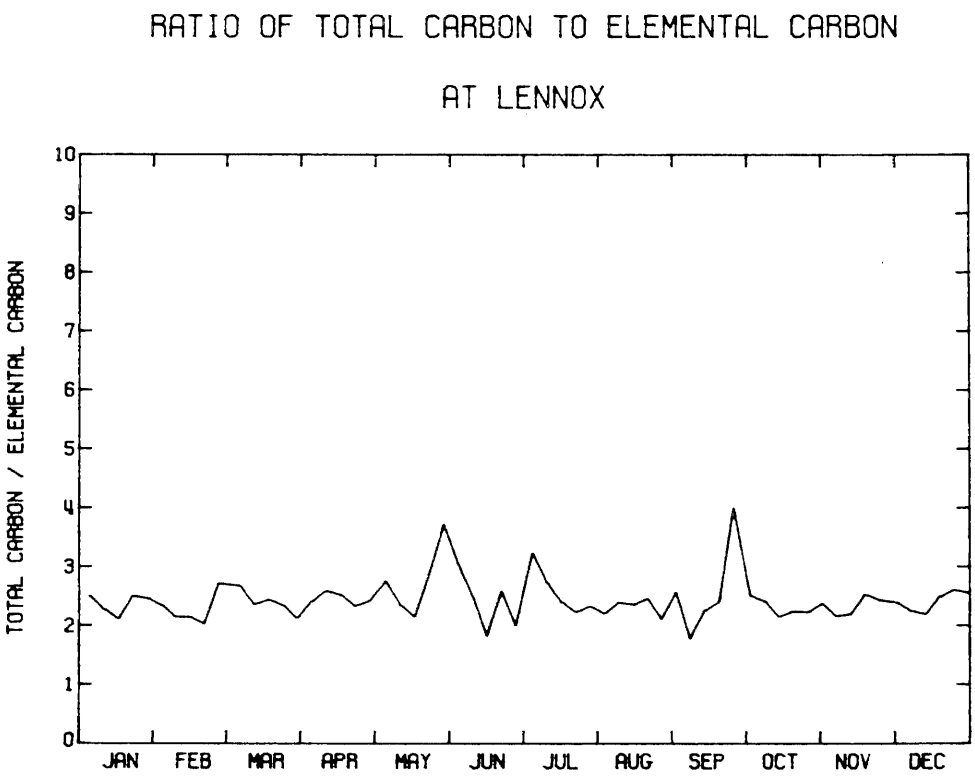

Figure 2.9a

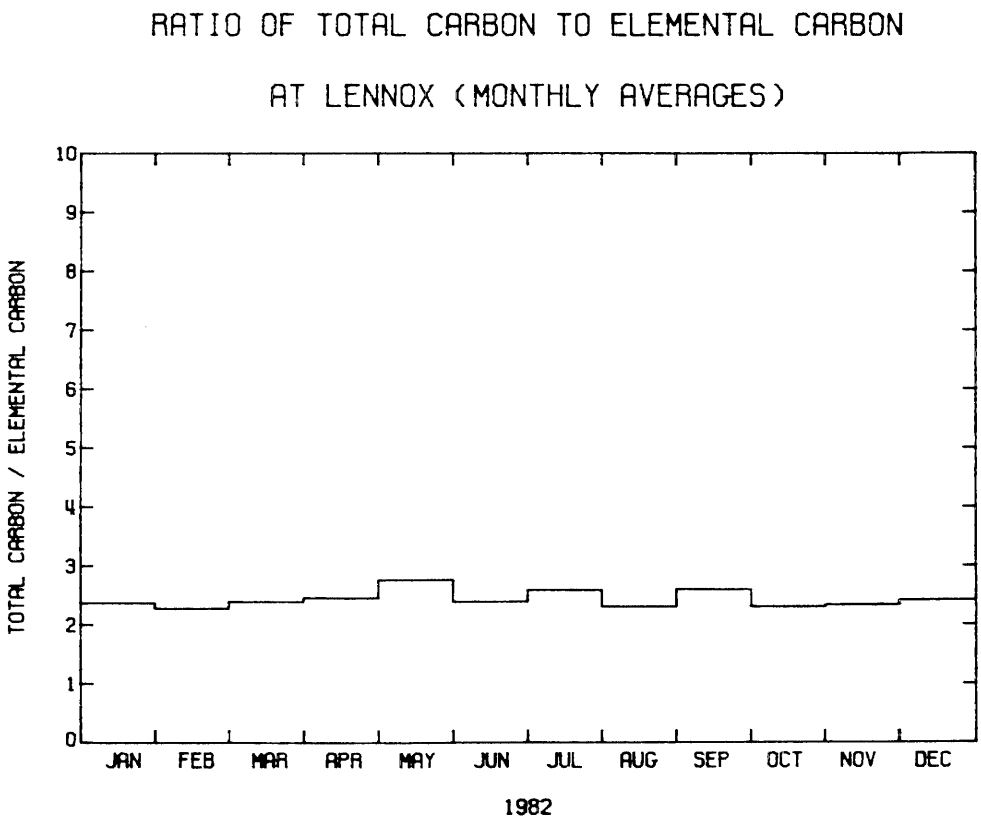

Figure 2.9b

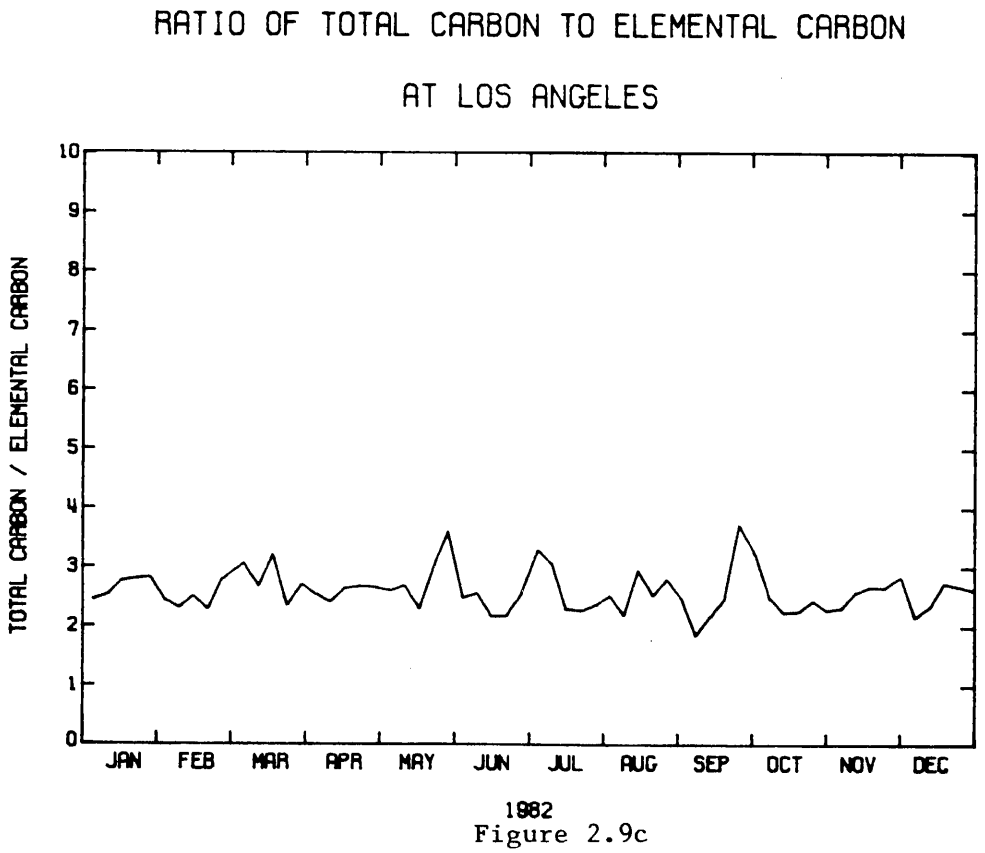

Figure 2.9c

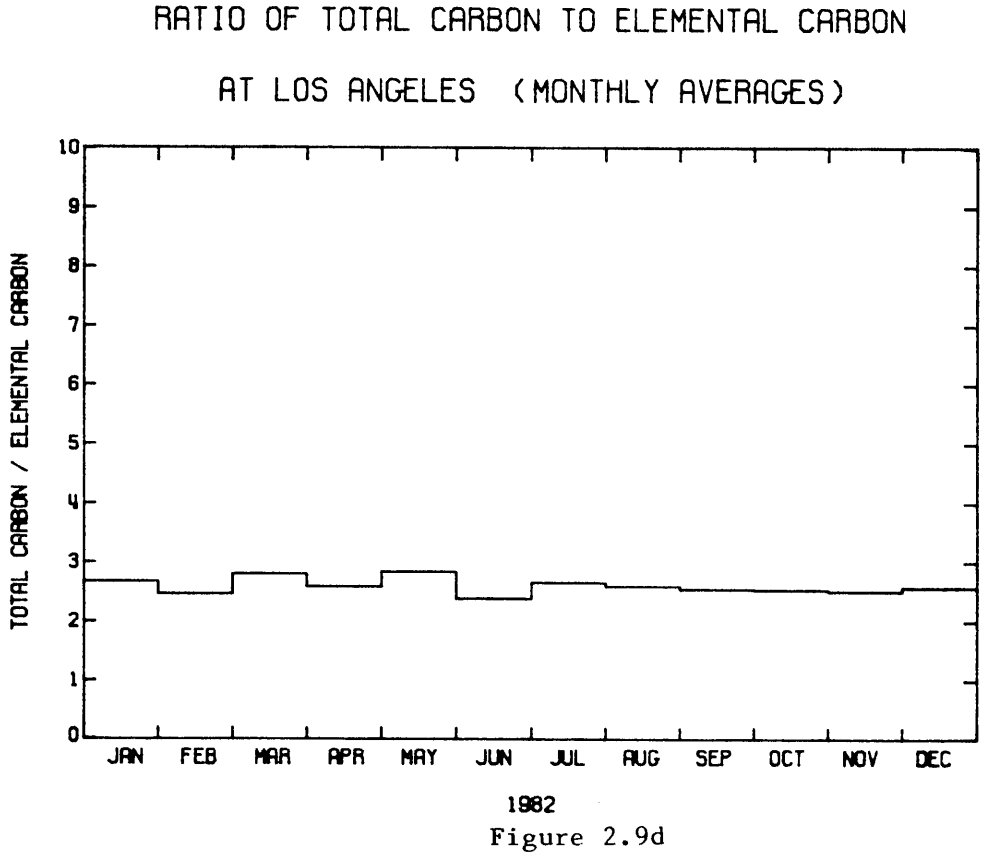

Figure 2.9d

RATIO OF TOTAL CARBON TO ELEMENTAL CARBON

AT PASADENA

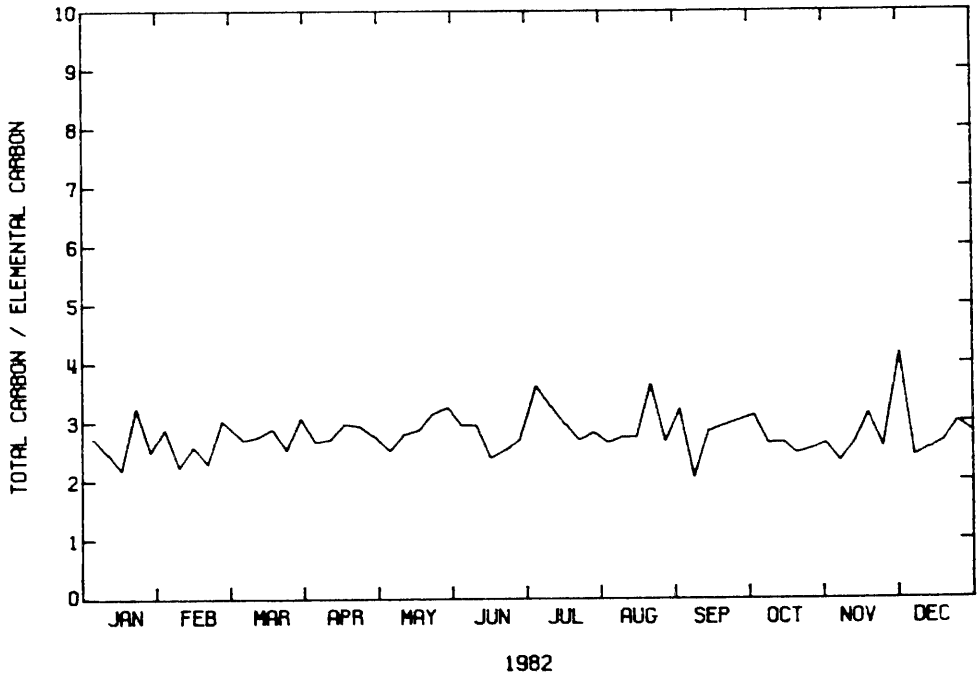

Figure 2.9e

RATIO OF TOTAL CARBON TO ELEMENTAL CARBON

AT PASADENA (MONTHLY AVERAGES)

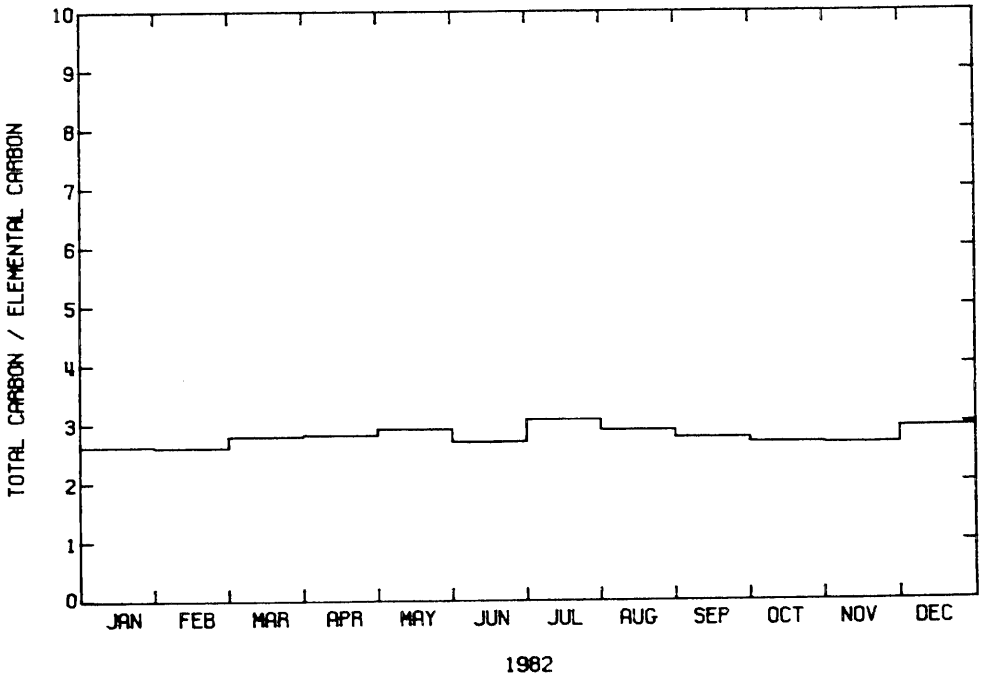

Figure 2.9f

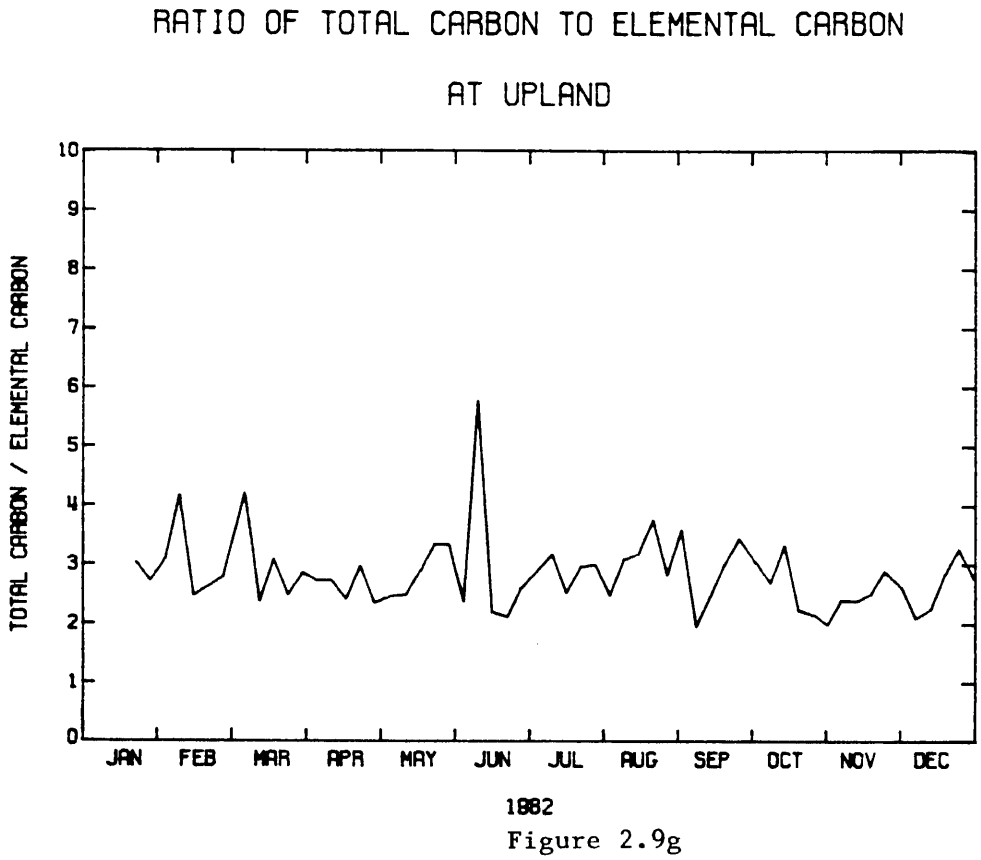

Figure 2.9g

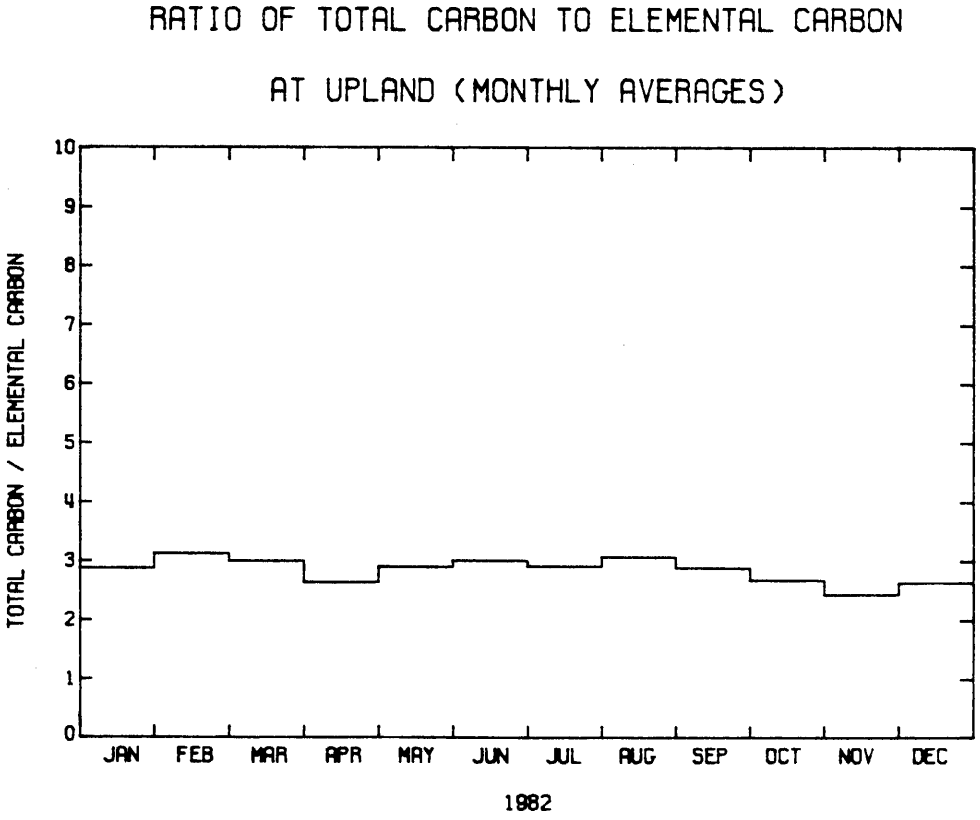

Figure 2.9h

RATIO OF TOTAL CARBON TO ELEMENTAL CARBON

AT RUBIDOUX

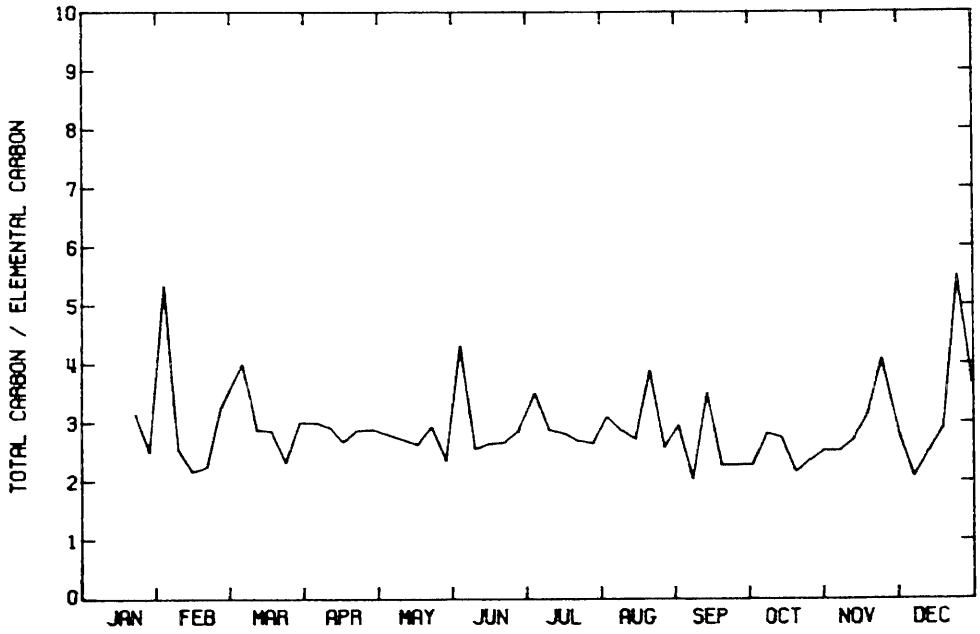

Figure 2.9i

RATIO OF TOTAL CARBON TO ELEMENTAL CARBON

AT RUBIDOUX (MONTHLY AVERAGES)

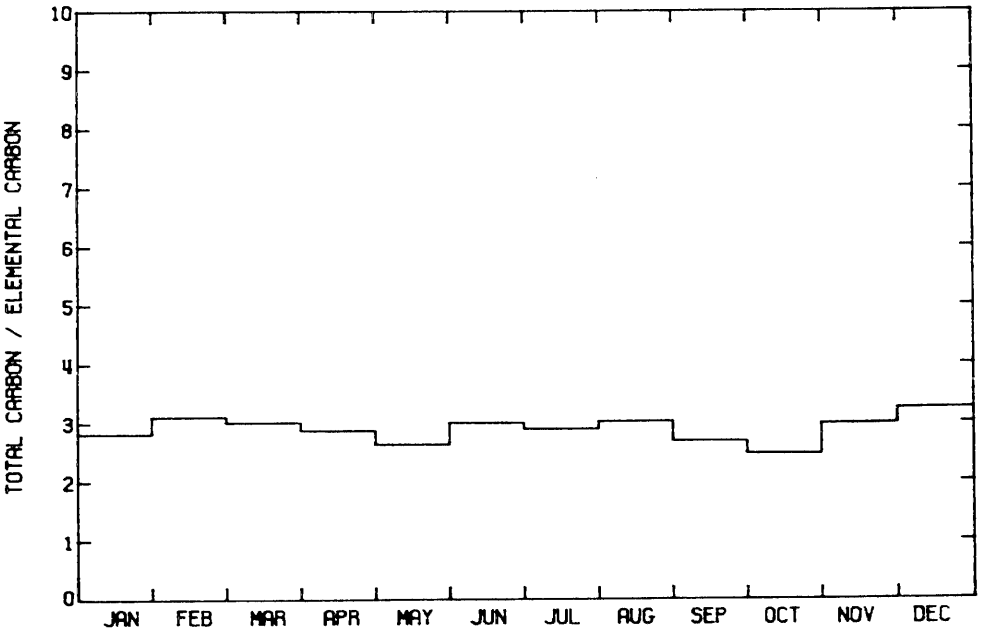

Figure 2.9j

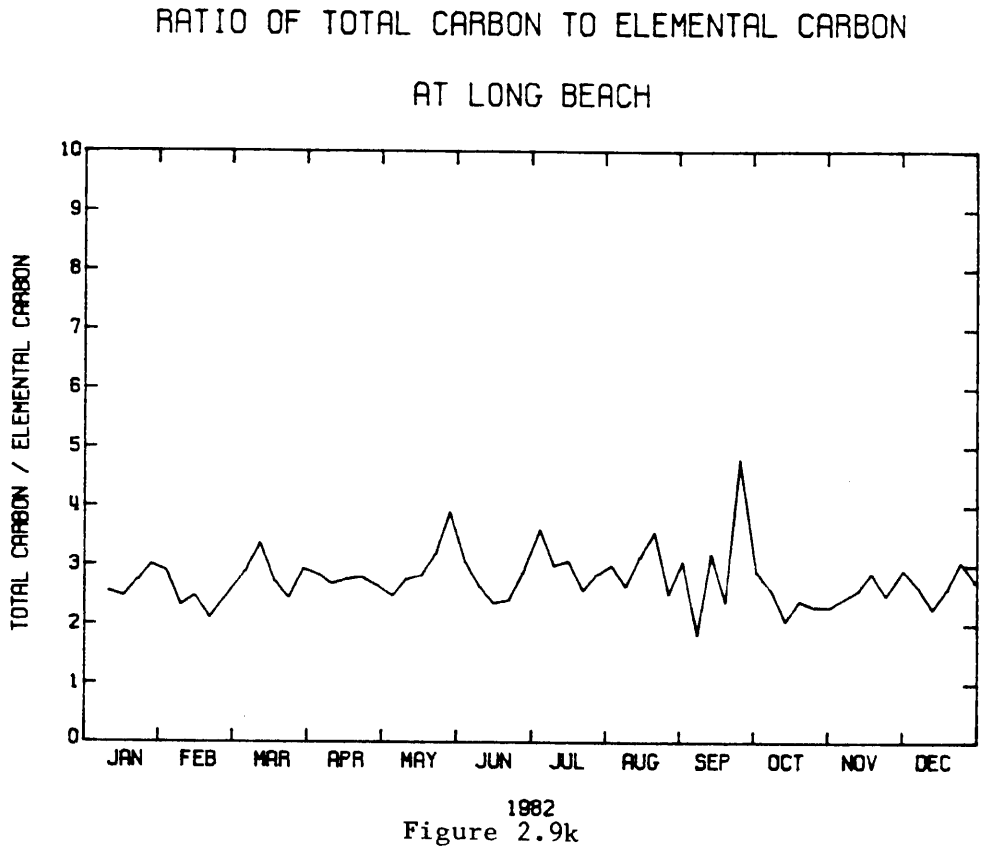

Figure 2.9k

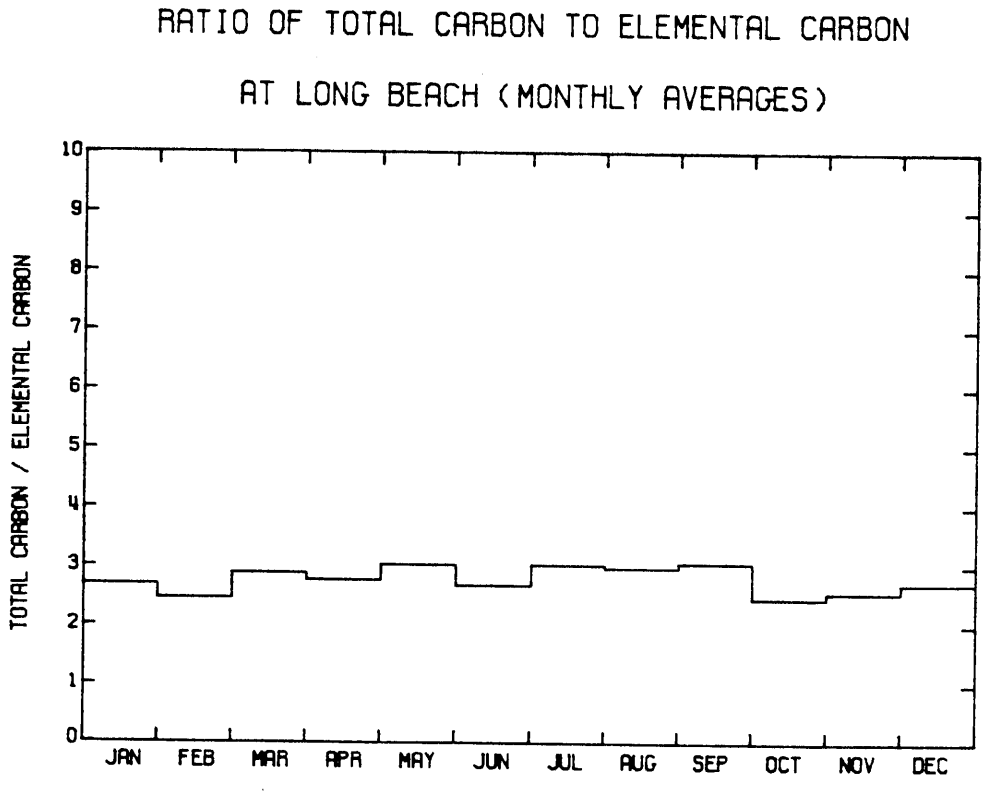

Figure 2.91

RATIO OF TOTAL CARBON TO ELEMENTAL CARBON

AT WEST LOS ANGELES

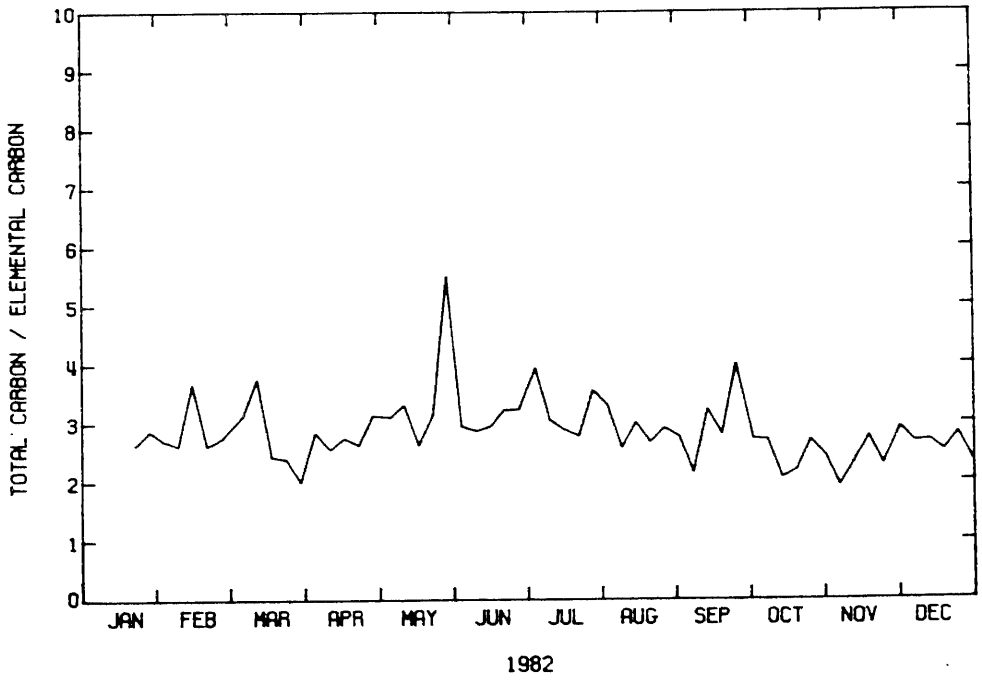

Figure 2.9m

RATIO OF TOTAL CARBON TO ELEMENTAL CARBON

AT WEST LOS ANGELES (MONTHLY AVERAGES)

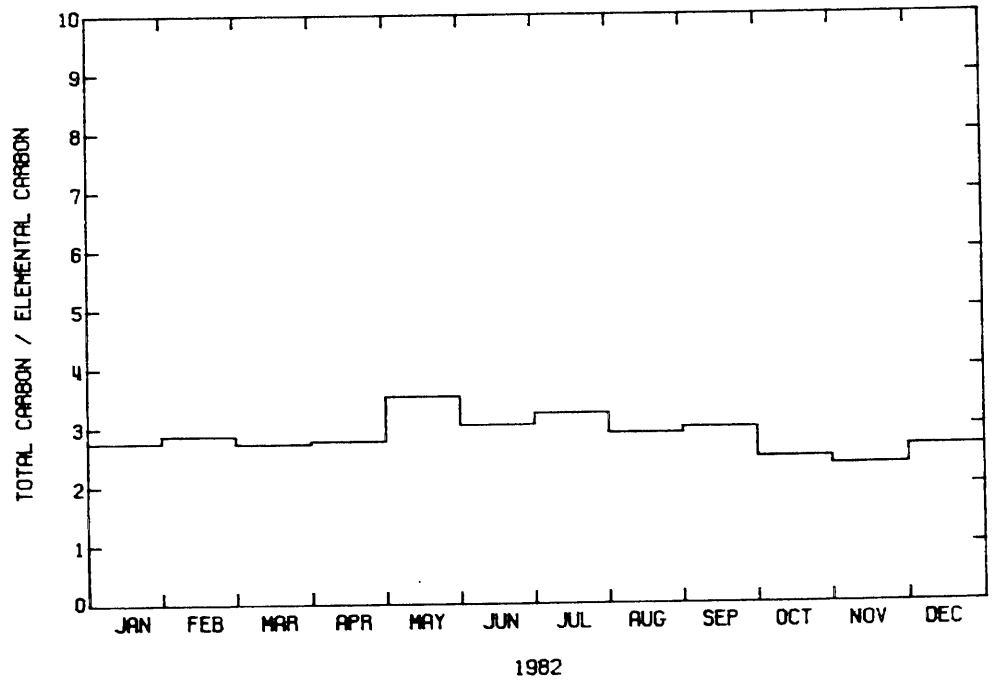

Figure 2.9n

RATIO OF TOTAL CARBON TO ELEMENTAL CARBON

AT ANAHEIM

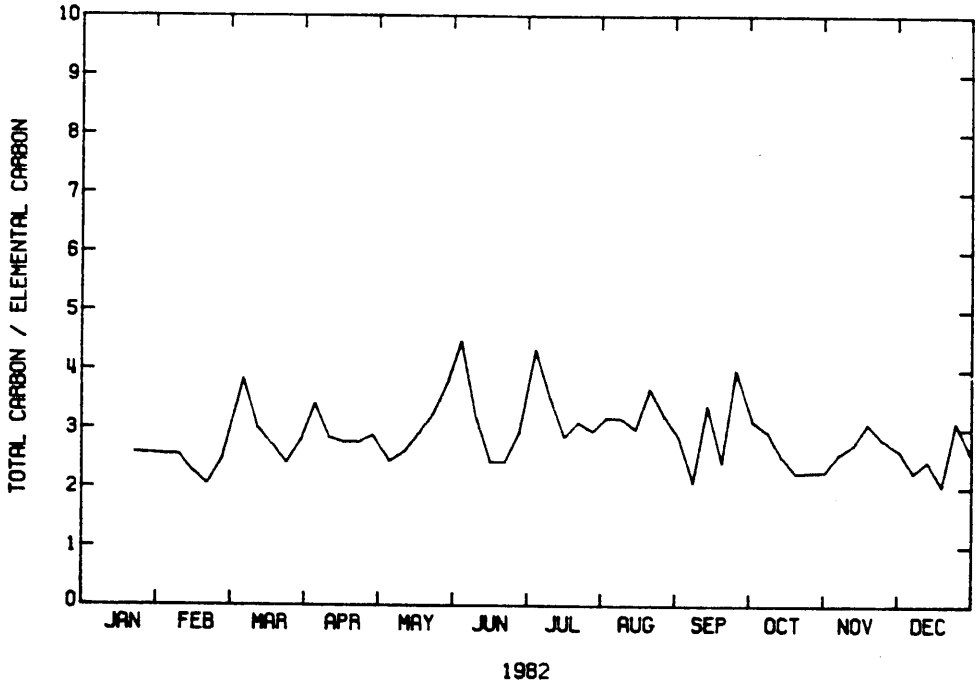

Figure 2.9o

RATIO OF TOTAL CARBON TO ELEMENTAL CARBON

AT ANAHEIM (MONTHLY AVERAGES)

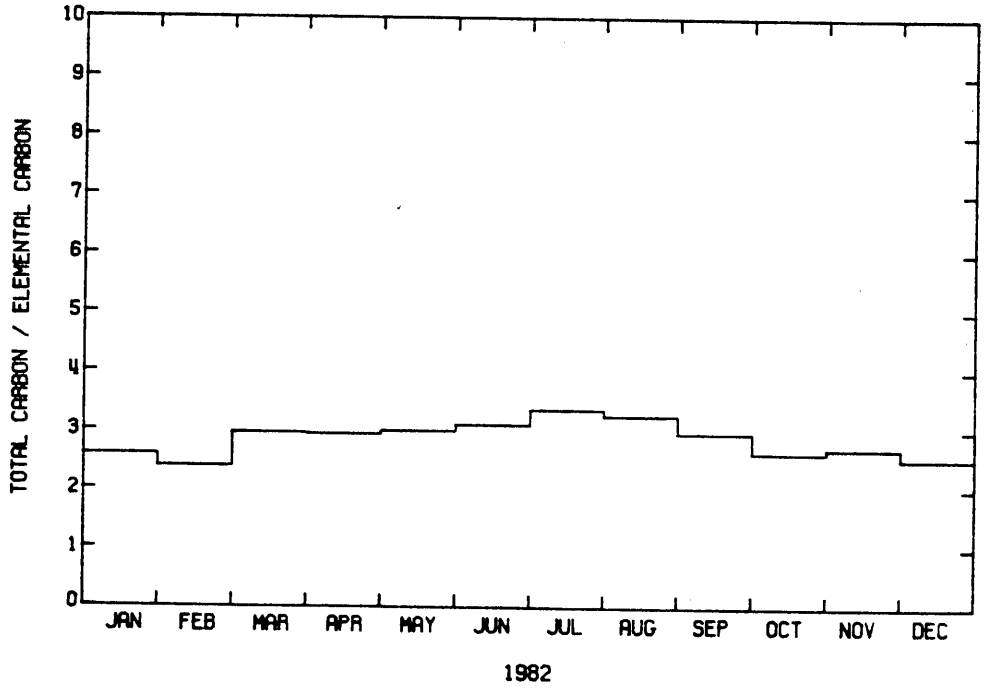

Figure 2.9p

RATIO OF TOTAL CARBON TO ELEMENTAL CARBON

AT AZUSA

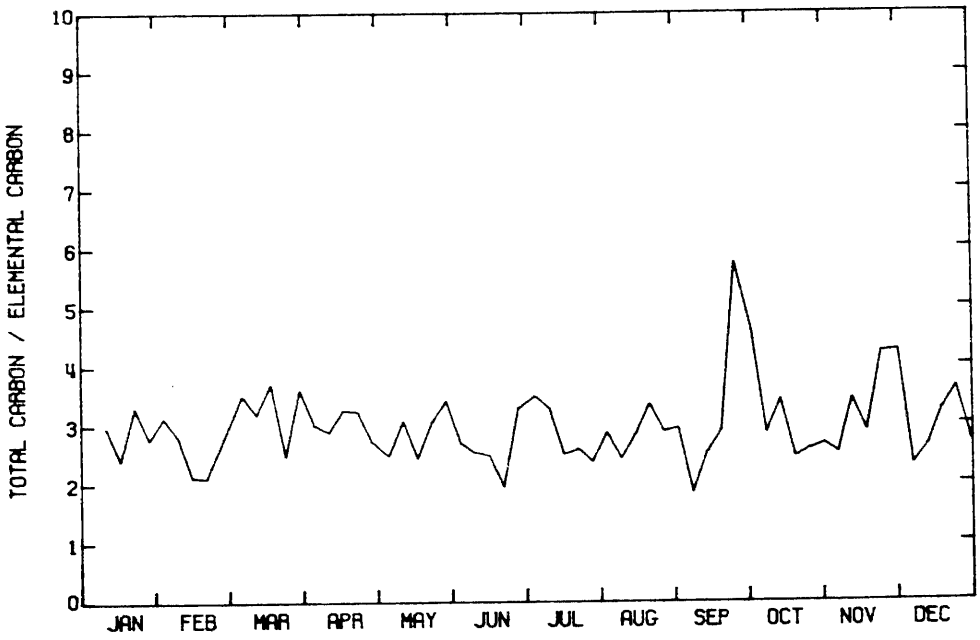

Figure 2.9q

RATIO OF TOTAL CARBON TO ELEMENTAL CARBON

AT AZUSA (MONTHLY AVERAGES)

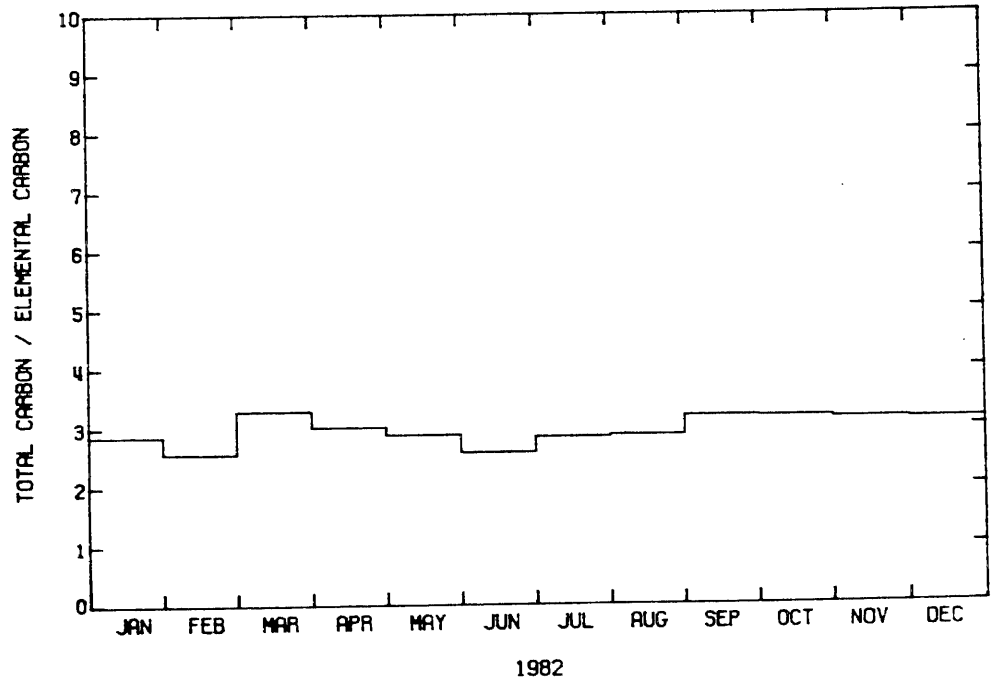

Figure 2.9r

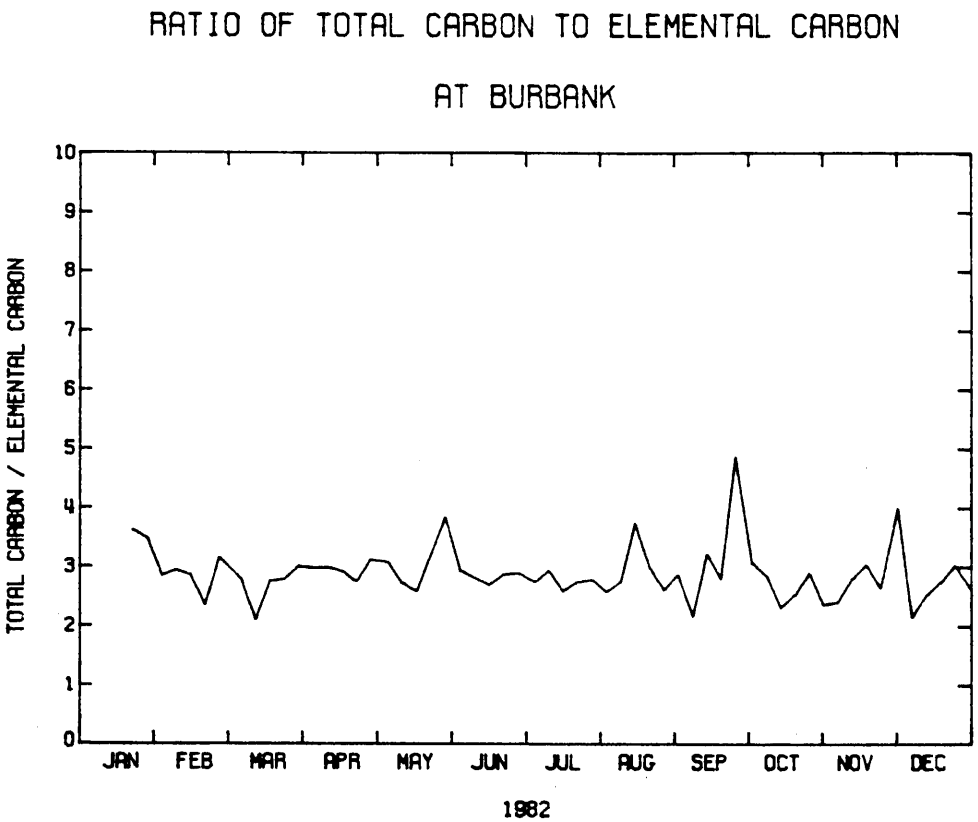

Figure 2.9s

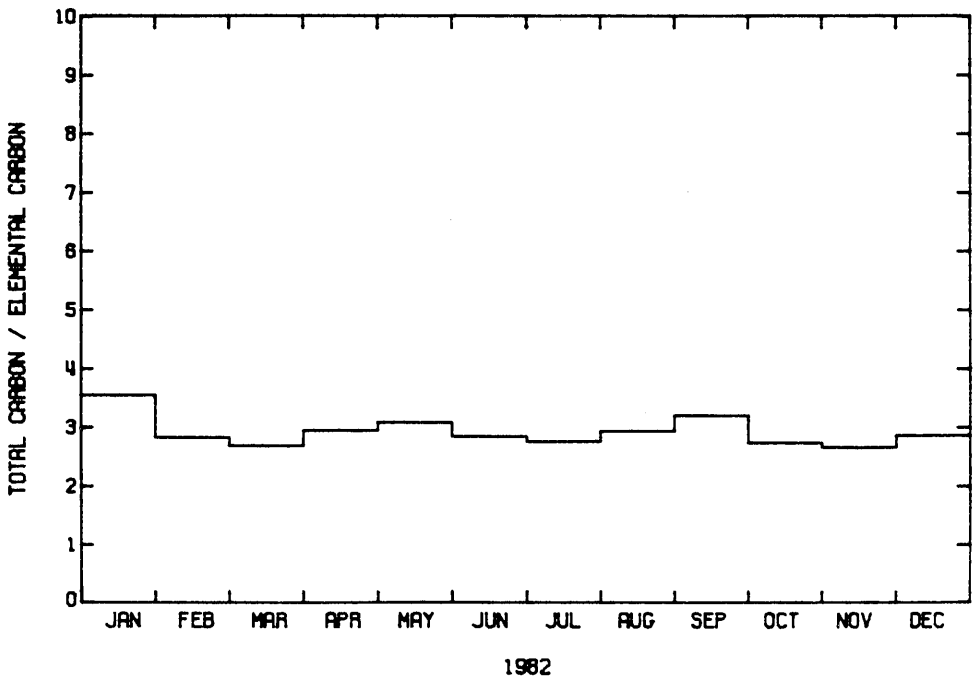

Figure 2.9t

ratio of 2.6:1, only slightly higher than at Lennox. Moving further inland to Pasadena, the annual average value of the daily TC to EC ratio rises to 2.8:1, again with little seasonal dependence (Figure 2.9ef). Air parcels reaching Upland on occasion are highly enriched in organics, with daily average TC to EC ratios often above 3:1, and on occasion approaching 6:1 (Figure 2.9gh). This may indicate periodic intrusion of heavy loadings of secondary organic aerosol at Upland. Nevertheless, Upland shows an annual average value of the daily TC to EC ratio of 2.8:1, not greatly different from Downtown Los Angeles. Aerosol behavior further downwind at Rubidoux near Riverside is similar to that at Upland (Figure 2.9ij). Occasional days with high TC to EC ratios are observed, but the monthly average value of the daily TC to EC ratio shows relatively little seasonal dependence. The annual average value of the daily TC to EC ratio at Rubidoux is 2.9:1, still not greatly different from the 1980 estimates of the TC to EC ratio in primary source emissions.

Daily values of the total carbon to elemental carbon ratios at each monitoring site have been averaged over the year 1982 and are shown in Figure 2.10. The lowest average TC to EC ratio is at Lennox adjacent to the San Diego Freeway on the western edge of the air basin, while the highest on-land values are at inland sites usually associated with heavy photochemical smog, like Azusa and Rubidoux. The TC to EC ratio of approximately 7:1 achieved at San Nicolas Island is due to the virtual absence of elemental carbon rather than to an anomalously high organic carbon loading.

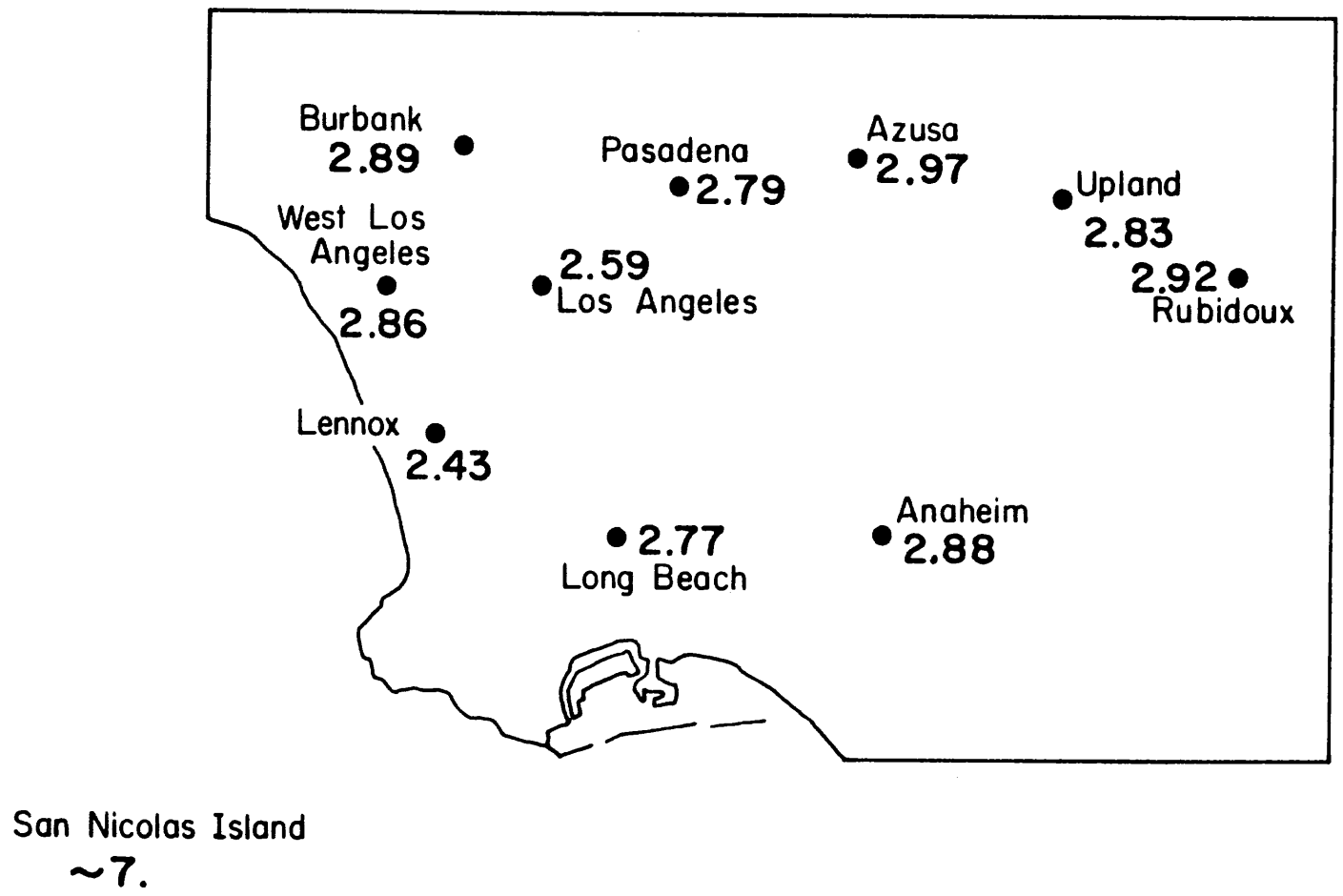

Figure 2.10 Annual average of the daily ratio of total carbon to elemental carbon in fine particles in the Los Angeles area--1982.

2.6 Summary and Discussion

An air quality monitoring protocol employing several parallel filter samples has been described that is capable of nearly closing a material balance on the chemical species contributing to atmospheric fine particle concentrations at all on-land sites other than Rubidoux. Application of this approach to the Los Angeles basin during 1982 shows that carbonaceous aerosols are the most abundant fine particle species present, accounting for roughly 40% of the average fine particle ($d_p < 2.1$ μm) loading at most air monitoring sites.

Fine organic and elemental carbon concentrations in the western Los Angeles basin peak in winter months, like CO and Pb concentrations at those sites. Less seasonal dependence is seen in the eastern basin near Upland and Rubidoux. When averaged over an annual cycle, fine organic and elemental carbon particle concentrations are highest in heavy traffic areas like Los Angeles, Lennox, and Burbank, and decline in downwind areas (Azusa, Upland, and Rubidoux). This spatial distribution and seasonal dependence is consistent with that expected of primary aerosol emissions from ground level sources in Los Angeles.

The comparison of the ratio of fine total carbon to fine elemental carbon in primary emissions versus ambient samples was explored as an indicator of the magnitude of secondary organic aerosol. Three characteristics might be expected if a large amount of secondary organics were present: (1) a ratio of TC to EC exceeding that in primary source emissions, (2) a summer seasonal peak in the ratio of TC to EC reflecting enhanced secondary organics production

during the summer photochemical smog season, and (3) an increase in the ratio of TC to EC in the prevailing inland transport direction.

Results of the 1982 field experiment show little seasonal dependence in the ratio of TC to EC. This is true at all monitoring sites on the average over periods of many months, although individual days at inland monitoring sites do show large levels of organic carbon enrichment. Either secondary organic aerosol formation in summer months is a reasonably small fraction of long-term average total carbon concentrations, or alternatively secondary organic aerosol as a fraction of total aerosol carbon is roughly the same in both summer and winter months. The annual average of the daily ratio of fine total carbon to fine elemental carbon averaged from 2.4:1 to 3.0:1 throughout the Los Angeles area during 1982 versus about 3.2:1 in 1980 estimates of local primary source emissions. Comparison of ambient data to emission data alone shows little evidence of a large enrichment in organic aerosol due to secondary aerosol formation on the average during 1982.

The best case that can be made for aerosol organic carbon enrichment of air parcels during transport in the prevailing inland wind direction is based on examination of differences in TC/EC and OC/EC ratios between stations. In the extreme, the annual average of the daily ratio of TC to EC rises from 2.43:1 at Lennox to 2.97:1 at Azusa and 2.92:1 at Rubidoux. These differences between Lennox and either Azusa or Rubidoux are statistically significant with greater than 95% confidence as can be seen by computing the standard error of

the TC/EC sample mean from the TC/EC population standard deviation given in Table 2.2. This enrichment of up to 0.54 parts organic carbon added to the 2.43:1 ratio observed at Lennox represents a + 22% increase in total carbon relative to elemental carbon from one end of the air basin to the other. A + 16% enrichment in total carbon relative to elemental carbon would be found between Lennox and Azusa if the analysis is based on differences in the ratio of the annual mean TC and EC values (see Figure 2.5) rather than on differences in the mean of the daily TC/EC ratios. The organic carbon enrichment can be isolated from total carbon by examining the ratio of OC to EC. The OC enrichment relative to EC between Lennox and Azusa is + 38% based on the mean of the daily ratio of OC to EC, but only + 27% if based on the ratio of the annual mean OC to EC values (see Figure 2.5). One reason for the difference in these statistics is that the OC enrichment relative to EC is favored slightly during summer months when total carbon levels are lower than average. Summaries based on the average of the daily OC to EC ratio treat that ratio each day as equally important to the annual mean, while the ratio of annual means is most affected by the highest concentration events that occur in winter months. Over long averaging times, between 16% and 22% of the total carbon and between 27% and 38% of the organic carbon at an inland location like Azusa or Rubidoux might be due to secondary aerosol formation in excess of that found at Lennox, the range depending on the statistical measure used. By all of these measures, this enrichment contributes a minority of the total carbon and organic

carbon present.

On the average over long periods of time, Los Angeles area fine aerosol carbon concentrations probably are dominated by primary source emissions. Secondary organic aerosols may be present, but they probably were not the overwhelming contributor to observed long term average fine carbon particle concentrations during 1982. This suggests that an emission control strategy that achieves a substantial reduction in primary aerosol carbon particle emissions could be expected to achieve a correspondingly large improvement in annual mean fine particle carbon concentrations in the atmosphere.

2.7 References for Chapter 2

Appel, B. R., E. M. Hoffner, E. L. Kothny, S. M. Wall, M. Haik, and R. L. Knights. 1979. Analysis of carbonaceous material in southern California atmospheric aerosols 2. Environmental Science and Technology 13:98-104.

Appel, B. R., Y. Tokiwa, and E. L. Kothny. 1983. Sampling of carbonaceous particles in the atmosphere. Atmospheric Environment 17:1787-96.

Cadle, S. H., P. J. Groblicki, and P. A. Mulawa. 1983. Problems in the sampling and analysis of carbon particulate. Atmospheric Environment 17:593-600.

Cass, G. R., P. M. Boone, and E. S. Macias. 1982. Emissions and air quality relationships for atmospheric carbon particles in Los Angeles. In Particulate carbon: Atmospheric life cycle, ed. G. T. Wolff and R. L. Klimisch. New York: Plenum Press.

Cess, R. D. 1983. Arctic aerosols: Model estimates of interactive influences upon the surface-atmosphere clear sky radiation budget. Atmospheric Environment 17:2555-64.

Conklin, M. H., G. R. Cass, L-C. Chu, and E. S. Macias. 1981. Wintertime carbonaceous aerosols in Los Angeles: An exploration of the role of elemental carbon. In Atmospheric aerosols: Source/air quality relationships, ed. E. S. Macias and P. K. Hopke. Washington, D.C.: American Chemical Society.

Countess, R. J., G. T. Wolff, and S. H. Cadle. 1980. J. Air Pollut. Control Assoc. 30:1194-1200.

Cronn, D. R., R.J. Charlson, R. L. Knights, A. L. Crittenden, and B. R. Appel. 1977. A survey of the molecular nature of primary and secondary components of particles in urban air by high-resolution mass spectrometry. Atmospheric Environment 11:929-37.

Davidson A., M. C. Hoggan, and M. A. Nazemi. 1979. Air quality trends in the South Coast Air Basin. South Coast Air Quality Management District. El Monte, California.

Groblicki, P. J., G. T. Wolff, and R. J. Countess. 1981. Visibility-reducing species in the Denver "brown cloud"--I. Relationships between extinction and chemical composition. Atmospheric Environment 15:2473-84.

Grosjean, D. 1977. Aerosols. In Ozone and other photochemical oxidants. Washington, D.C.: National Academy of Sciences.

Grosjean, D. 1983. Polycyclic aromatic hydrocarbons in Los Angeles air from samples collected on Teflon, glass and quartz filters. Atmospheric Environment 17:2565-73.

Grosjean, D., and S. K. Friedlander. 1975. Gas-particle distribution factors for organic and other pollutants in the Los Angeles atmosphere. J. Air Pollut. Control Assoc. 25:1038-44.

Hoggan, M. C., A. Davidson, and D. C. Shikiya. 1980. Seasonal and diurnal variation in air quality in California's South Coast Air Basin. South Coast Air Quality Management District. El Monte, California.

Huntzicker, J. J., R. L. Johnson, J. J. Shah, and R. A. Cary. 1982. Analysis of organic and elemental carbon in ambient aerosols by a thermal-optical method. In Particulate carbon: Atmospheric life cycle, ed. G. T. Wolff and R. L. Klimisch. New York: Plenum Press.

IARC Working Group. 1980. An evaluation of chemicals and industrial processes associated with cancer in humans based on human and animal data. Cancer Research 40:1-12.

John, W., and G. Reischl. 1980. A cyclone for size-selective sampling of air. J. Air Pollut. Control Assoc. 30:872-76.

Johnson, R. L., J. J. Shah, R. A. Cary, and J. J. Huntzicker. 1981. An automated thermal-optical method for the analysis of carbonaceous aerosols. In Atmospheric aerosols: Source/air quality relationships, ed. E. S. Macias and P. K. Hopke. Washington, D.C.: American Chemical Society.

Lin, C., M. Baker, and R. J. Charlson. 1973. Absorption coefficient of atmospheric aerosol: A method for measurement. Applied Optics 12:1356-63.

Mueller, P. K., B. V. Mendoza, J. C. Collins, and E. A. Wilgus. 1978. In Ion chromatographic analysis of environmental pollutants, ed. E. Sawicki, J. D. Mulik, and E. Wittgenstein. Ann Arbor, Michigan: Ann Arbor Science.

Muhlbaier, J. L., and R. L. Williams. 1982. Fireplaces, furnaces and vehicles as emission sources of particulate carbon. In Particulate carbon: Atmospheric life cycle, ed. G. T. Wolff and R. L. Klimisch. New York: Plenum Press.

Patterson, E. M., B. T. Marshall, and K. A. Rahn. 1982. Radiative properties of the Arctic aerosol. Atmospheric Environment 16:2967-77.

Pierson, W. R., and P. A. Russell. 1979. Aerosol carbon in the Denver area in November 1973. Atmospheric Environment 13:1623-28.

Pierson, W. R., R. A. Gorse, A. C. Szkarlat, W. W. Brachaczek, S. M. Japar, F. S-C. Lee, R. B. Zweidinger, and L D. Claxton. Mutagenicity and chemical characteristics of carbonaceous particulate matter from vehicles on the road. 1983. Environmental Science and Technology 17:31-44.

Pitts, J. N. 1983. Formation and fate of gaseous and particulate mutagens and carcinogens in real and simulated atmospheres. Environ. Health Perspect. 47:115-40.

Porch, W. M., and M. C. MacCracken. 1982. Parametric study of the effects of Arctic soot on solar radiation. Atmospheric Environment 16:1365-71.

Rosen, H., A. D. A. Hansen, L. Gundel, and T. Novakov. 1978. Identification of the optically absorbing component in urban aerosols. Applied Optics 17:3859-61.

Rosen, H., T. Novakov, and B. A. Bodhaine. 1981. Soot in the Arctic. Atmospheric Environment 15:1371-74.

Rosen, H., A. D. A. Hansen, L. Gundel, and T. Novakov. 1982. Graphitic carbon in urban environments and the Arctic. In Particulate carbon: Atmospheric life cycle, ed. G. T. Wolff and R. L. Klimisch. New York: Plenum Press.

Schuetzle, F., D. Cronn, A. L. Crittenden, and R. J. Charlson. 1975. Molecular composition of secondary aerosol and its possible origin. Environmental Science and Technology 9:838-45.

Shaw, G., and K. Stamnes. 1980. Ann. N.Y. Acad. Sci. 338:533-39.

Siegla, D. C., and G. W. Smith, ed. 1981. Particulate carbon: Formation during combustion. New York: Plenum Press.

Solorzano, L. 1967. Limnol. Oceanogr. 14:799-801.

Van Vaeck, L., G. Broddin, W. Cautreels, and K. Van Cauwenberghe. 1979. Aerosol collection by cascade impaction and filtration: Influence of different sampling systems on the measured organic pollutant levels. Sci. Tot. Environ. 11:41-52.

Waggoner, A. P., and R. J. Charlson. 1977. In Proc. symp. on Denver air pollution study--1973, ed. P. A. Russell. Vol. 2. U.S. Environmental Protection Agency EPA-600/9-77-001.

Wagner, H. G. G. 1978. Soot formation in combustion. In 17th symposium (international) on combustion. The Combustion Institute. Pittsburgh.

Witz, S. 1982. Suspended particulate matter in the atmosphere of the South Coast Air Basin and southeast desert areas--1980. South Coast Air Quality Management District. El Monte, California.

Wolff, G. T., P. J. Groblicki, S. H. Cadle, and R. J. Countess. 1982. Particulate carbon at various locations in the United States. In Particulate carbon: Atmospheric life cycle, ed. G. T. Wolff and R. L. Klimisch. New York: Plenum Press.

CHAPTER 3

DEVELOPMENT OF A SIMULATION MODELING TECHNIQUE FOR LONG-TERM AVERAGE PRIMARY CARBON PARTICLE AIR QUALITY

3.1 Introduction

A procedure for computing the relationship between emissions of an inert pollutant, such as elemental carbon, and long-term average air quality is sought that can be applied in the Los Angeles area. If meteorological information on wind velocities were known with certainty at all locations at all times, then the path of an air parcel leaving an emission source could be tracked exactly. Of course, exact information concerning the transport of air parcels over an air basin is impossible to obtain due to the extremely small length scales for some of the motion which occurs in the atmosphere. However, by combining routine measurements on hourly average wind speed and direction, for which some information is available, and applying a probabilistic approach to the smaller scales of motion, a mathematical description of the transport of pollutants over an air basin may be developed which can be used to predict long-term average primary carbon particle concentrations in the Los Angeles area.

The model described in this chapter is designed to predict the long-term average concentration of elemental carbon in the Los Angeles area by simulating the transport of emissions by atmospheric processes such as advection, diffusion, and deposition. Los Angeles often is

characterized by "unsteady" meteorology--light winds and shifting wind patterns over time scales shorter than that necessary to remove pollutants from the air basin. In this study, a Lagrangian marked particle modeling technique has been employed which simulates the motion and deposition of pollutants in an air basin that experiences unsteady meteorological conditions and a fluctuating temperature inversion aloft. In addition, the model is designed with special attention paid to the extent of vertical mixing of pollutants at locations near to their source.

In the following sections of this chapter, a short review of modeling techniques for predicting long-term average pollutant concentrations will be presented. The choice of a model for computing long-term average primary carbon particle concentrations in the Los Angeles area will be discussed, and the applicable mathematical equations will be formulated. In the next chapter, the model will be used to predict fine primary aerosol carbon concentrations in the central portion of the air basin that surrounds Los Angeles. Model predictions will be verified against monthly average elemental carbon concentrations observed during 1982 at a number of locations in the air basin.

3.2 An Overview of Long-term Average Air Quality Models

Emissions to air quality models directly simulate atmospheric fluid transport processes. These models are classified as Eulerian or Lagrangian, depending on the coordinate system employed. Both types

of model are based on the atmospheric diffusion equation that mathematically describes the system of atmospheric transport.

Eulerian models are constructed by examining a volume element, fixed in space, and then accounting for all sources and sinks of a pollutant species within that control volume and across its boundaries. This is described mathematically for an inert pollutant (no chemical reactions) by the following set of continuity equations:

$$\frac{\partial c(x,t)}{\partial t} + \frac{\partial u_i(x,t)c(x,t)}{\partial x_i} = D \frac{\partial^2 c(x,t)}{\partial x_i \partial x_i} + S(x,t) \qquad (3.1)$$

$$i = 1,2,3$$

where

$c(x,t)$ is pollutant concentration at location $x = (x_1,x_2,x_3)$ and time t,

$u_i(x,t)$ is fluid velocity in the i^{th} coordinate direction at location x and time t,

D is the molecular or Brownian diffusivity of the pollutant species in air,

$S(x,t)$ is the source strength of emissions at location x and time t.

To apply the above equation to an air basin, one would need to know the fluid velocities at all locations. Because wind velocity fluctuates over length scales smaller than those that can be resolved by conventional wind monitors, the mass balance approach used in

equation (3.1) cannot be applied as written. An approximate relationship for the ensemble mean concentration of a pollutant can be developed from equation (3.1), however, by separating the fluid transport into an advection term describing the mean wind motion and an eddy diffusion term that accounts for small scale features of atmospheric turbulence with periods less than about one-half hour (see Lamb and Seinfeld 1973):

$$\frac{\partial \langle c(x,t) \rangle}{\partial t} + \frac{\partial}{\partial x_i}\left(\bar{u}_i(x,t) \langle c(x,t) \rangle \right) = \frac{\partial}{\partial x_i}\left(\bar{K}_{ij} \frac{\partial \langle c(x,t) \rangle}{\partial x_j} \right) + S(x,t) \tag{3.2}$$

$$i = 1,2,3 \quad j = 1,2,3$$

where

$\langle c(x,t) \rangle$ is the ensemble mean pollutant concentration at location x and time t,

$\bar{u}_i(x,t)$ is average wind velocity in the i^{th} coordinate direction at location x and time t,

$\bar{K}_{ij}$ is the atmospheric eddy diffusivity tensor (usually it is assumed that $\bar{K}_{ij} = 0$ for $i \neq j$).

In the Lagrangian approach to air quality modeling, air parcels are represented by hypothetical mass points, the trajectories of which are computed from a stochastic solution to the atmospheric diffusion equation. Pollutant concentrations are determined by the probability that an air parcel (representing some pollutant mass) exists at location x and time t, given that it was present at a known location x', at an earlier time t'.

The ensemble mean pollutant concentration at location x and time t is found by integrating initial pollutant concentrations and continuing source emissions over all possible starting locations, weighted by the probability densities of displacement to x, for all times leading up to t:

$$\langle c(x,t)\rangle = \int_{-\infty}^{\infty}\int_{-\infty}^{\infty}\int_{-\infty}^{\infty} Q(x,t|x_o,t_o)\ \langle c(x_o,t_o)\rangle dx_o$$

$$+\int_{-\infty}^{\infty}\int_{-\infty}^{\infty}\int_{-\infty}^{\infty}\int_{t_o}^{t} Q(x,t|x',t')\ S(x',t')dt'dx' \qquad (3.3)$$

where

$\langle c(x,t)\rangle$ is the ensemble mean pollutant concentration at location x and time t,

$Q(x,t|x',t')$ is the transition probability density that a fluid particle existing at location x' and time t' will undergo a displacement to location x at time t,

$S(x',t')$ is the spatial and temporal distribution of emissions, evaluated at location x' at time t',

x_o and t_o are the initial conditions for location and time.

Equation (3.3) is the general Lagrangian expression developed for use in air quality modeling by Lamb for the case of a nonreactive pollutant (see Lamb 1971, Lamb and Neiburger 1971). The interested reader will find a discussion of the theoretical relationship between the Eulerian modeling approach of equation (3.2) and the Lagrangian solution of equation (3.3) in Lamb and Seinfeld (1973).

3.3 A Simulation Model for Long-term Average Primary Carbon Particle Air Quality under Unsteady Meteorological Conditions

To compute a time-averaged pollutant concentration, equation (3.2) or equation (3.3) could be solved for a large number of nearly instantaneous time increments, and then the results could be averaged. However, if a simulation model is to be run over a period of months, the computing resources required by that approach will become very large if the simulation used to compute the transition probability densities is at all realistic. Therefore, a method for directly computing long-term average concentrations can be developed. The long-term average pollutant concentration at x, over a time interval of duration T (typically one month), starting at time t_s, is defined as:

$$\overline{\langle c(x;T,t_s)\rangle} = \frac{1}{T}\int_{t_s}^{t_s+T} \langle c(x,t)\rangle dt \qquad (3.4)$$

Inserting equation (3.3) into equation (3.4) for the case of $\langle c(x_o,t_o)\rangle = 0$ (this can be accomplished by setting $t_o = -\infty$) gives equation (3.5):

$$\overline{\langle c(x;T,t_s)\rangle} = \frac{1}{T}\int_{t_s}^{t_s+T}\int_{-\infty}^{\infty}\int_{-\infty}^{\infty}\int_{-\infty}^{\infty}\int_{-\infty}^{t} Q(x,t|x',t')\, S(x',t')dt'dx'dt \qquad (3.5)$$

Changing the order of integration between dt and dx' and introducing a change of variable, $t' = t - \tau$ gives:

$$\overline{\langle c(x;T,t_s)\rangle} = \int_{-\infty}^{\infty}\int_{-\infty}^{\infty}\int_{-\infty}^{\infty}\frac{1}{T}\int_{t_s}^{t_s+T}\int_{0}^{\infty} Q(x,t|x',t-\tau)S(x',t-\tau)\,d\tau\,dt\,dx' \tag{3.6}$$

For the case where the diurnal variation of emission source strength for a given source class is independent of location, then $S(x',t-\tau)$ may be written as $\bar{S}(x')\omega(t-\tau)$, where $\bar{S}(x')$ is the time-averaged source strength at location x' and $\omega(t')$ is the normalized diurnal fluctuation for this source class; note that $\omega(t') = \omega(t' + 24 \text{ hours})$. Then equation (3.6) becomes:

$$\overline{\langle c(x;T,t_s)\rangle} = \int_{-\infty}^{\infty}\int_{-\infty}^{\infty}\int_{-\infty}^{\infty}\left[\frac{1}{T}\int_{t_s}^{t_s+T}\int_{0}^{\infty} Q(x,t|x',t-\tau)\omega(t-\tau)\,d\tau\,dt\right]\bar{S}(x')\,dx' \tag{3.7}$$

The term in brackets in equation (3.7) may be defined as the time-averaged source-to-receptor transport probability density function:

$$\bar{Q}(x|x';T,t_s) = \frac{1}{T}\int_{t_s}^{t_s+T}\int_{0}^{\infty} Q(x,t|x',t-\tau)\omega(t-\tau)\,d\tau\,dt \tag{3.8}$$

Then equation (3.7) may be rewritten as:

$$\overline{\langle c(x;T,t_s)\rangle} = \int_{-\infty}^{\infty}\int_{-\infty}^{\infty}\int_{-\infty}^{\infty}\bar{Q}(x|x';T,t_s)\bar{S}(x')\,dx' \tag{3.9}$$

The meteorology in Los Angeles would be characterized as unsteady. A daily land breeze/sea breeze wind reversal occurs regularly due to differential solar heating of the land and sea. During the morning and early evening hours, the winds often are

stagnant, with no predominant direction during typical short averaging times of one hour. In addition, there is a strong diurnal variation in the height of the base of the temperature inversion. Low overnight inversions rise during the day due to solar heating of the land. In the evening, the inversion base descends again because of a sinking motion induced by the Pacific Anticyclone. The volume of air below the inversion base is often vertically well mixed, so that quick changes in the inversion base height may drastically alter pollutant dilution in the vertical direction. Because of this unsteady behavior in the meteorology, an analytical solution for $\bar{Q}(x|x';\ T,t_s)$ using pseudo-steady state parameterization cannot be obtained.

Lamb and Seinfeld (1973) suggest that the only feasible method of predicting source-to-receptor transport probabilities, $\bar{Q}(x|x';\ T,t_s)$, for an arbitrary sequence of unsteady meteorological events is by means of a simulation model. One straightforward way to estimate $\bar{Q}$ is to launch hypothetical mass points into a numerical simulation of atmospheric fluid flow, and observe their positions over time. The number of particles falling within each volume element of a geographical grid system can be counted to determine by inspection the probability, $P(x,t|x',t-\tau)$, that a particle released at location x' at time $t-\tau$ will be in the grid cell volume element Δx_1, Δx_2, Δx_3 that surrounds location x at time t. Then

$$\bar{Q}(x|x';T,t_s) = \frac{1}{T\Delta x_1 \Delta x_2 \Delta x_3} \int_{t_s}^{t_s+T} \int_{o}^{\tau_c} P(x,t|x',t-\tau)\omega(t-\tau)\,d\tau\,dt \qquad (3.10)$$

In practice, evaluation of equation (3.10) does not require integration of air parcel starting times over all past history. Integration over τ from $\tau = 0$ to $\tau = \tau_c$ is sufficient, where τ_c is the longest retention time for an air parcel within the airshed of interest.

In the following sections, a simulation model will be formulated which will follow the trajectory of statistical "marked" particles. A Lagrangian particle-in-cell air quality model, previously developed by Cass (1977, 1981), will be improved to handle near-source dispersion from ground level sources. Each particle, which represents an air parcel containing a known mass of pollutant, is numerically transported in accordance with a time sequence of meteorological events. First, a set of rules will be written that governs the motion of a single particle over time after it has been released from an air pollutant source of interest. The source-to-receptor probability calculation is broken down into components, each representing a stochastic process in a chain of meteorological events. From the simulation of many such particles representing emissions from a number of urban source types, the probabilities concerning the existence of pollutant mass at given locations can be computed and, hence, may be used to evaluate long-term average pollutant concentrations.

In each of the following sections, the numerical simulation procedure will be given that describes how individual physical processes affect a single particle. Probabilities of transition will

be derived based on an idealized meteorological situation representing Los Angeles air basin conditions. Finally, an algorithm will be constructed for computing the overall source-to-receptor transition probabilities, $P(x,t|x',t-\tau)$ (from equation [3.10]), due to all physical processes for each source type in the air basin. Then $\bar{Q}$ can be evaluated from equation (3.10) for each separate source type. When combined with data on the spatial distribution of emission source strength as in equation (3.9), a multiple source urban air quality model results. Numerical solution of equation (3.9) is achieved by replacing the integrals with summations over discrete spatial intervals in the horizontal plane, (x_1,x_2). Concentrations are computed at a single height, x_3, near ground level. Contributions from all sources are added to an estimate of regional background air quality to arrive at the predicted long-term average pollutant concentration.

3.3.1 Single Particle Transport in the Horizontal Plane

The horizontal trajectory of an air parcel may be computed by integrating wind vectors instantaneously along the path of the air parcel. This calculation is impossible given data available in an actual urban air basin, however, since wind measurements are made only at a limited number of locations and generally are time-averaged over one-hour periods. Large scales of motion in an air basin are resolvable with such wind data, but there exist many smaller scale motions with periods of less than about one-half hour that are not

measured directly. The cumulative effect of these small scale features of atmospheric turbulence is known as eddy diffusion and can be modeled as a random fluctuation in air parcel location about the path computed from hourly averaged wind data. It should be pointed out that the separation of horizontal transport into advection and diffusion merely reflects the observer's frame of reference. An air parcel experiences motion due to all scales of atmospheric turbulence acting together.

Mean air parcel trajectories in the horizontal plane will be computed by head-to-tail progressive addition of observed wind vectors. Eddy diffusion will be simulated by adding small random displacements to the air parcel location computed from hourly averaged wind data. A very sophisticated wind field generation scheme based on interpolation of all available hourly averaged wind measurements could be used to determine the mean wind components. However, the data entry effort and computer time necessary to construct highly accurate wind fields hourly over the period of a year can become extremely costly. Therefore, an approximation is sought that will simplify the computation of trajectories for an air basin such as Los Angeles.

Cass (1977) showed that a uniform parallel flow approximation at any single hour adequately represents transport over the flat portion of the Los Angeles coastal plain when used in this type of long-term average air quality modeling calculation. Under the parallel flow approximation, a single centrally located wind station is used to represent flow over the coastal plain. During near-

stagnant conditions this approximation will not yield great accuracy, but during periods of higher wind speeds, flow becomes quite organized. Over long averaging times, experience shows that the approximation yields reasonable results.

Given that approximation, the trajectory computation for a single particle proceeds as follows. The reported hourly mean wind direction measurements are resolved only to within the 22.5° of arc which make up sectors of the 16-point compass reading. Therefore, a random direction is chosen from a uniform distribution of those possible directions within the sector of interest to be used as the mean direction for each hour. The two-dimensional random variable representing mean hourly horizontal wind speed, $\underset{\sim}{V}$, may be broken down into its two orthogonal components, V_1 and V_2, which are computed from the following equations:

$$V_1(t) = w(t) \cos (\theta(t)) \tag{3.11}$$

$$V_2(t) = w(t) \sin (\theta(t)) \tag{3.12}$$

where

$V_1(t)$ and $V_2(t)$ are the components of wind speed for hour t in the x_1 and x_2 directions, respectively,

ws(t) is the reported hourly averaged wind speed during hour t,

and

$$\theta(t) = d(t) + 22.5\ U\ [-0.5,0.5] \tag{3.13}$$

where

$\Theta(t)$ is the randomized mean wind direction at hour t, in degrees,

$d(t)$ is the reported mean wind direction during hour t, in degrees measured counterclockwise from an axis pointing toward the east (direction x_1),

$U[a,b]$ is a uniform random variable with mean zero and range from a to b.

The randomized location due to the advective displacement from $\underline{x}' = (x'_1, x'_2)$ to $\underline{X}'' = (X''_1, X''_2)$ during the time from t_o to t is computed for a uniform parallel flow regime as:

$$X''_1 (t|x'_1, t_o) = \int_{t_o}^{t} V_1(t')dt' + x'_1(t_o) \tag{3.14}$$

$$X''_2 (t|x'_2, t_o) = \int_{t_o}^{t} V_2(t')dt' + x'_2(t_o) \tag{3.15}$$

Since the wind measurements are recorded as hourly averages, the integrals in equations (3.14) and (3.15) may be replaced by summations, with Δt = 1 hour:

$$X''_1 (t|x'_1, t_o) = \sum_{n=0}^{N-1} V_1(t_o + n\Delta t)\Delta t + x'_1(t_o) \tag{3.16}$$

$$X''_2 (t|x'_2, t_o) = \sum_{n=0}^{N-1} V_2(t_o + n\Delta t)\Delta t + x'_2(t_o) \tag{3.17}$$

where $N = \dfrac{(t - t_o)}{\Delta t}$.

In addition to the mean displacement due to advective transport, small scale turbulent fluctuations occur that randomize an air parcel's location about its mean trajectory. This process of eddy diffusion is simulated as a two-dimensional Gaussian random variable with mean zero and standard deviation $(\sigma_1(\tau), \sigma_2(\tau))$. Mean trajectory end points X''_1, X''_2 are perturbed at each hour by adding small distance increments $\delta X''_1$ and $\delta X''_2$ drawn at random from the family of displacements having a Gaussian distribution $(\sigma_1(\tau), \sigma_2(\tau))$.

Now, consider the probability distribution, $P_a(\underline{x}'', t|\underline{x}', t - \tau)$, for the displacement <u>by advection</u> (and eddy diffusion) of a single particle from starting point $\underline{x}'$ to ending point $\underline{x}''$ during the time interval from $t_o = (t - \tau)$ to t. A single particle can be only in one place. Therefore, for the case of P_a estimated from a single trajectory calculation with spatial location defined over a grid system based on discrete spatial intervals:

$$P_a(\underline{x}'', t|x', t - \tau) = \lambda(x^* - \underline{X}'') \tag{3.18}$$

where $\lambda\ (\underline{x}^* - \underline{X}'')$ is a proximity function defined as

$$\lambda\ (\underline{x}^* - \underline{X}'') = \begin{array}{l} 1 \text{ if } |(x_i^* - X''_i)| < \dfrac{\Delta x_i}{2} \text{ for } i = 1,2 \\ 0 \text{ otherwise} \end{array} \tag{3.19}$$

and $\underline{x}^*$ is the center of the grid cell in the horizontal plane of the modeling region that contains location $\underline{x}''$. $P_a(x'', t|x', t - \tau)$ could be computed repeatedly for many single particle trajectories and then averaged to obtain an accurate spatially distributed probability

density function $\langle P_a(x'',t|x',t-\tau)\rangle$ describing the fate of pollutants released at location x' at time $t-\tau$.

The instantaneous parallel flow assumption allows for a great savings in computation time, since the probability of finding the particle in the area element surrounding $\underset{\sim}{x}''$ at time t, given that it was at location $\underset{\sim}{x}'$ at time t_o, is only a function of the displacement $(\underset{\sim}{x}'' - \underset{\sim}{x}')$ and the specific time interval (t_o, t). The probability of a particle's experiencing a displacement $(\underset{\sim}{x}'' - \underset{\sim}{x}')$ in the horizontal plane is not a function of starting location. Therefore, trajectory calculations for hundreds of different source starting locations may be collapsed into one source-to-receptor probability distribution calculation that may be applied to any starting location, $\underset{\sim}{x}'$, by simply subtracting the change in starting location from all possible endpoints of interest. The result is that $P_a(\underset{\sim}{x}'',t|\underset{\sim}{x}',t-\tau)$ may be rewritten as $P_a(\underset{\sim}{x}'' - \underset{\sim}{x}',t,t-\tau)$.

3.3.2 Exchange in the Vertical Direction

Up to this point, the motion of an air parcel has been described only in two dimensions. The probabilities of transport presented thus far have dealt with the frequency of occurrence of air parcel transport to particular horizontal locations. The air parcel's motion in the vertical direction also may be simulated.

The geographic region of interest is assumed to experience an idealized stable temperature inversion aloft at all times. The base of the inversion generally rises during the day and falls at night due

to the radiative heating and cooling of the earth. An air parcel containing particulate matter may reside in the stable layer above the inversion base or in the unstable layer below the inversion base. In addition, dry deposition of particulate matter occurs at the ground. In this section, a set of rules that describes the exchange of particulate-laden air parcels between these two vertical layers in the atmosphere will be constructed, and ground level dry deposition will be considered. Mathematical expressions for the probabilities associated with finding a particular fluid particle in each vertical compartment in the model will be formulated. These probability calculations will be discussed in two regimes. First, the case of an air parcel that has been emitted into the stable temperature inversion aloft or that has resided below the inversion base long enough to become fully mixed from the ground to the inversion base will be considered. In that case, the air parcel, <u>if</u> it is below the inversion base, will have equal probability of being found at any particular elevation within the mixed layer, and calculation of the air parcel's probability of affecting ground level air quality is particularly easy. The second case, where the air parcel has not yet had time to become fully mixed within the ground level layer of the model, occurs for fresh emissions from low-level sources and on occasion from elevated sources when the inversion base is at a high elevation. That case of non-uniform vertical mixing will be treated later in Section 3.3.3.

The following set of rules, developed by Cass (1977), is

adopted by which the probability may be computed that an air parcel containing particulate matter resides in one of three compartments in the model. At the time of emission, an air parcel is placed either into the mixed layer below the inversion base or into the inversion layer above, depending on the effective stack height of the source. Then a procedure is outlined that computes the probability that that air parcel resides above or below the inversion base at the end of each time step, or that it has undergone dry deposition at the earth's surface prior to the end of that time step. This probability depends upon the conditions at the beginning of the time step and upon inversion base motion that causes air parcels to be transferred between the mixed layer below the inversion and the stable layer within the inversion.

The following definitions are made:

$P_b(t|t-\tau)$ is the probability that an air parcel is <u>below</u> the inversion base at time t, given that it was emitted at time $t_o = t - \tau$,

$P_i(t|t-\tau)$ is the probability that an air parcel is in the <u>inversion</u> layer above the inversion base at time t, given that it was emitted at time $t_o = t - \tau$,

$P_g(t|t-\tau)$ is the probability that an air parcel has been deposited at the <u>ground</u> sometime between the time of emission, $t_o = t - \tau$, and time t,

$h(t)$ is the height of the inversion base separating the inversion layer above from the mixed layer below,

$h_m(t,t-\tau)$ is the maximum inversion base height, h(t), over the time interval from $t_o = t - \tau$ to t,

$H(t_o)$ is the effective stack height of emissions.

At the time of release, an air parcel is assumed to reside below the inversion base if the effective stack height of the source is below the inversion base. Otherwise, the air parcel's initial location is assumed to be stratified at the effective stack height within the stable inversion layer. This is shown schematically in Figure 3.1. The initial conditions for the probability of finding the particle in a given compartment of the model are as follows:

$$P_b(t_o) = \begin{cases} 1 & H(t_o) \leq h(t) \\ 0 & h(t) < H(t_o) \end{cases} \tag{3.20}$$

$$P_i(t_o) = 1 - P_b(t_o) \tag{3.21}$$

$$P_g(t_o) = 0 \tag{3.22}$$

and

$$h_m(t_o) = h(t_o) \tag{3.23}$$

Dry deposition of particulate matter from the mixed layer to the ground may be represented as a first order process. The rate of removal from the mixed layer due to dry deposition alone is:

Figure 3.1 Air parcel insertion into the atmosphere (from Cass 1977).

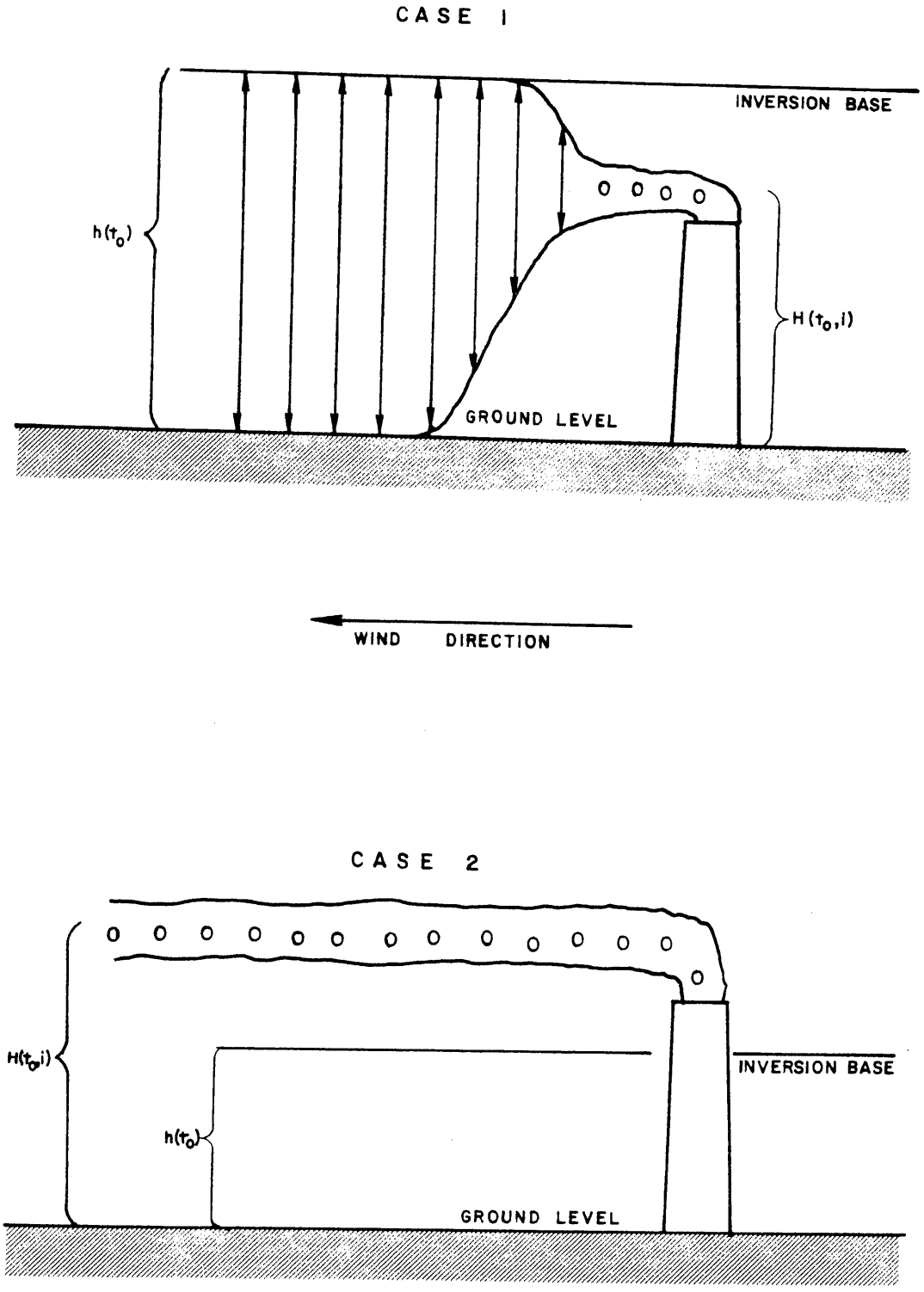

$$\frac{dP_b(t)}{dt} = -\frac{V_g}{h(t)} P_b(t) \tag{3.24}$$

where V_g is the effective deposition velocity for particles of a given size range. (This is not actually a settling velocity, but rather the ratio between pollutant flux to the ground and atmospheric concentration.)

Solving equation (3.24) for a short interval time, Δt, where $h(t + \Delta t) \simeq h(t) \simeq h$:

$$P_b(t + \Delta t) = P_b(t) \exp\left[\frac{-V_g}{h} \Delta t\right] \tag{3.25}$$

This is the probability that an air parcel residing in the mixed layer below the inversion at time t remains in the mixed layer after Δt, i.e., it is not deposited at the ground. Therefore, the probability that an air parcel has been deposited by time $t + \Delta t$ is:

$$P_g(t + \Delta t) = P_g(t) + P_b(t) \left\{1 - \exp\left[\frac{-V_g}{h} \Delta t\right]\right\} \tag{3.26}$$

The probability of transfer of an air parcel from the mixed layer to the ground represented in equations (3.25) and (3.26) now must be coupled with the process by which an air parcel may move between the mixed layer and the inversion layer. The mixed layer has a depth, changing with time, equal to the current inversion base height. The inversion base height above ground level, and hence the mixing depth, will be taken as independent of horizontal location at any single time. Justification for this approximation over the western portion of the Los Angeles basin is provided by Cass (1977). This approximation when combined with previous assumptions about

horizontal transport allows for calculation of vertical motions independently of horizontal location in the air basin.

Consider the fate of an air parcel emitted from an elevated source at night into the stable inversion aloft. That air parcel will remain at the effective height of emission until such time as the inversion base rises to intercept the air parcel, transferring it to the layer below the inversion base. Once below the inversion base, that air parcel has equal probability of being found at any elevation (i.e., pollutants fumigated down from high elevation become fully mixed between the inversion base and the ground). If the inversion base descends over time, an air parcel located below the inversion base within the mixed layer has some probability of becoming trapped within the inversion layer. Assuming that pollutant-laden air parcels are well mixed below the inversion base, then the probability that a particular air parcel remains in the mixed layer and is not transferred to the inversion layer is equal to the ratio of the inversion base heights before and after the descent of the inversion base. Inversion base descent through a polluted mixed layer results in stabilization of a thick polluted air mass within the inversion itself. The depth of this thick pollutant layer within the inversion is equal to the distance between the previous maximum mixing depth and the current lower inversion base height. If the inversion base subsequently rises into this thick polluted layer aloft, the probability that an air parcel is transferred from the inversion layer back into the mixed layer is taken in proportion to the change in

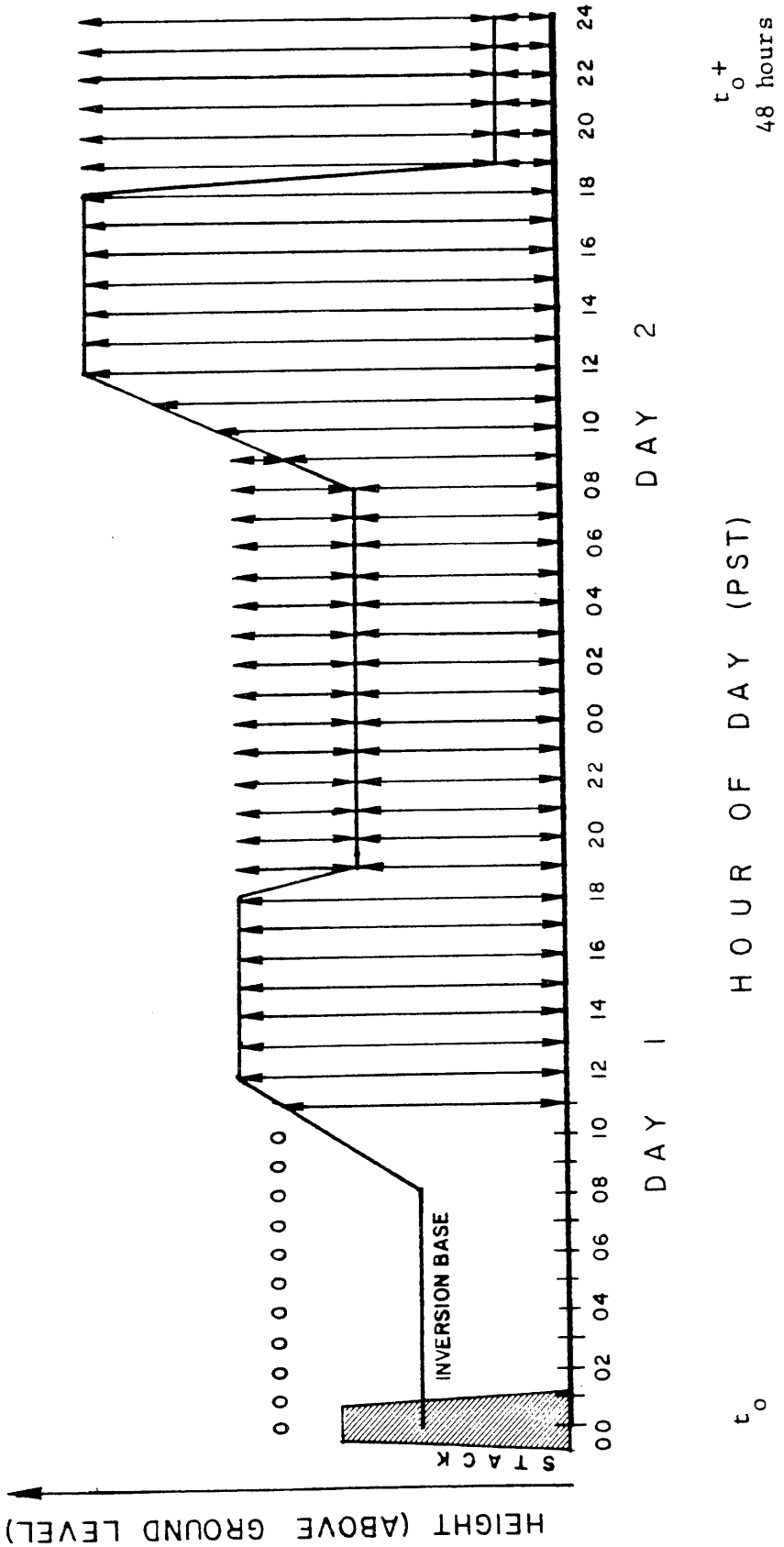

Figure 3.2 Hypothetical time history of interaction between the inversion base and a fluid particle released at time t_o (from Cass 1977).

inversion base height relative to the previously established maximum mixing depth. This process is described graphically in Figure 3.2.

The initial conditions in equations (3.20) through (3.23), when combined with the following stepwise procedure for computing probabilities of transfer of air parcels between each vertical layer over a time interval, Δt, can be used to propagate the probabilities that an air parcel resides in each layer of the model during the history of the air parcel's trajectory. For each time interval $(t, t + \Delta t)$ perform the following steps:

1. Compute f_d, the probability that an air parcel in the mixed layer has deposited at the ground during this time interval:

$$f_d = 1 - \exp\left[\frac{-V_g \Delta t}{h(t + \Delta t)}\right] \tag{3.27}$$

2. If $h(t + \Delta t) > h_m(t)$, then set maximum inversion height $h_m(t + \Delta t)$, to new maximum $h(t + \Delta t)$, else $h_m(t + \Delta t) = h_m(t)$.

3. Determine the parameter f_s which is related to the air mass that is exchanged between the inversion layer and the mixed layer when the inversion base moves. If the inversion base is rising, f_s will be negative.

   For effective stack height, $H(t_o) > h_m(t + \Delta t)$:

$$f_s = 0 \tag{3.28}$$

For $H(t_o) \leq h_m(t + \Delta t)$:

$$f_s = \begin{cases} P_b(t) \left[\dfrac{h(t) - h(t + \Delta t)}{h(t)}\right] & \text{inversion base falling: } h(t + \Delta t) < h(t) \\ 0 & \text{steady: } h(t + \Delta t) = h(t) \\ P_i(t) \left[\dfrac{h(t) - h(t + \Delta t)}{h_m(t) - h(t)}\right] & \text{rising: } h(t) < h(t + \Delta t) < h_m(t) \\ -P_i(t) & \text{rising: } h(t) \leq h_m(t) < h(t + \Delta t) \end{cases} \tag{3.29}$$

4. Compute new probabilities at end of time increment $t + \Delta t$:

$$P_i(t + \Delta t) = P_i(t) + f_s \tag{3.30}$$

$$P_b(t + \Delta t) = (P_b(t) - f_s)\ (1 - f_d) \tag{3.31}$$

$$P_g(t + \Delta t) = P_g(t) + \left[P_b(t) - f_s\right] f_d \tag{3.32}$$

If this procedure is executed repeatedly for time steps from $t_o = t - \tau$ to t, then the result will be the three probabilities, $P_i(t|t - \tau)$, $P_b(t|t - \tau)$, and $P_g(t|t - \tau)$ that the air parcel is within the stable inversion, or below the inversion base within the mixed layer, or has deposited at the ground by time t, given that it was emitted at time $t - \tau$. Note that the summation of equations (3.30), (3.31), and (3.32) results in:

$$P_i(t + \Delta t) + P_b(t + \Delta t) + P_g(t + \Delta t) = P_i(t) + P_b(t) + P_g(t) \qquad (3.33)$$

The sum of these probabilities always will be 1.0 since $P_i(t_o) + P_b(t_o) + P_g(t_o) = 1.0$ (see equations [3.20] through [3.22]). Therefore, mass is conserved during this process.

3.3.3 Vertical Profile below Inversion Base

Particulate matter residing below the inversion base may not always be completely mixed in the vertical direction. Although the ground level computational cell in the model is called the "mixed layer," there are times when the probabilities of finding a polluted air parcel at different heights within that cell are unequal. If the pollutant were assumed to be fully mixed below the inversion base, then the probability of finding an air parcel at any height (or, more specifically, within Δx_3 of any height) below the inversion base would be inversely proportional to inversion base height, h(t). This assumption becomes unreasonable when polluted air parcels are near their sources and the pollutant has not had sufficient time to become fully mixed.

In order to accurately predict particulate concentrations near ground level in the vicinity of ground level sources, a model must include the effect of short travel times on vertical mixing. In this section, the probability of finding a polluted air parcel at a particular elevation within the mixed layer is computed for the first few time steps after release from a source with effective stack height

below the inversion base.

A vertical profile of probable air parcel location is formulated assuming a Gaussian distribution of plume spread from an effective source height, H. Three regimes are possible, depending on the degree of dispersion and the height of the inversion base: (1) when the inversion base height, h, is very high (or the air parcel's travel time is very short), there is no effect of the inversion base on the vertical dispersion of the plume; (2) as the air parcel moves away from its source, the vertical dispersion increases until the stable layer aloft begins to trap the air parcel below the inversion base; (3) when the plume has traveled sufficiently far, it becomes fully mixed between the ground and the inversion base. It is necessary that each of these three regimes be considered and that the transitions between the regimes be smooth. This is accomplished by utilizing basic analytical procedures for estimating dispersion as outlined by Turner (1969).

Assume that the probable location of a pollutant-laden air parcel has a Gaussian distribution, centered along the mean horizontal wind trajectory, in both the crosswind and vertical directions. Further assume that there is a total reflection of the plume at the earth's surface (deposition is accounted for elsewhere; see Section 3.3.2). Then the normalized concentration at location $x = (x_1, x_2, x_3)$ due to a continuous unit source located at $x_1 = x_2 = 0$ with effective stack height H, for the case of transport in the x_1 direction when the inversion base is high relative to the

characteristic scale for vertical mixing (i.e., $\sigma_3 << h$), may be computed as follows (from Turner 1969):

$$C(x_1,x_2,x_3;H) = \frac{1}{2\pi\sigma_2\sigma_3 u} \exp\left[-\tfrac{1}{2}\left(\frac{x_2}{\sigma_2}\right)^2\right] \left\{\exp\left[-\tfrac{1}{2}\left(\frac{x_3 - H}{\sigma_3}\right)^2\right] + \exp\left[-\tfrac{1}{2}\left(\frac{x_3 + H}{\sigma_3}\right)^2\right]\right\} \quad (3.34)$$

where σ_2 and σ_3 are the standard deviation of plume spread in the crosswind and vertical directions, respectively, u is wind speed, C is pollutant concentration (mass per unit volume of air) resulting from a source of one mass unit per unit time. Note that σ_2 and σ_3 are increasing functions of x_1, the distance along the centerline of the plume trajectory, and hence σ_2 and σ_3 depend on the travel time, τ, of the air parcel from its time of release until reaching location x, downwind. If a slice is taken across the plume at distance x_1 downwind and that slice is integrated in the crosswind direction, one determines the probability of finding a polluted air parcel at a specific height x_3 or, more specifically, within the small differential height element Δx_3 about x_3 at time t given that it was released at time $t - \tau$:

$$P_v(x_3,t|H,t-\tau) = \frac{\Delta x_3}{\sqrt{2\pi}\,\sigma_3}\left\{\exp\left[-\tfrac{1}{2}\left(\frac{x_3-H}{\sigma_3}\right)^2\right] + \exp\left[-\tfrac{1}{2}\left(\frac{x_3+H}{\sigma_3}\right)^2\right]\right\} \tag{3.35}$$

Equation (3.35) is used when a fresh air parcel is released below the inversion base while $\sigma_3 << h$. When the magnitude of σ_3 grows to approach the location of the inversion base, the presence of the inversion base begins to affect material in the upper tail of the Gaussian plume, and a correction to equation (3.35) is necessary. Bierly and Hewson (1962) have suggested the addition of numerous terms to equation (3.35) that account for the multiple reflections from both the ground and the stable layer:

$$P_v(x_3,t|H,t-\tau) = \frac{\Delta x_3}{\sqrt{2\pi}\,\sigma_3}\left(\exp\left[-\tfrac{1}{2}\left(\frac{x_3-H}{\sigma_3}\right)^2\right] + \exp\left[-\tfrac{1}{2}\left(\frac{x_3+H}{\sigma_3}\right)^2\right]\right.$$
$$+ \sum_{n=1}^{J}\left\{\exp\left[-\tfrac{1}{2}\left(\frac{x_3-H-2nh(t)}{\sigma_3}\right)^2\right] + \exp\left[-\tfrac{1}{2}\left(\frac{x_3+H-2nh(t)}{\sigma_3}\right)^2\right]\right.$$
$$\left.\left. + \exp\left[-\tfrac{1}{2}\left(\frac{x_3-H+2nh(t)}{\sigma_3}\right)^2\right] + \exp\left[-\tfrac{1}{2}\left(\frac{x_3+H+2nh(t)}{\sigma_3}\right)^2\right]\right\}\right) \tag{3.36}$$

where J = 4 is sufficient to include the important reflections.

Equation (3.36) may be used for all three regimes discussed above. When the inversion base is very high ($\sigma_3 << h$), the reflection terms are near zero so equation (3.36) becomes the same as equation (3.35). As the plume moves farther downwind, σ_3 continues to grow rapidly, until the plume becomes completely mixed between the ground and the base of the temperature inversion. At this point, $P_v(x_3,t|H,t-\tau)$ approaches $\Delta x_3/h(t)$, which means it is equiprobable that a polluted air parcel from this plume will be found at any elevation below the inversion base. Computation on equation (3.36) for the case of $\sigma_3 >> h$ gives the desired result (as h/σ_3 approaches zero, it is necessary to increase J for convergence):

$$P_v(x_3,t|H,t-\tau) \rightarrow \frac{\Delta x_3}{h(t)} \quad \text{as} \quad \frac{h}{\sigma_3} \rightarrow 0 \tag{3.37}$$

Since equation (3.36) collapses into equation (3.35) when the inversion base has no effect, and into equation (3.37) when complete mixing occurs, it can be used for the general case to compute the probability that an air parcel resides within a particular domain within the mixed layer during the first few time steps after its release below the inversion base.

In practice, Turner (1969) suggests using an equation like (3.35) for $\sigma_3 < h^* = 0.47\ h$. At the time when σ_3 equals h^*, the error in $P_v(x_3,t|H,t-\tau)$ associated with not using the additional reflection terms found in equation (3.36) is only 0.02% (for $x_3 = H =$

0). Equation (3.36) is used when $\sigma_3 > h^*$. At some point, however, σ_3 will become large enough that the air parcels may be considered well mixed below the inversion base and $P_v(x_3,t|H,t-\tau)$ will approach $\Delta x_3/h(t)$ as in equation (3.37). It can be seen that when σ_3 increases to 2.5 h^*, the use of equation (3.37) instead of equation (3.36) results in an error in $P_v(x_3,t|H,t-\tau)$ of only 0.22% (for $x_3 = H = 0$). As time increases, σ_3 increases so that when σ_3 increases beyond 2.5 h^* and equation (3.37) has been chosen once, that portion of an air parcel that is located below the inversion base is considered fully mixed between the ground and inversion base for all subsequent time steps. It should be understood that the imposition of the vertical profile in this section will be operative only for the first few time steps of an air parcel's travel from its source. The vertical profile approximation constructed in this section, therefore, is employed as a correction for close-to-source, pollutant-laden air parcels during periods when σ_3 is small relative to the inversion base height.

3.3.4 Computational Procedure for Air Quality Model Simulation

The methods described in the previous sections for calculating probable air parcel motion over time due to individual physical processes may be combined to compute the overall source-to-receptor transport relationship in three-dimensional space. Let $P(x,t|x',t-\tau)$ be the probability of finding an air parcel within the air volume $x_i - \frac{\Delta x_i}{2} \leq x_i < x_i + \frac{\Delta x_i}{2}$, $i = 1,2,3$ surrounding near-ground

level location x given that it was released at location x' at time $t - \tau$. That probability density function can be constructed by multiplying the separate probabilities that the air parcel is (1) in the horizontal domain $x_i - \frac{\Delta x_i}{2} \leq x_i < x_i + \frac{\Delta x_i}{2}$, $i = 1,2$, and (2) resides below the inversion base, and (3) that the particle is at elevation $x_3 - \frac{\Delta x_3}{2} \leq x_3 < x_3 + \frac{\Delta x_3}{2}$ given that it is below the inversion base:

$$P(x,t|x',t-\tau) = P_a(x - x',t,t-\tau)\ P_b(t|t-\tau)\ P_v(x_3,t|x'_3,t-\tau) \tag{3.38}$$

By integrating equation (3.10) over time for many particle trajectories defined by equation (3.38) and then over many source locations using equation (3.9), long-term average pollutant concentration estimates are obtained. The computer program written to perform this integration works on the basis of a numerical simulation. Hypothetical mass points are released successively at small time intervals, Δt, from source location x' at the effective stack height of the source of interest. The pollutant mass associated with each particle is weighted by the diurnal source strength function appropriate to that source. Then for each time increment, the horizontal displacement of each of the many particles released is computed as a random variable in accordance with the probabilities of transition due to advection and horizontal diffusion as detailed in

Section 3.3.1. This is followed by the simulation of vertical exchange during the time increment, with probabilities computed as in Section 3.3.2. Finally, the probability that each mathematical particle is near the specified height, x_3, is computed for this time increment from equations in Section 3.3.3. At each time increment, Δt, of interest during the averaging time interval (t_s, $t_s + T$), a grid system is laid down over the air basin. The number of particles falling within each grid cell and the pollutant mass associated with each particle are summed. The pollutant mass is divided by the volume of the cell in order to obtain pollutant concentration in mass/unit volume of air. This procedure is described graphically in Figure 3.3 for the case of Δt = 1 hour and T = 1 month.

Results for the same time of day on each day during (t_s, $t_s + T$) are superimposed and then averaged in order to obtain the average diurnal variation of predicted pollutant concentration. Results at all times during the period (t_s, $t_s + T$) are superimposed and averaged in order to compute the long-term average pollutant concentration as a function of grid cell location in the air basin.

This simulation procedure is executed separately for each source class (e.g., automobiles, jet aircraft, power plants, etc.), resulting in a separate estimate of the contribution to pollutant concentration due to each source class. The incremental impacts from all source classes are added to form a total air quality impact at each horizontal grid cell location and height x_3 due to local pollution sources. Finally, an estimate of background pollutant

Figure 3.3

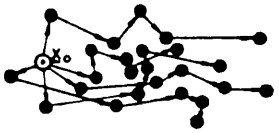

STEP 1

SUPERIMPOSE STREAKLINES CONTAINING ALL FLUID PARTICLES OBSERVED: ONE STREAKLINE FOR EACH HOUR OF THE MONTH

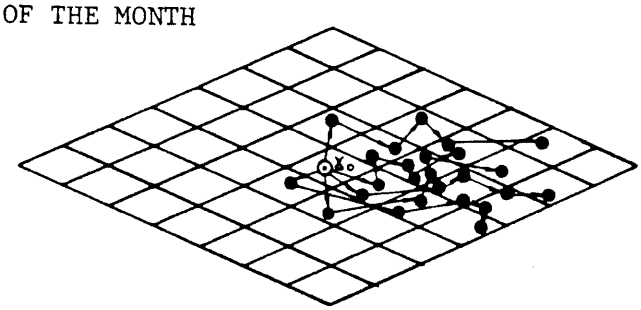

STEP 2

LOCATE PARTICLES WITHIN THE CELLS OF A RECEPTOR GRID

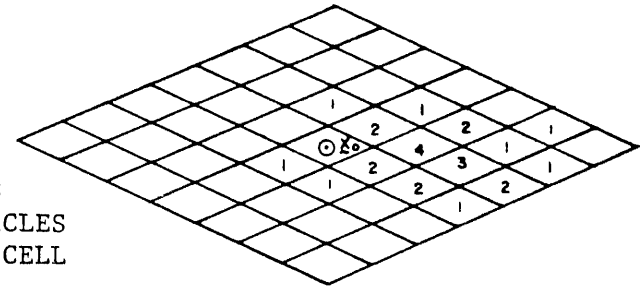

STEP 3

ACCUMULATE THE MAGNITUDES ASSOCIATED WITH THE PARTICLES FALLING WITHIN EACH GRID CELL

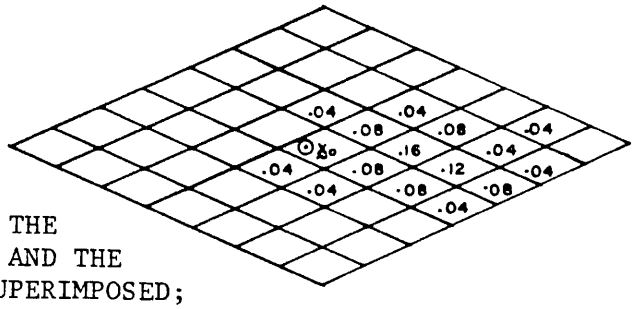

STEP 4

DIVIDE THE ACCUMULATED POLLUTANT MASS LOADING BY THE SIZE OF THE RECEPTOR CELL AND THE NUMBER OF "HOURS" BEING SUPERIMPOSED; CORRECT FOR INCOMPLETE VERTICAL MIXING NEAR SOURCES

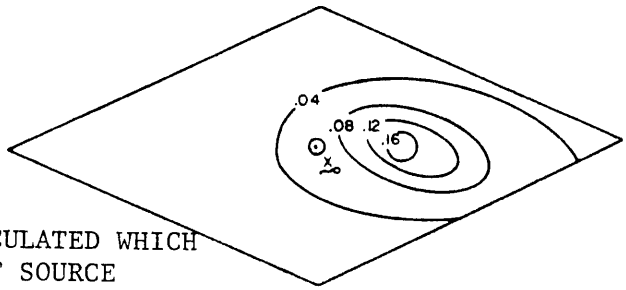

RESULT

THE SOURCE TO RECEPTOR RELATIONSHIP HAS BEEN CALCULATED WHICH MAPS EMISSIONS FROM A UNIT SOURCE AT LOCATION $\underset{\sim}{X}_0$ INTO AVERAGE POLLUTANT CONCENTRATION OBSERVED

concentration is added to the computed pollutant concentration from all local pollution sources to arrive at a predicted long-term average pollutant concentration.

In practice, the order of integration in the above description may be changed. Simulations may be carried out such that all trajectories ending (not starting) at a specific time are computed together. This enables one to readily examine long-term average diurnal concentration patterns. Also, computation time is saved because trajectories may be constructed by integrating backwards in time such that one mathematical trajectory represents the current locations of $\tau_c/\Delta t$ air parcels which were released from a single location during the preceding $\tau_c/\Delta t$ time increments. This one trajectory calculation replaces $\tau_c/\Delta t$ separate trajectory calculations to arrive at the same information (see Cass 1977).

3.4 Summary

In this chapter, a mathematical model has been stated that is suited to the computation of long-term average primary carbon particle air quality in an urban air basin. A Lagrangian simulation model has been constructed that tracks a large number of statistical air parcels, representing the transport of air pollutants under unsteady meteorological conditions. Each physical transport process is modeled as an independent stochastic process. Pollutant transport is simulated between the mixed layer adjacent to the ground and the atmosphere within a stable temperature inversion aloft. The model

also imposes a vertical (crosswind integrated) Gaussian concentration profile to compute the impact of emissions close to their sources.

A procedure was outlined for computing the long-term average concentrations of a primary (inert) pollutant that is released from a number of sources. In addition to predicting total pollutant concentrations, the model separates the individual source class contributions to air quality. In Chapter 4, this procedure will be applied to the prediction of monthly averaged concentrations of fine carbonaceous particulate matter from a variety of sources in the Los Angeles area.

3.5 References for Chapter 3

Bierly, E. W., and E. W. Hewson. 1962. Some restrictive meteorological conditions to be considered in the design of stacks. J. Appl. Meteorol. 1:383-90.

Cass, G. R. 1977. Methods for sulfate air quality management with applications to Los Angeles. Ph.D. thesis, California Institute of Technology, Pasadena.

Cass, G. R. 1981. Sulfate air quality control strategy design. Atmospheric Environment 15:1227-49.

Lamb, R. G. 1971. The application of a generalized Lagrangian diffusion model to air pollution simulation studies. In Proceedings of the symposium on air pollution, turbulence and diffusion, ed. H. W. Church and R. E. Luna. (Paper presented at symposium, 7-10 December, at New Mexico State University, Las Cruces.)

Lamb, R. G., and M. Neiburger. 1971. An interim version of a generalized urban air pollution model. Atmospheric Environment 5:239-64.

Lamb, R. G., and J. H. Seinfeld. 1973. Mathematical modeling of urban air pollution--general theory. Environmental Science and Technology 7:253-61.

Turner, D. B. 1969. Workbook of atmospheric dispersion estimates. National Air Pollution Control Administration. U.S. Public Health Service Publication no. 999-AP-26. Cincinnati.